ANKARA YILDIRIM BEYAZIT UNIVERSITY

GRADUATE SCHOOL OF NATURAL AND APPLIED SCIENCES



MULTI-WAVELENGTH GENERATION OF BRILLOUIN STOKES SIGNALS FOR (DWDM) COMMUNICATION SYSTEMS

Ph.D. Thesis by

MOHAMMED KAMIL SALH AL-MASHHADANI

Department of Electrical and Electronics Engineering

September 2021

ANKARA

MULTI-WAVELENGTH GENERATION OF BRILLOUIN STOKES SIGNALS FOR (DWDM) COMMUNICATION SYSTEMS

A Thesis Submitted to

The Graduate School of Natural and Applied Sciences of

Ankara Yıldırım Beyazıt University

In Partial Fulfillment of the Requirements for the Degree of Doctor of Philosophy in Electrical and Electronic Engineering, Department of Electrical and Electronics Engineering

by

MOHAMMED KAMIL SALH AL-MASHHADANI

September 2021

ANKARA

Ph.D. THESIS EXAMINATION RESULT FORM

We have read the thesis entitled **"MULTI-WAVELENGTH GENERATION OF BRILLOUIN STOKES SIGNALS FOR (DWDM) COMMUNICATION SYSTEMS"** completed by **MOHAMMED KAMIL SALH AL-MASHHADANI** under the supervision of **PROF. DR. HALIM HALDUN GOKTAS** and **ASSOC. PROF. DR. THAMER AL-MASHHADANI** and we certify that in our opinion it is fully adequate, in scope and in quality, as a thesis for the degree of Doctor of Philosophy.

Prof. Dr. Halim Haldun GOKTAŞ

Supervisor

Assoc. Prof. Dr. Thamer Al-Mashhadani

Co-supervisor

Prof. Dr. Fatih V. ÇELEBİ

Jury Member

Prof. Dr. Murat YÜCEL

Jury Member

Prof. Dr. İsa NAVRUZ

Jury Member

Assoc. Prof. Dr. Mustafa Burunkaya

Jury Member

Prof. Dr. Sadettin ORHAN

Director

Graduate School of Natural and Applied Sciences

I hereby declare that, in this thesis which has been prepared in accordance with the Thesis Writing Manual of Graduate School of Natural and Applied Sciences,

- All data, information and documents are obtained in the framework of academic and ethical rules,
- All information, documents and assessments are presented in accordance with scientific ethics and morals,
- All the materials that have been utilized are fully cited and referenced,
- No change has been made on the utilized materials,
- All the works presented are original,

and in any contrary case of above statements, I accept to renounce all my legal rights.

Date: **Signature: ……..**

Name & Surname:…….

ACKNOWLEDGMENTS

Firstly, I would like to express my sincere gratitude to my supervisor, **Prof. Dr. Halim Haldun GOKTAS** and **Assoc. Prof. Dr. Thamer AL-MASHHADANI** for his tremendous support and motivation during my study. His immense knowledge and precious recommendations constituted the milestones of this study. His guidance assisted me all the time of my research and while writing this thesis.

I would like to thank **Prof. Dr. Fatih V. ÇELEB** for his time, comments and supporting. I also want to offer special thanks to **Prof. Dr. Murat YÜCEL** for his generous explanations and giving me the opportunity to be in his lab.

I am proud and grateful to **my mother**, **my father**, **my brothers,** and **sisters** for being so helpful and supportive through my study. Last but not least special thanks to **my wife** for being so understanding and encouraging. I truly appreciate the commands of my friends in the lab. My special thanks to my aunt **Sukynh**, who taught me the first letter in my life. Thanks to **Ahmed Ebu-Duaaira** for his support during my study.

2021, September **MOHAMMED AL-MASHHADANI**

MULTI-WAVELENGTH GENERATION OF BRILLOUIN STOKES SIGNALS FOR (DWDM) COMMUNICATION SYSTEMS

ABSTRACT

In this study, firstly, the tunability of the multiwavelength Brillouin erbium fiber laser is experimentally enhanced by utilizing an absorber passive erbium doped fiber. The laser comb shows a wide tuning range of 65 nm in the absence of self lasing cavity. 62.5 % enhancement in the tuning range in our proposed structure compared with the configuration without passive Erbium doped fiber. In addition, the number of the generated Stokes lines was not affected and up to 13 single Brillouin frequency shift output channels having a peak power of 6 dBm are generated. Secondly, the stimulated Brillouin scattering threshold is experimentally investigated based on ring cavity Brillouin fiber laser. Threshold power for the 1st Stokes signal is improved and reduced up to 90% in ring cavity structure compared to its value in conventional technique. Thirdly, we experimentally propose simple and widely tunable multiwavelength Brillouin erbium fiber laser with triple Brillouin frequency spacing. In the developed structure, we achieved six triple Stokes lines with high peak power and large optical signal to noise ratio of more than 45 dB. Wide tuning range of 50 nm in the absence of self lasing cavity modes is recorded. Fourthly, we propose and experimentally demonstrate quadruple Brillouin-shift wavelength spacing utilizing multiwavelength Brillouin–Erbium fiber laser (MBEFL) cavity. The proposed structure has a tuning range of 60 nm (1530 nm–1590 nm) in the absence of self lasing cavity modes. Four stable Brillouin Stokes with high output power are achieved. Finally, we experimentally proposed widely tunable multiwavelength Brillouin erbium fiber laser with quintuple Brillouin frequency spacing. In the developed structure, at port1, we achieved four quintuple Stokes lines of about 10 dB peak power and large optical signal to noise ratio of more than 50 dB. Wide tuning range of 40 nm (1540–1580 nm) in the absence of free running modes is recorded.

Keywords: MBEFL, Brillouin fiber laser, Passive Erbium Doped Fiber, Laser Tunability, Triple Brillouin frequency spacing, Quadruple channel spacing, Quintuple channel spacing.

(DWDM) HABERLEŞME SİSTEMLERİ İÇİN BRILLOUIN STOKES SİNYALLERİNİN ÇOKLU DALGA BOYU ÜRETİMİ

ÖZ

Bu çalışmada, ilk olarak, çoklu dalga boylu Brillouin erbiyum fiber lazerin ayarlanabilirliği, bir emici pasif erbiyum katkılı fiber kullanılarak deneysel olarak arttırılmıştır. Lazer tarağı, kendinden lazerli boşluğun yokluğunda 65 nm geniş bir ayar aralığı gösterir. PEKF'siz konfigürasyona kıyasla önerilen yapımızda ayar aralığında % 62,5 artış gözlendi. Ek olarak, oluşturulan Stokes hatlarının sayısı etkilenmedi ve 6 dBm'lik bir tepe gücüne sahip 13 adete kadar tek Brillouin frekans kayması çıkış kanalı üretildi. İkinci olarak, uyarılmış Brillouin saçılma eşiği, halka kaviteli Brillouin fiber lazere dayalı olarak deneysel olarak araştırılmıştır. Birinci Stokes sinyali için eşik gücü konvansiyonel teknikteki değerine kıyasla halka kavite yapısı iyileştirilmiş ve %90'a kadar azaltılmıştır. Üçüncüsü, deneysel olarak, üçlü Brillouin frekans aralığına sahip basit ve geniş ölçüde ayarlanabilen çok dalga boylu Brillouin erbium fiber lazer öneriyoruz. Geliştirilen yapıda, yüksek tepe gücüne ve 45 dB'den fazla büyük optik sinyal gürültü oranına sahip altı adet üçlü Stokes hattı elde edildi. Kendinden kalıcı boşluk modlarının yokluğunda 50 nm'lik geniş ayar aralığı. Dördüncü olarak, çok dalga boylu Brillouin-Erbium fiber lazer (MBEFL) boşluğunu kullanarak dörtlü Brillouin-kaydırma dalga boyu aralığını öneriyoruz ve deneysel olarak gösteriyoruz. Önerilen yapı, kendiliğinden kalıcı boşluk modlarının yokluğunda 60 nm'lik (1530 nm–1590 nm) bir ayar aralığına sahiptir. Yüksek çıkış gücüne sahip dört kararlı Brillouin Stokes elde edilir. Son olarak, beşli Brillouin frekans aralığına sahip deneysel olarak geniş ölçüde ayarlanabilir çok dalga boylu Brillouin erbium fiber lazer önerdik. Geliştirilen yapıda, port1'de, yaklaşık 10 dB tepe gücü ve 50 dB'den fazla büyük optik sinyal gürültü oranı olan dört beşli Stokes hattı elde ettik. Serbest çalışma modlarının yokluğunda 40 nm'lik (1540–1580 nm) geniş ayar aralığı kaydedilir.

Anahtar Kelimeler: ÇBEFL, Brillouin fiber lazer, Pasif Erbium Katkılı Fiber, Lazer Ayarlanabilirlik, Üçlü Brillouin frekans aralığı, Dörtlü kanal aralığı, Beşli kanal aralığı.

CONTENTS

Ph.D. THESIS EXAMINATION RESULT FORM ii
ACKNOWLEDGMENTS iv
ABSTRACT v
ÖZ vi
NOMENCLATURE x
ACRONYMS xi
LIST OF TABLES xii
LIST OF FIGURES xiii

CHAPTER 1 INTRODUCTION 1
1.1 Overview of DWDM Communication System 1
1.2 Problem Statements 4
1.3 Research Objectives 7
1.4 Scope of the Work 8
1.5 Thesis outlines 9
CHAPTER 2 THEORETICAL BACKGROUND AND LITERATURE REVIEW 11
2.1 Introduction 11
2.2 Fiber Nonlinearity 11
2.2.1 Self-Phase Modulation (SPM) 14
2.2.2 Cross Phase Modulation (XPM) 14
2.2.3 Four Wave Mixing (FWM) 14
2.2.4 Stimulated Raman Scattering (SRS) 15
2.2.5 Stimulated Brillouin Scattering (SBS) 15
2.3 Brillouin Stokes Threshold in Single Mode Fiber 19
2.4 Review of Multiwavelength Brillouin Stokes frequency shift Laser comb. 21
2.4.1 Previous Works of Single Channel Spacing (0.08 nm, 10 GHz) 22
2.4.2 Previous Works of Double Channel Spacing (0.16 nm, 20 GHz) 33
2.4.3 Previous Works of Triple Channel Spacing (0.25 nm, 33 GHz) 43
2.4.4 Previous Works of Quadruple Channel Spacing (0.33 nm, 40 GHz) ... 48
CHAPTER 3 RESEARCH METHODOLOGY 51
3.1 Introduction 51

3.2 General Research Flow 51
3.3 Equipment and components 53
3.4 Single Brillouin Frequency Shift Generation Flowcharts 55
3.5 Double Brillouin Frequency Shift Generation Flowcharts 57
3.6 Triple, Quadruple, and Quintuple Brillouin Frequency Shift Generation Flowcharts 59
CHAPTER 4 RESULTS AND DISCUSSION 61
4.1 Introduction 61
4.2 Single Brillouin Frequency Shift (10 GHz) 61
4.2.1 Experimental Setup 61
4.2.2 Free Running Modes 62
4.2.3 Pump Powers Required for the First Brillouin Stokes. 63
4.2.4 Output Spectrum for the Generated Stokes at Threshold Pump Power. 64
4.2.5 Tunability of the Output Laser Comb 67
4.2.6 Spectrum of the Brillouin Stokes at Different BP Wavelengths 68
4.2.7 Effect of the 1480 Pump Power on the Numbers of the Generated Stokes Signals and Tuning Range 70
4.2.8 Impact of BP Power Variation on the Tuning Range and the Number of the Generated Stokes 71
4.3 Double Brillouin frequency spacing (20 GHz) 72
4.3.1 Experimental Setup 72
4.3.2 First Stokes Power at Different BP power 74
4.3.3 First Stokes Threshold as a Function of SMF Length 74
4.3.4 Maximum First Stokes power and the addition gain vs SMF length 76
4.3.5 Output Optical Spectrum 77
4.3.6 First Stokes Power and Threshold Comparison in Different Cavities 78
4.4 Triple Brillouin Frequency Shift (30 GHz) 79
4.4.1 Experimental Setup 79
4.4.2 Self Lasing Cavity Mode Oscillations 80
4.4.3 Stokes Spectrum at Threshold Power 81
4.4.4 Output Channels Tunability 83
4.4.5 Spectrum of the Output Laser Comb at Various BP Wavelengths 84
4.4.6 Stokes Signals Power Stability 86
4.5 Quadruple Brillouin frequency shift (40 GHz) 86
4.5.1 Experimental setup 86

4.5.2 Free Running Cavity Modes (Erbium Gain) 88
4.5.3 Threshold Power (1480 nm Pump Power Required) 88
4.5.4 Stokes Power Variation as a Function of BP Power 90
4.5.5 Output Laser Comb Spectrum of the Multi-Output Ports 91
4.5.6 Output Channels Tunability 93
4.5.7 Impact of wave selective coupler on the performance 94
4.5.8 Output Spectrum of the Generated Stokes Signals 95
4.5.9 Peak Brillouin Stokes power stability 97
4.6 Quintuple Brillouin frequency shift (50 GHz) 97
4.6.1 Experimental Setup 97
4.6.2 Self Lasing Cavity Modes 99
4.6.3 Output Spectrum for The Generated Stokes Signals at the Threshold Power 100
4.6.4 The Output Laser Comb Spectrum of the Multi-Output Ports 101
4.6.5 Output Channels Tunability 103
4.6.6 Output Spectrum of Stokes Signals Generated at Different BP Wavelength 105
4.6.7 Stokes Peak Power Fluctuation 107
CHAPTER 5 CONCLUSIONS AND FURTHER WORKS 108
5.1 Conclusions 108
5.2 Novelty Contribution 109
5.3 Recommendations for Further Work 110
REFERENCES 111
CURRICULUM VITAE 127

NOMENCLATURE

A_{eff}	effective core area
c	light velocity
D	flux density
E	electric field
f	frequency
g_B	Brillouin gain coefficient
Ip	intensity of Brillouin pump
Is	Stokes power
L_{eff}	effective fiber length
n	refractive index
P	polarization
P_S	output power of the Stokes signals
R	reflectivity of optical mirrors
ν_a	acoustic velocity
ε_0	permittivity in free space
χ_0	electric susceptibility of the material
α	attenuation constant of the fiber

ACRONYMS

BEFL	Brillouin Erbium fiber laser
BFL	Brillouin fiber laser
BP	Brillouin pump
Bi-BFL	Bidirectional Brillouin fiber laser
CSBS	Cascade stimulated Brillouin scattering
DWDM	Dense wavelength division multiplexing
EDF	Erbium doped fiber
EDFA	Erbium doped fiber amplifier
FBG	Fiber Bragg grating
FWM	Four wave mixing
HNLF	Highly nonlinear fiber
MBEFL	Multiwavelength Brillouin Erbium fiber laser
MBEL	Multiwavelength Brillouin fiber laser
NZ-DSF	Non-zero dispersion shifted fiber
OSNR	Optical signal to noise ratio
OSA	Optical spectrum analyzer
PCF	Photonic crystal fiber
SBS	Stimulated Brillouin scattering
SMF	Single mode fiber
SRS	Stimulated Raman scattering
SPM	Self-phase modulation
TLS	Tunable laser source
Uni-BFL	Unidirectional Brillouin fiber laser
VOA	Variable optical attenuator
VOC	Variable optical coupler
WDM	Wavelength division multiplexing
XPM	Cross-phase modulation

LIST OF TABLES

Table 1.1 Nominal central frequencies of the DWDM grid 3

Table 2.1 Summary of tunability enhancement technique in a single Brilloiun frequency shift MBEFL 33

Table 2.2 Summary of tunability enhancement technique in a double Brilloiun frequency shift MBEFL 42

Table 2.3 Summary of the triple Brillouin frequency shift in MBEFL 48

Table 2.4 Summary of the quadrable Brillouin frequency shift in MBEFL 50

Table 3.1 Components and equipment used in the experimental and theoretical study 53

LIST OF FIGURES

Figure 1.1 Blok diagram of a Basic WDM system 2

Figure 1.2 Multi-wavelength sources as a transmitter in DWDM systems 3

Figure 1.3 Multi-wavelength sources as a transmitter in DWDM systems 9

Figure 2.1 Linear and non-linear interaction..... 12

Figure 2.2 Schematic of the nonlinear effects in fibre optics..... 13

Figure 2.3 Stimulated Brillouin and Raman Scattering (SBS) (SRS) in optical fiber [52]. 16

Figure 2.4 Schematic setup of linear cavity MBFL reported by [58]. 18

Figure 2.5 variation of the transmitted and Stokes power in SMF [59]. 20

Figure 2.6 Experimental setup which reported by (a) [100] (b) [101] (c) [102] (d) [103] 30

Figure 2.7 Output spectrum of the structures which presented by (a) [100] (b) [101] (c) [102] (d) [103] 31

Figure 2.8 The output spectra at different BP wavelengths of the cavities which proposed by (a) [100] (b) [101] (c) [102] (d) [103] 31

Figure 2.9 MBFL reported by [108] (a) Experimental setup (b) output spectrum.... 34

Figure 2.10 Experimental setup of MBFL reported by [110] 35

Figure 2.11 Output spectrum of MBFL reported by [110] 36

Figure 2.12 Experimental setup of MBFL reported by [121] 40

Figure 2.13 MBFL reported by [121] (a) Output spectrum of odd and even Stokes lines (b) Tuning range 40

Figure 2.14 Experimental setup which reported by (a) [37] (b) [38] (c) [125] (d) [40] (e) [41] (f) [42] 46

Figure 2.15 output spectrum of the structures proposed by (a) [37] (b) [38] (c) [125] (d) [40] (e) [41] (f) [42]..... 47

Figure 2.16 Experimental schemes which reported by (a) [125] (b) [126] (c) [127] (d) [43] 49

Figure 2.17 Output spectrum of the generated Stokes for the cavities proposed by (a) [125] (b) [126] (c) [127] (d) [43] 50

Figure 3.1 Research Process Flowchart. 52

Figure 3.2 Single Brillouin frequency shift generation flowchart. 56

Figure 3.3 Double Frequency Shift Brillouin Stokes signal characteristics flowchart. 58

Figure 3.4 Generation of 30, 40, and 50 GHz Brillouin frequency shift flowchart. . 60

Figure 4.1 Experimental setup of both configurations with and without PEDF. 62

Figure 4.2 Peak gain of the free running cavity modes at 230mW of 1480 pump power with and without PEDF. 63

Figure 4.3 Required pump power for generating the 1st Stokes signal of the two configurations. 64

Figure 4.4 Output Spectrum for the generated Stokes signals of proposed structure at the threshold power (a) without PEDF (b) with PEDF. 65

Figure 4.5 Output Spectrum for the generated Stokes signals at the maximum pump power (a) without PEDF (b) with PEDF 66

Figure 4.6 Output channels tunability of MBEFL cavity at different wavelengths at maximum of BP and 1480 nm powers of 10 dBm and 230 mW respectively (a) without PEDF (b) with PEDF 67

Figure 4.7 Output spectrum of Stokes signals generated at different BP wavelength within the entire tuning range(a) without PEDF (b) with PEDF 69

Figure 4.8 Tuning range and numbers of output channels of proposed cavity as a function of 1480 nm pump power. 70

Figure 4.9 Tuning range and number of output channels for proposed configuration as a function of BP power. 71

Figure 4.10 Ring BFL cavity and conventional technique structures. 72

Figure 4.11 First Stokes signal variation as a function of BP power in 5km SMF for ring BFL cavity and conventional technique. 74

Figure 4.12 First Stokes threshold power as a function of SMF length for both Structures. 75

Figure 4.13 Maximum 1st Stokes power and the addition gain vs SMF length in both structures. 76

Figure 4.14 Output optical spectrum for the conventional technique, and ring BFL cavity at a) 5 km SMF length and (b) 18 km fiber length. 78

Figure 4.15 Maximum of 1st Stokes signal power and threshold for linear and ring BFL cavities as a function of SMF length. 79

Figure 4.16 Experimental setup of the proposed MBEFL cavity. 80

Figure 4.17 Self lasing cavity modes Erbium gain without BP at the maximum pump power of 220 mW. 81

Figure 4.18 (a) Stokes spectrum at threshold power. (b) Stokes power variation versus pump power. 82

Figure 4.19 Output channels tunability of MBEFL cavity. 84

Figure 4.20 Output spectrum of Stokes signals generated at different BP wavelength (a) 1530, (b) 1540, (c) 1550, (d) 1562, (e) 1570, (f) 1580 nm. 85

Figure 4.21 Peak power stability of Brillouin Stokes signals at a pump power of 220 mW. 86

Figure 4.22 Experimental setup of the proposed MBEFL cavity. 87

Figure 4.23 Self lasing cavity modes (Erbium gain) at the maximum pump power of 225 mW. 89

Figure 4.24 Threshold power for S4, S8, and S12. (a) Stokes power variation as a function of 1480 pump power, (b, c, and d) output spectrum for S4, S8, and S12 at the threshold power of 70, 120, and 170 mW respectively. 89

Figure 4.25 (a) Stokes power variation as a function of BP power, (b, c, and d) output spectrum for S4, S8, and S12 at the different BP power of 12, 13, and 14 dBm respectively. 91

Figure 4.26 The output spectrum of the multi-output ports laser comb at a maximum pump power of 225 mW and BP power of 20 mW (a) out1 (b) out2 (c) out3 (d) out4. 92

Figure 4.27 Output channels tunability of MBEFL cavity at different wavelengths with BP and pump powers of 20 mW and 225 mW, respectively. 93

Figure 4.28 Output spectrum at the maximum 1480 pump power of 225 mW, (a) the residual 1480 nm pump power at WSC. (b) free running modes at out4 with and without WSC with 10% output ratio. 94

Figure 4.29 Output spectrum of the generated Stokes signals at different BP wavelength at the maximum 1480 nm pump powers of 225 mW and 20 mW of Bp power 96

Figure 4.30 Peak power stability within a period of one hour for the Bp, S4, S8, and S12 Brillouin Stokes signals at a pump power of 225 mW and a BP wavelength of 1560 nm with a power of 20 mW 97

Figure 4.31 Experimental setup of the proposed MBEFL cavity. 98

Figure 4.32 Free running modes (Erbium gain) at the maximum pump power of 220mW. 100

Figure 4.33 (a): Quintuple Stokes signals power vs 1480 pump power. (b): Output Spectrum for the generated Stokes signals at the threshold power (required 1480 pump power for each Stokes signal 101

Figure 4.34 The output spectrum of the multi-output ports laser comb at a maximum pump power of 220 mW and BP power of 20 mW (a) port1 (b) port2 (c) port3 (d) port4 (e) port5 (f) All ports. 102

Figure 4.35 Output channels tunability of MBEFL cavity at different wavelengths at maximum of BP and 1480 nm powers of 20 mW and 220 mW respectively 104

Figure 4.36 Free running modes with and without WSC2 with output ratio 10% after EDFA2 section 105

Figure 4.37 Output spectrum of Stokes signals generated at different Bp wavelength (a) 1540 (b) 1550 (c) 1562 (d) 1570 (e) 1580 (f) quintuple Stokes peak powers at different Bp wavelength. 106

Figure 4.38 Peak power stability within a period of one hour for the BP, S5, S10, and S15 Brillouin Stokes signals at a pump power of 220mW and a Bp wavelength of 1562 nm with power of 20 mW. 107

CHAPTER 1

INTRODUCTION

1.1 Overview of DWDM Communication System

Optical fiber allows multiple wavelength signals to be transmitted in one single fiber without interfering with each other. This gives a promising solution to the high-capacity demands. There is currently an increasing demand for transmission bandwidth used for dense wavelength-division-multiplexing (DWDM) optical communication systems as resulted from the remarkable advancement both in the data traffic and the internet [1, 2]. Basically, there are three different techniques to increase the transmitted capacity per fiber in DWDM technology [3]; the first approach is by increasing the number of the transmitted channels by using a narrow channel spacing. The second technique is by increasing the bit rate per channel, and the third approach is by increasing the total transmission bandwidth. Relatively Low bit rate per channel is required in the first approach that gives it significant advantages as compared to the others two techniques. For that no complicated dispersion compensation technique is required and low electrical circuits speed can be implemented. In other word, in this technique the DWDM system is effectively increasing the bandwidth per single optical fiber as the total system bandwidth is the sum of the bit rates of each different wavelength channels.

DWDM has a potential transmission system with large number of closely spaced channels through optical fiber. In addition, employment of optical amplifiers for regenerating the multi-channel light wave without requiring to demultiplexing of individual channels makes a revolution in multi-wavelength optical system designs. This makes a demand for multi-wavelength light source. In order to fulfil such a demand, using the multi-channel laser source has turned into a noticeable and conceivable solution. Multi-wavelength fiber lasers are highly desirable for the cost and size reduction, improvement of system integration and their compatibility with optical communication networks.

To generate, isolate, distribute, and amplify the inserted optical signal in DWDM optical communication system, many optical elements are included as shown in Figure 1.1. Different optical channels with several wavelengths are transmitted along the same fiber. Before they inserted into the optical span, these channels are multiplexed via an optical multiplexer. Within the entire optical link, a fiber optical amplifiers are used to supress the optical span loss and to keep the signal level at certain value. In addition, to reverse a positive dispersion that comes from the optical fiber span, dispersion compensators are utilized. The optical nodes also could be used to add or drop any channel within the optical link. At the receiver side, the transmitted multiplexed channels need to be multiplexed to be detected by the photodetectors [4].

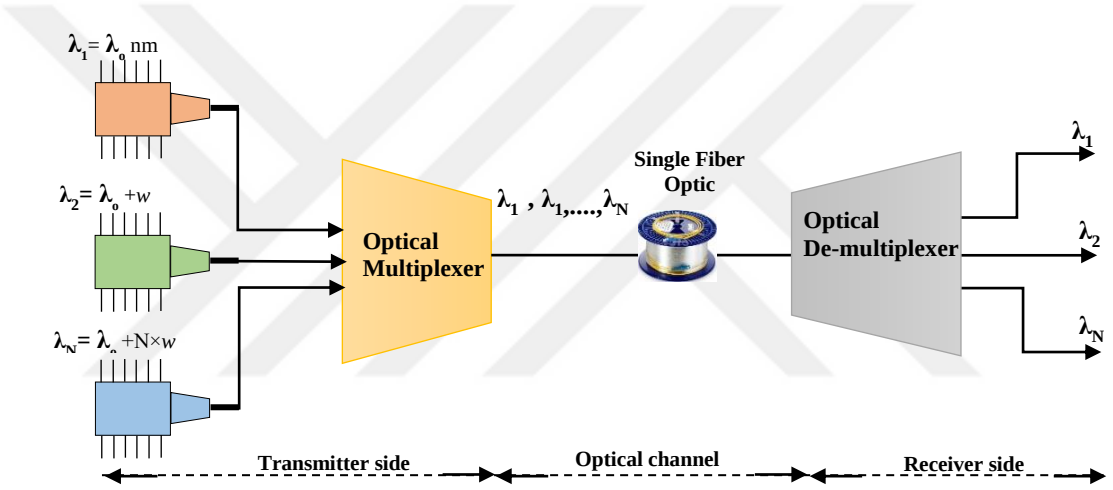


Figure 1.1 Blok diagram of a Basic WDM system

For DWDM communication system, a multiple channel sources are required. Generally, these multiple channels are provided by an individual laser sources to be used like an optical carrier as illustrated in Figure 1.1. Using such individual optical carriers, more complexity is added to the system especially when the number of the channel is increased. Subsequently, the number of the laser and temperature controllers will be increased. To avoid such complexity, a multiwavelength sources operation could be incorporated as an optimal solution for DWDM system and at the same time no optical multiplexer is needed at the transmitter side as shown in Figure 1.2. Still an optical demultiplexer is needed before the receiver side to demultiplex the transmitted signals.

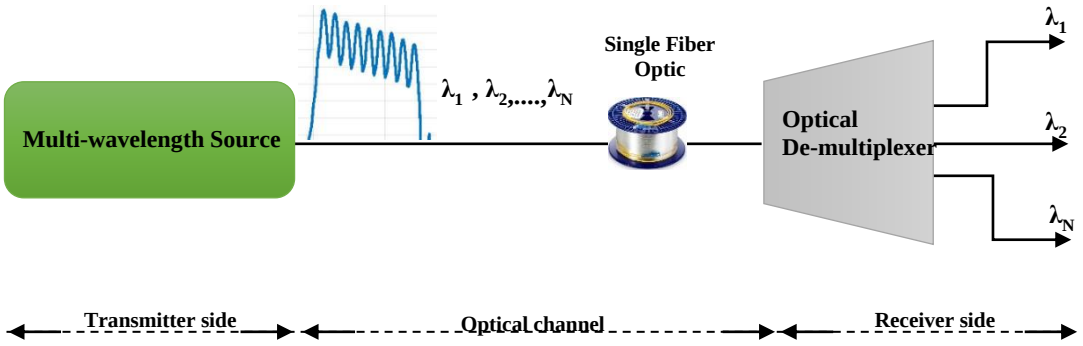


Figure 1.2 Multi-wavelength sources as a transmitter in DWDM systems

Multiple optical sources can be achieved through several methods. One of the most used method is by using a fiber nonlinearities. Although such fiber nonlinearities are considered as a drawback in optical communication system (saturate the transmitted optical power), they be used beneficially for multiwavelength sources generation. Different fiber nonlinearities such as four wave missing (FWM), stimulated Raman scattering (SRS), and stimulated Brillouin scattering (SBS) were incorporated to generate multiple channel sources.

SBS is the nonlinear phenomenon in optical fiber that occurs once the incident optical power exceeds the threshold level. Scattering backward Stokes's signal is generated with down shifting frequency of about 10 GHz corresponding to the input signal [5]. The dynamics of cascaded-order Brillouin lasers make them able to generate different frequency shift, according to the kind of the cavity, such as 10 GHz for the fundamental Brillouin shift in addition to 20, 30, 40, and 50 GHz for double, triple, quadruple, and quintuple space respectively. This property of the Brillouin laser makes it suitable for multi-wavelength sources generation.

The International Telecommunication Union (ITU) provided a guidelines for DWDM wavelength channels and the channel spacing determination [6]. They provided the suitable channel frequency shift of 1.25, 50, and 100 GHz for DWDM applications. One example of the frequency grid is illustrated in Table 1.1. Due to the dense wavelength spacing, the frequencies or the wavelength should be rigid and stable to be

used for real time application. To prevent wavelengths drifting in DWDM systems, a control of precision temperature of the carrier is important.

Table 1.1 Nominal central frequencies of the DWDM grid reported by [6]

Nominal central frequencies (THz) for spacings of:				**Approximate nominal central wavelengths (nm)**
12.5 GHz	**25 GHz**	**50 GHz**	**100 GHz and above**	
.	.	.	.	.
.	.	.	.	.
195.8875	-	-	-	1530.4318
195.8750	195.875	-	-	1530.5295
195.8625	-	-	-	1530.6271
195.8500	195.850	195.85	-	1530.7248
195.8375	-	-	-	1530.8225
195.8250	195.825	-	-	1530.9203
195.8125	-	-	-	1531.0180
195.8000	195.800	195.80	195.8	1531.1157
195.7875	-	-	-	1531.2135
195.7750	195.775	-	-	1531.3112
195.7625	-	-	-	1531.4090
195.7500	195.750	195.75	-	1531.5068
195.7375	-	-	-	1531.6046
195.7250	195.725	-	-	1531.7024
195.7125	-	-	-	1531.8003
195.7000	195.700	195.70	195.7	1531.8981
195.6875	-	-	-	1531.9960
.	.	.	.	.
.	.	.	.	.
.	.	.	.	.
184.5000	184.500	184.50	184.5	1624.8914

1.2 Problem Statements

Multiwavelength Brillouin-Erbium fiber laser (MBEFL) is of great importance due to of its possible functions many applications such as: millimeter wave generation, microwave photonics, dense wavelength-division-multiplexing (DWDM) communication system, and fiber sensing [7, 8]. However, the main drawback of such fiber lasers cavities is the instability caused by the free running modes which is highly increased with the increment of the pump power in the EDF section. Subsequently, Enough Brillouin pump power, close to the center wavelength of the self lasing cavity

modes, is required to eliminate such unwanted oscillations. Many techniques have been implemented to accomplish broad tuning range. High Brillouin pump (BP) power was utilized in [9], an optical filter like Sagnac loop filter [10] and bandpass filter [11] were used for the same purpose. However, using such optical filters can be resulted into two setbacks in terms of complexity and cost issues. Avoiding using such optical filters, [12, 13] presented an acceptable tuning range using single and double pass pre-amplification for the inserted BP power. MBEFL tuning range's cavity was expanded to 23 nm via passive erbium doped fiber (PEDF) and variable optical attenuator (VOA) inside the laser cavity [14]. However, using both of PEDF and VOA inside the cavity, the number of the generated Stokes was limited only to 11 Stokes signals, and the Stokes power was below -23 dBm. A tunable L-band MBEFL that uses PEDF as an absorber section was presented by [15]. In this work, a comparison between with and without PEDF was illustrated. Inclusion PEDF enhanced the cavity tunability by 31% and up to 16 Stokes signals were tuned over 24.4 nm. However, the number of the generated Stokes signals were a bit decreased via PEDF due to the small Brillouin gain absorption within it.

Stimulated Brillouin scattering (SBS) represents the backbones of generating multiple Brillouin Stokes signal inside the fiber [16–18]. The threshold of SBS for conventional technique in which there is no signal circulation or feedback has been studied by many researchers [19, 20]. To reduce the SBS threshold, two techniques of bidirectional laser pump and recycling technique were used [21,22]. In these two techniques, the researchers claim that the SBS threshold was reduced due to the long signal interacting within the structure. The threshold for SBS was reduced up to 50 % in these two-techniques compared to conventional technique. In addition, the SBS threshold reduction ratio in linear BFL cavity was studied in [23]. In which, the SBS threshold was reduced up to 75% and 50% in linear cavity as compared to its values in conventional and recycling techniques. However, it can be known from the literature that the SBS threshold was reduced either by bidirectional pump or by recycling technique as compared to conventional technique. In addition, it also can be found the SBS threshold ratio in linear BFL cavity. Therefore, more investigation study should be conducted to find the SBS threshold reduction ratio in ring cavity BFL. This ratio is too important by estimating the SBS threshold value for the ring BFL cavity by

returning into the standard conventional technique threshold equation for certain SMF length [24].

DWDM systems has been supported by multiwavelength fiber laser due to its potential application that can provide dense laser wavelength spacing. However, MBEFL has limitation related to cavity tunability [25,26] and narrow line spacing of 0.08 nm [27, 28] which is presented as the major limitation of such laser cavity to be used in optical communication system applications. Various techniques were presented to enhance the laser cavity tunability [12,13,15,29–32]. Real challenge is related to de-multiplexing process in receiver side which is complicated to be recognized using narrow dense line spacing of 0.08 nm. Thus, double Brillouin frequency spacing of 0.17 nm has been implemented by many researchers [33–36]. In order to expand the line channel spacing which makes de-multiplexing process easier, triple Brillouin frequency spacing of 0.25 nm were proposed by fewer researchers [37–42]. Tunable and switchable frequency shift MBEFL cavity that uses three cascade single mode fiber (SMF) was proposed by [37]. However limited number Stokes and power were achieved. Two ring laser cavities with long SMF length of 50 km that generated ten Brillouin Stokes lines with triple wavelength spacing and a real tuning range of 35 nm in the absence of self lasing cavity mode were presented by [38]. However, high pump power of 600 mW at 980 nm was used and the Stokes peak powers were below −4 dBm. Again, cascade SMFs lengths of 70 km was implemented in ring laser cavity to achieve switchable MBEFL [39]. SMF sections were added or removed manually to produce switchable feature within the cavity. Using such long SMF length in addition to use high pump power of 1.2 W made the proposed setup hard to be realized in real application. MBEFL structure that was able to generate six Brillouin Stokes lines with triple wavelength spacing was proposed by [40]. However, two EDFA sections and 20 km of two-dispersion compensation fiber (DCFs) were used. In addition, the tunability range was limited to 19 nm at 100 mW pump power for the second EDFA section. At such pump power, the number of the triple Stokes lines was limited to four only. Further switchable Brillouin Stokes spacing in MBEFL cavity was reported by [41]. Nine Stokes lines with a peak power of −15 dBm and a channel spacing of 0.259 nm at the center frequency of 1565 nm were generated. However, two erbium– ytterbium amplifier sections were used, and the laser cavity tunability was limited to the central

wavelength of self-lasing cavity at 1565 nm. In another word, tuned BP wavelength a way from 1565 nm, self lasing cavity modes appeared at the output laser comb. The proposed previous triple Brillouin frequency structures [37–41] suffer from the drawbacks of self-mode competition that restricts the laser cavity tunability. Recently, tunable MBEFL cavity with triple Brillouin spacing lines was reported by [42]. Four Stokes lines that tuned over 40 nm (limited to the erbium emission band 1530–1570 nm) were recorded. However, high pump power of 370 mW and two Brillouin gain media (DCF length of 12 km and 10 km of SMF) were used. Using such long DCF length led to additional loss of the transmitted signal power since the Brillouin gain was already saturated at such length. Furthermore, few research have presented fourth Brillouin spacing of 0.33 nm (40 GHz) [39, 43]. Only one quadruple Brillouin Stokes signal with a 40 GHz wavelength spacing shifted from the first Stokes wavelength was reported by adjusting BP and variable attenuator [43]. In addition, fiber Bragg grating was utilized as a filter to obtain these two wavelength signals. Four cascade SMFs spools with total length of 112 km, two EDFA sections, and high pump power about 1.1 W were used for generating four quadruple Stokes signals [39]. Low achieved Stokes power (about −2 dBm) compared to the long SMF used made the proposed setup out of the reality application. Up to date, to the best of our knowledge, no study has been reported on fifth Brillouin frequency shift.

1.3 Research Objectives

The research study presented in this thesis focuses on the design, analysis and development of the multiwavelength fiber laser based on Brillouin and hybrid gain mediums. The main research objectives of the entire study can present as follows:

1 Enhance the tunability of the MBEFL cavity using PEDF in simple ring cavity design.

2 Investigate and estimate the threshold equation of the SBS in ring cavity corresponding to the SBS threshold equation in conventional technique.

3 Improve the performance of the triple Brillouin space cavity in terms of tuning range and the number of the generated Stokes signals.

4 Generate quadruple Brillouin frequency shift (40 GHz) Brillouin Stokes signals.

5 Expand the Brillouin frequency shift to 50 GHz in order to be more detectable in receiver side of the DWDM optical communication system.

1.4 Scope of the Work

The flowchart of the research scopes of this study is shown in Figure 1.3. Ring cavity structure is implemented within the entire work. At first, the tuning range of the multiwavelength Brillouin erbium fiber laser (MBEFL) with single Brillouin frequency shift of 0.08 nm (10 GHz) is improved by using simple passive EDFA. In addition, the proposed new setup avoided the trade-off in the number of generated Stokes lines and the number of the Stokes lines was same in the proposed design as compere to the conventional ring laser cavity. For the second stage, the threshold equation for the stimulated Brillouin scattering (SBS) is experimentally estimated in ring laser cavity with double Brillouin frequency shift (20 GHz) and the threshold equation of the SBS signal is derived according to the reduction ratio achieved by the experimental conducted results. In the context of the enhancement study, the tuning range and the number of the generated Stokes channels are improved in triple Brillouin frequency shift (30 GHz) cavity. In the last section of this study, a generation of quadruple and quintuple (40 and 50GHz) Brillouin stokes lines is proposed for the first time as a multiwavelength laser source generation for DWDM communication system

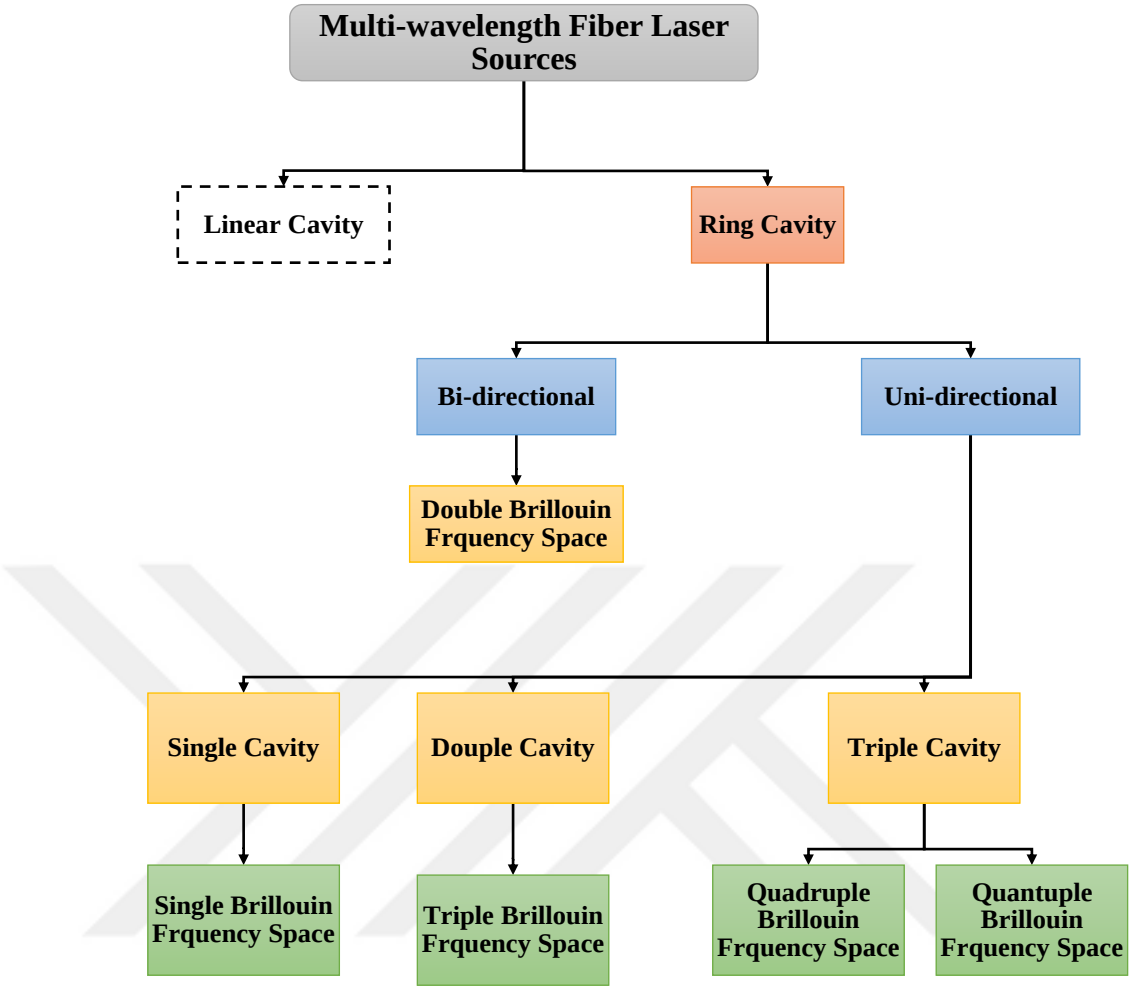


Figure 1.3 Multi-wavelength sources as a transmitter in DWDM systems

1.5 Thesis outlines

This thesis shows the design and analysis of the multiwavelength Brillouin fiber laser channels with different frequency shift for DWDM communication system application. This experimental study is structured into five chapters. The possible application of the multiwavelength fiber laser sources in DWDM communication system and the brief introduction of the DWDM system is presented in chapter 1. In addition, the problem statement, objective, and research scope are also contained in this chapter. Chapter 2 presents the theoretical background of the nonlinear effect phenomena as well as a critical review of different generated Brillouin frequency shift Stokes lines. The flowchart of the general research methodology and the individual

experimental proposed structure are covered in chapter 3. The explanation for each experimental part that show how the proposed design is work are also presented in chapter 3. Chapter 4 focuses on different proposed ring fiber laser cavities that generates different Brillouin frequency shift started from 10 to 50 GHz channel spacing. The chapter started with enhancing the laser performance of the 10, 20, and 30 GHz cavities. Then the generation of new 40 and 50 GHz channel spacing cavities are presented at the end of this chapter. Finally, the individual conclusion corresponding to the different experimental studies is included in chapter 5.

CHAPTER 2

THEORETICAL BACKGROUND AND LITERATURE REVIEW

2.1 Introduction

In this Chapter, firstly, the studies of Brillouin Stokes signal and threshold mathematical equations in optical fiber are presented. Then the chapter focuses on a review of multiwavelength fiber laser sources, based on first, second, third, and fourth Brillouin frequency shift MBEFL.

2.2 Fiber Nonlinearity

The nonlinearity is characterized as the impact of the magnitude of the electric field on the output [3, 24]. Dielectric material can be utilizing in order to explain the nonlinear effect. Applying the electric field on the material, the movement of the positive charge will be in the same direction of the field, while the negative charge displaced in reverse direction of the electric field that produces the dielectric polarization. Optical fiber is a kind of the dielectric media in which the electric field intensity causes the nonlinear phenomenon.

The linear relationship between the electric field and flux density inside the optical fiber, dielectric material, at low intensity of the field is given by equation (2.1)

$$D = \varepsilon_0 E + P \qquad (\mathbf{2.1})$$

where *P* is the polarization induced in the optical fiber.

The polarization P which given in equation (2.2) is linearly relat to the electric field in linear and isotropic optical media and it is in the forward direction as *D*.

$$P = \varepsilon_0 \chi_0 E \qquad (\mathbf{2.2})$$

where ε_0 represents the permittivity in free space and where χ_0 (chi) is a dimensionless quantity called the electric susceptibility of the material.

The electrons alternate with the similar frequency of the applied field when the electric field has low intensity. In this case the optical parameter like absorption coefficient and refractive index are invariable. However, when the intensity of the field goes up, the electrons inside the media will be in an harmonic motion form that produce a new frequency different from the incident frequency [4] as shown in equation 2.3

$$P = \varepsilon_0(\chi^1 E + \chi^2 E^2 + \chi^3 E^3 + \cdots) \qquad (\mathbf{2.3})$$

linear and nonlinear interactions between the input and the output in both conditions, low and high input intensity, are shown in Figure 2.1.

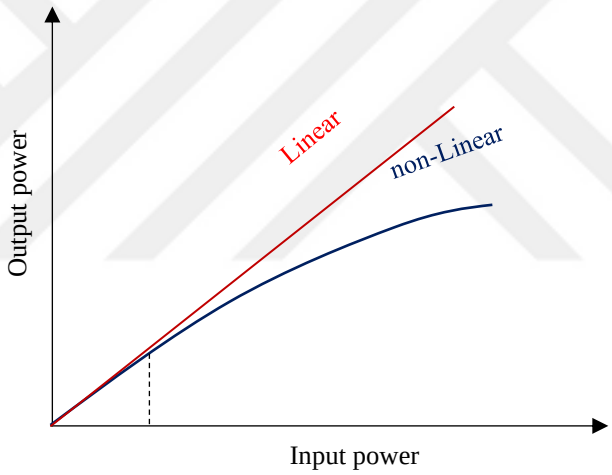


Figure 2.1 Linear and non-linear interaction

The polarization equation, Equation (2.3), state the relation of the polarization with the electric susceptibility of the material numbers. It can be seen that the main parameter in this equation are χ^1 the χ^2 which influenced by the second harmonics production and sum of frequency generation. On the other hand, the third susceptibility parameter χ^3 caused the lowest order nonlinear impact. The equation (2.3) explains that the intensity of the light, E, changes the susceptibility [44]. Indeed,

In reality, this connection is far from material with absorption parameter and refractive index. The direction of the molecules is modified as the electric field (E) inside the

optical fiber increase which produces many nonlinear effects such as inelastic scattering and refractive index as shown in Figure 2.2.

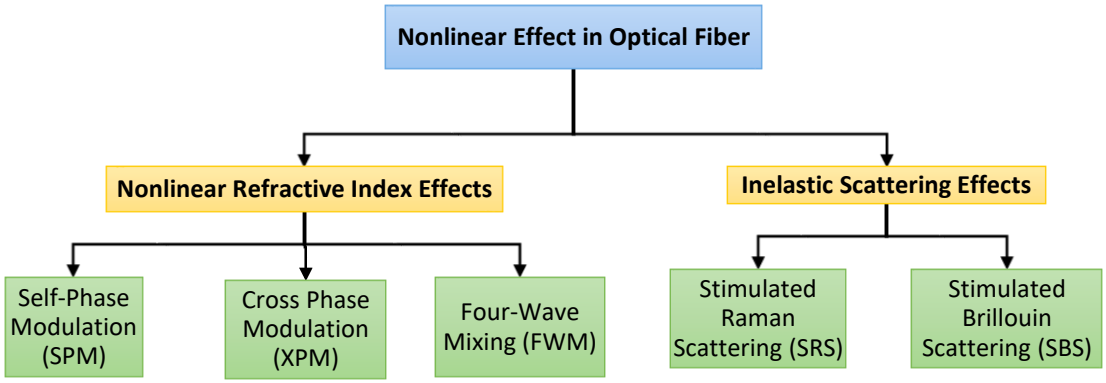


Figure 2.2 Schematic of the nonlinear effects in fibre optics

The nonlinear phenomenon in optical fiber can be divided into two categories: elastic (nonlinear refractive index) and inelastic. The elastic phenomenon in which the energy does not transfer between the lunched light and the media. Because the refractive index of the media varies with the incident light intensity, several nonlinear phenomena such as cross-phase modulation (XPM), four-wave mixing (FWM), and self-phase modulation (SPM) occur related to the type of the input light. On the other side, when the part of the optical energy exchange to the medium, inelastic scattering effect happened. These nonlinear effects are known as stimulated Brillouin scattering (SBS) and stimulated Raman scattering (SRS) [44].

The inelastic interaction between the incident photons and the acoustic phonon resulted in frequency shifting in the scattered photons which directly affected by the sound velocity characteristics of the medium. These two inelastic phenomena; SBS and SRS have some major differences between them. While the SBS phenomenon generates a coherent laser beam which propagation in opposite direction of the input light, the SRS may be scattered in both forward and backward directions. In addition, the SBS produces a light with around 10 GHz frequency shift according to the launched signal, whereas the large frequency shift of about 13 THz is achieved in SRS.

The main difference between them is that the SRS occurs due to the optical phonons participate while SBS is generated through acoustic phonons [45].

2.2.1 Self-Phase Modulation (SPM)

When the light is travelling in an optical medium, it will induce a varying refractive index of the medium due to the optical Kerr effect. This variation in refractive index will produce a phase modulation on itself, leading to a change of the pulse's frequency spectrum. The phenomenon in which the phase modulation of the optical light occurs by itself is called SPM. The SPM happens if the system has only single wavelength signal. The refractive index of the optical fiber is many depend on the intensity of the incident light, so the high input power of the laser vary this index and it will spread the pulses as a result the overlap will be acquired. The pulse spreading make the signal in receiver side difficult to be recognized. In order to avoid the SPM to be occurred, low level of the input power should be considered.[46]

2.2.2 Cross Phase Modulation (XPM)

Cross-phase modulation (XPM) is a nonlinear optical effect where one wavelength of light can affect the phase of another wavelength of light through the optical Kerr effect. When the optical power from a wavelength impacts the refractive index, the impact of the new refractive index on another wavelength is known as XPM. The XPM is similar to the SPM but the origin of the spectral broadening of the pulses are other pulses propagating at the same time in the optical fiber; they will mutually influence each other [47]. This is especially important for WDM systems where a huge number of pulses with different carrier wavelengths will be transmitted in one fiber.

2.2.3 Four Wave Mixing (FWM)

As illustrated by nonlinearity interaction formula (Equation 2.3), the 3-rd order parameter $\chi 3$ can generate the FWM phenomenon. When a two different wavelength of a laser beam are incident to the optical fiber, the refractive index changes depending on the power and the frequency of the incident signals then the index modulation will be happened. Two additional wavelengths will be created from the two different frequency of the input signals [1]. If the laser which lunched to the fiber have f_1 and f_2 frequency, the output signals will be with four different frequency f_1, f_2, f_3, and f_4.

These two new frequencies can be calculated by the formula: $f_3=f_1-(f_2-f_1)$ and $f_4=f_2+(f_2-f_1)$.

2.2.4 Stimulated Raman Scattering (SRS)

Unlike the previous phenomena in which the intensity of the incident signal changes the refractive index, part of the energy of the input signal will be transferred to a new photon that generates a new signal which called Raman Stokes. This process is called SRS in which an optical phonon will be produced by molecular vibrations. Once the pump power exceeds the certain value in optical fiber, the Raman Stokes signal will be initiated a scattered in both directions, forward and backward direction, according to the input signal. Depending on the amount of the transferred energy, the SRS will be produced with different large frequency shift, related to the power and frequency of the pump signal, within a wide band width with a number of the THz shifting. This wide band operating range makes the SRS phenomenon useful in many applications such as Raman amplifiers and multiwavelength source generation [48].

2.2.5 Stimulated Brillouin Scattering (SBS)

SBS is the nonlinear phenomenon in optical fiber that occurs once the incident optical power exceeds the threshold level. Scattering backward Stokes signal with down shifting frequency of about 10 GHz corresponding to the input signal was generated as depicted in Figure 2.3. Compared this shifting with SRS in which the shift is around 13 THz, 10 GHz is more suitable in multiwavelength sources since the spacing between the channels in WDM system is a few GHz. Ippen and Stolen presented that when the input power increase, some of the power is reflected in opposite direction of the lunched signal this is called SBS [49].One of the differences between the SRS and SBS is a high pump power is needed to generate the SRS while, depending on the characteristic of the optical fiber, a few milli-watts is required to produce the SBS.[50, 51].The interaction between “photon-phonon” is occurred in SBS phenomenon. The created phonon is the vibrational modes of atoms, also called a propagation density wave. The interaction between more than two signals inside the optical fiber is considered as physical process of the SBS [52, 53].

When a laser beam is injected to the fiber laser as a pump power, an acoustics signal will be produced by the electrostriction process since the intensity of the lunched field affects the refractive index of the optical optical fiber.

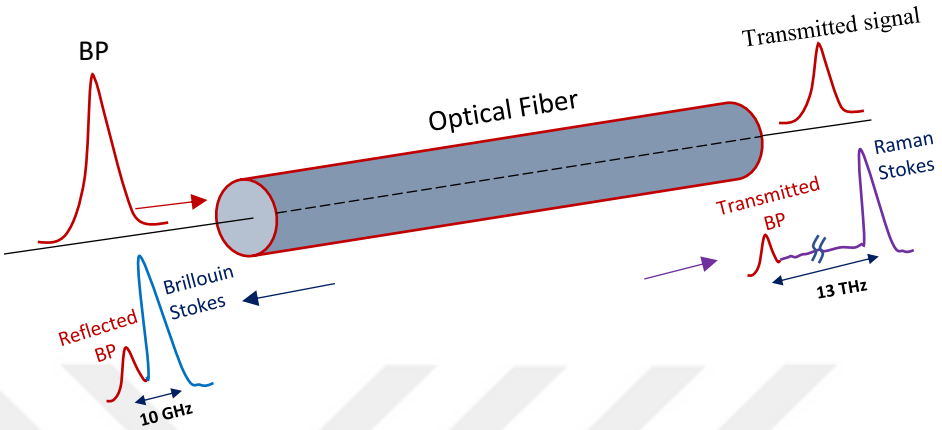


Figure 2.3 Stimulated Brillouin and Raman Scattering (SBS) (SRS) in optical fiber [52].

The value of laser source that initiate the Brillouin scattering is called as Brillouin pump (BP) whereas, according to the frequency shift, the reflected signal is defined as Stokes or anti-Stokes. The Stokes is generated when the frequency shift greater that the injected signal while if it is lower than the BP, the anti-Stokes is obtained.

The nonlinear relation between the BP and the generated Stokes signal can be described by the following coupled equations [54]:

$$\frac{dI_P}{dz} = -g_B I_P I_S - \alpha I_P \qquad (\mathbf{2.4})$$

$$\frac{dI_S}{dz} = -g_B I_P I_S + \alpha I_S \qquad (\mathbf{2.5})$$

where *Ip is* the intensity of Brillouin pump, *Is* represents Stokes power, g_B is the Brillouin gain coefficient, α is the attenuation constant of the optical fiber.

The generation of the successive Stokes continues until the amount of the Stokes signal power is not enough to produce a new Brilloiun Stokes. This continuous development

produces a multiple signal that have different frequency *fs* from its Brillouin pump frequency, f_{BP} and is given by equation (2.6)

$$f_s = \frac{2ncv_a}{f_{BP}} \tag{2.6}$$

Where *c* is the speed of light, *n* represent refractive index, and v_a is an acoustic velocity.

Tang, et al. in 1966 resolved the equation (2.4) and equation (2.5) by neglecting the attenuation constant of the fiber (α = 0) [54] as flowing:

$$I_P(z) = [I_P(0) - I_S(0)] \times \frac{I_P(0)exp\{g_B[I_P(0) - I_S(0)]\, z\}}{I_P(0)exp\{g_B[I_P(0) - I_S(0)]\, z\} - I_S(0)} \tag{2.7}$$

$$I_S(z) = [I_P(0) - I_S(0)] \times \frac{I_S(0)}{I_P(0)exp\{g_B[I_P(0) - I_S(0)]\, z\} - I_S(0)} \tag{2.8}$$

However, the attenuation factor is so important in optical fiber, therefore, Agrawal in 1995 proposed a solution that includes this coefficient. Agrawal's solution was depend on the Enns and Batr solution in 1969 in which the exact solving for SRS was considered [55]. Agrawal solution was criticized by Liang Chen and X. Bao in 1998 [56]. They showed that only the sign of $\frac{dI^R{}_S}{dz}$ is the different between the SBS and SRS equations. In addition, they replaced the negative sign according to the counter propagating of the Brilloiun Stokes signal corresponding the pump signal direction. Only the first term of the right-hand side of equation (2.5) in Agrawal solution, was replaced to negative sign.

Instead, Liang Chen and X. Bao presented an exact solution using transformation equations:

$$\int_{\Delta_0}^{\Delta(z)} \frac{d_x}{\sqrt{(\sum_0^2 - \Delta_0^2)\, exp\left\{\left(\frac{g_B}{\alpha}\right)[x - \Delta_0]\right\} + x^2}} \tag{2.9}$$

where $\sum_0^2$ and Δ_0 represents the correspondence values at the near end of the fiber at z = 0.

Equation (2.9) represent an integral form solution and no systematic form solving has been proposed. In this context, Ou, Zhonghua et al., presented an analytical solution for the coupled equations in which the attenuation factor was considered to describe the distribution of the Stokes and pump signals along the fiber length [57]. Based on the light propagation inside the optical fiber and according to the linear relationship, the pump and the Stokes signal distribution equations along the fiber can be derived as follows:

$$I_P(z) = \frac{[I_P(0) - I_S(0)]I_P(0)exp\{g_B[I_P(0) - I_S(0)]\ (1 - e^{\alpha z})/\alpha\}e^{-\alpha z}}{I_P(0)exp\{g_B[I_P(0) - I_S(0)]\ (1 - e^{\alpha z})/\alpha\}e^{-\alpha z} - I_S(0)} \quad (\mathbf{2.10})$$

$$I_{PS}(z) = \frac{[I_P(0) - I_S(0)]I_S(0)e^{-\alpha z}}{I_P(0)exp\{g_B[I_P(0) - I_S(0)]\ (1 - e^{\alpha z})/\alpha\}e^{-\alpha z} - I_S(0)} \quad (\mathbf{2.11})$$

Recently, T. F. AL-MASHHADANI et al., derived the dependence of the generated Stokes signal on the input power, in a BFL linear cavity which shown in Figure 2.4.

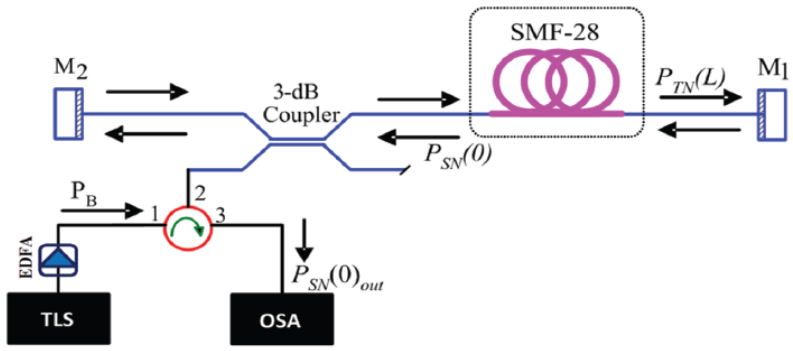


Figure 2.4 Schematic setup of linear cavity MBFL reported by [58].

as well as on the successive transmitted power, the cascade-stimulated Brillouin Stokes model can was written as [58]:

$$P_{S1}(0) = P_B\alpha_{12}/2 + P_{T2}(L)exp(-\alpha L)R_1 + P_{T1}(L)exp(-\alpha L)R_1R_2/4 - P_0 \quad (\mathbf{2.12})$$

$$P_{S2}(0) = [P_B\alpha_{12}/2 + P_{T2}(L)exp(-\alpha L)R_1 - P_0]\,R_2/4 + P_{T3}(L)exp(-\alpha L)R_1 - P_0 \quad (\mathbf{2.13})$$

where R1 and R2 denote the reflectivity of optical mirrors M1 and M2, respectively, P_0 is the SBS threshold for the SMF, α_{12} is the loss factor through the circulator between ports 1 and 2, N is an integer value (N = 1, 2, 3, ….), P represents the successive pump power.

$$P_{SN}(0) = \left[\begin{array}{c} \frac{1}{2 \times 4^{N-1}} P_B \alpha_{12} + \sum_{n=1}^{N} \frac{1}{4^{N-n} R_2^{n-1}} P_T(n+1)\, exp(-\alpha L) R_1 \\ - \sum_{n=1}^{N} \frac{1}{4^{N-n} R_2^{n-1}} P_0 \end{array} \right] R_2^{N-1} \qquad (\mathbf{2.14})$$

$$P_{SN}(0)_{out} = \left(\left[\begin{array}{c} \frac{1}{2 \times 4^{N-1}} P_B \alpha_{12} + \sum_{n=1}^{N} \frac{1}{4^{N-n} R_2^{n-1}} P_T(n+1)\,.\, exp(-\alpha L) R_1 \\ - \sum_{n=1}^{N} \frac{1}{4^{N-n} R_2^{n-1}} P_0 \end{array} \right] R_2^{N-1} \right)^{\alpha_{23}/2} \qquad (\mathbf{2.15})$$

where $P_{SN}(0)_{out}$ is the output of the Nth-order Stokes signals

2.3 Brillouin Stokes Threshold in Single Mode Fiber

The Brillouin threshold was defined as the inserted optical signal power to the Brillouin gain medium at the first order Brillouin Stokes signal generated at the near end of the optical fiber as shown in Figure 2.5. The transmitted optical signal at the far end of the fiber was saturated due to the appearance of the Brillouin Stokes signal [58]. In the conventional transmission span of optical communication system in which there is no feedback was presented by [59]. This model was built on integrating equation (2.5) over the fiber length as follow:

$$\frac{g_B P_{cr} L_{eff}}{A_{eff}} = 21 \qquad (\mathbf{2.16})$$

where L_{eff} and A_{eff} represent the effective fiber length and the effective core area respectively.

Under the typical condition in C-band optical communication system at 1.55-μm, g_B = 5×10^{-11} m/W, L_{eff} = 20 km, and A_{eff} = 50 μm, an SBS threshold of 1 mW was recorded. Due to the low Brillouin Stokes signal threshold power, such Stokes signal was considered as a limitation parameter in optical communication system since the transmitted optical power will be saturated [60].

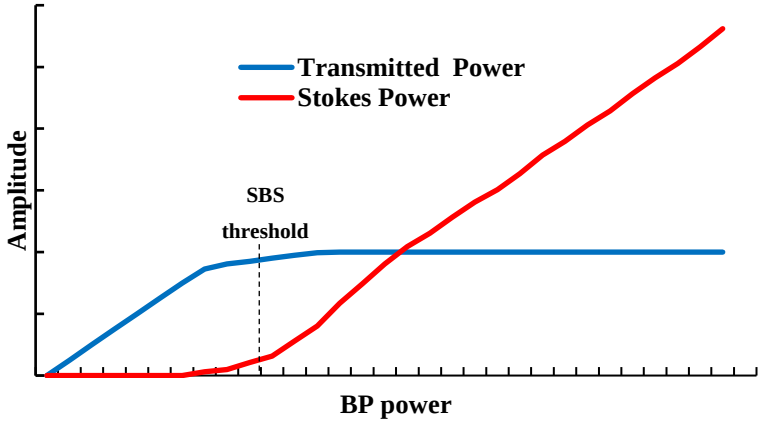


Figure 2.5 variation of the transmitted and Stokes power in SMF [59].

Referring to equation (2.16), the Brillouin Stokes threshold can be effectively increased to delay the transmitted power saturation. In this context, using light source polarization in the instated optical signal power was beneficially increased the Stokes threshold by 50 % [61]. Since the Brillouin gain is affected by the inhomogeneities of the fiber and by varying the doping level within the z-direction, thus, the SBS threshold power can depend on the variations of silica dopant along the fiber length [62]. The Brillouin shift (ΩB) can also reduce the Brillouin gain that can led to increase the SBS threshold power [63]. Changing the core radius was another method presented by [64] to increase the SBS threshold power to 30 mW. Related to polarization factor (K), [65] was reported an SBS threshold evaluation in SMF as follow:

$$P_{SBS} = 21\frac{KA_{eff}}{g_B L_{eff}}\frac{\Delta v_B + \Delta v_L}{\Delta v_B} \qquad (\mathbf{2.17})$$

where $\Delta\nu_B$ is the Brillouin gain bandwidth and $\Delta\nu_L$ is the laser linewidth.

Thus, the influence of the SBS signal can be effectively suppressed by adopting Δ_{vL} to delay the optical transmission saturation [66, 67]. In addition, both of [68]and [69] were presented the impact of g_B on the Stokes signal threshold. An evaluation experimental work method that study the effect of the SBS signal on the transmitted power limitation was reported by [70].

Moreover, optical communication system in the presence of optical feedback was presented by many works [16, 22, 71–73]. They found that by recycling the optical signal at the far end of the fiber, the SBS threshold power was reduced. By implementing an excellent reflectivity at the far fiber end utilizing an optical mirror, a reduction of 50 % was achieved in the SBS threshold power [22]. The analytical model for such SBS threshold reduction of 50 % was reported by [71] by solving the steady state coupled equation in both of forward and backward direction and by ignoring the pump depletion. In this model both of forward and backward Brillouin gain was included. Finally, the SBS analytical expression was derived as follow:

$$P_{th} = C\frac{A_{eff}}{g_B L_{eff}} \tag{2.18}$$

where

$$C = \frac{P_{sb} + R_1(1-\alpha L)P_{sf}(0)}{\frac{\alpha A_{eff}}{\alpha_{cb} g_B} + \alpha R^2 L_{eff} P_{sf}(0)} \tag{2.19}$$

$$L_{eff1} = \frac{e^{-\alpha\alpha_{cf}L}}{\alpha} \qquad and \;\; L_{eff} = \frac{1-e^{-\alpha L}}{\alpha}$$

2.4 Review of Multiwavelength Brillouin Stokes frequency shift Laser comb.

In this section a review of different Brillouin Stokes frequency shift of single space (0.08nm), double space (0.16 nm), triple space (0.25 nm) and quadruple frequency space (0.33 nm) will be discussed. In addition, the advantages, and the limitations, related to the number of generated Stokes, output comb tunability and optical signal to noise ratio, of each frequency shift will be presented.

2.4.1 Previous Works of Single Channel Spacing (0.08 nm, 10 GHz)

The first generation of the proposed BEFL was the Single space shift of Brillouin Stokes signal in MBEFL. Many studies have been considered for such kind of channel spacing. The first structure design of the single Brillouin shift frequency was demonstrated by [74]. Two gain media, nonlinear Brillouin gain in single-mode optical fiber and linear gain in erbium-doped fiber, were used. A laser comb with 10-GHz line spacing has been demonstrated through internal and external cascade schemes. Up to 6 Brillouin Stokes signals were tuned over low tuning range of 2 nm. Multiwavelength twin-cavity Brillouin erbium fiber laser (TBEFL) was implemented by [75]. The TBEFL configuration consists of two identical erbium-doped fiber ring lasers (EDFL) that share a single mode fiber SMF to produce interdependent bi-directional Stokes signals. This cavity produced 24 channels at 1560 nm. A new design of multi-wavelength Brillouin Erbium fibre laser in a linear cavity was proposed to generate 18 Brillouin Stokes in C-band region [76]. The design used only a 980 nm pump laser and a coil of Erbium doped fibre for its multiple wavelength's operation. The proposed laser system exhibited low threshold 980 nm pump power of 5.5 mW only. In the same year, Y. J. Song et al., presented a tunable multi-wavelength comb in BEFL using the Sagnac loop filter [77]. Using the Sagnac loop filter with 18-cm PMF, the generation of 12 Brillouin wavelengths with 14.5-nm tuning range was obtained. The experiment also demonstrated that the tunable range is closely equal to the 3-dB bandwidth of Sagnac loop filter due to its periodic transmission profile. In addition, Mohamad K. Abdullah et al. presented a MBEFL to generate a stable single channel spacing of 0.08 nm utilizing a ring cavity [78]. The EDFA section was used with 980 nm pump power to amplify the Stokes signals. The generated Brillouin Stokes was tuned over 36.7 nm band from 1529.8 to 1566.5nm at Bp of 8 mW. The effect of the BP power and wavelength on the tunability and Stokes power was studied in this work.

In order to expand the tuning range in MBEFL, M. H. Al-Mansoori et al., presented double-pass pre-amplifier technique [9]. This was achieved by injecting high Brillouin pump powers to saturate the Erbium gain in the laser cavity. A tuning range of 60 nm has been achieved from 1525 to 1585 nm. A direct injection Brillouin pump in linear cavity of hybrid Brillouin/Erbium fibre laser (BEFL) was proposed by [79]. The

optimal condition for the new configuration of BEFL in a linear cavity was found when the BP power was 0.44 dBm at 1557.5 nm and the 980nm pump power was 100mW. Twenty-two Stokes lines of the linear cavity BEFL were obtained in this condition. Two EDFA section were utilized in different loop to enhance the performance of the S-band BEFL setup and up to 8 Brillouin Stokes signals was achieved [80]. The number of the output channels was enhanced related to the Stokes flatness and maximum line power compared with the conventional structure. The incorporation of additional EDFA also increases the tuning range of the BEFL, which the maximum tuning range of 1.8nm was obtained with the single-pass scheme. The S-band BEFL has constant spacing of 0.09 nm or 11 GHz, which has a potential application in dense wavelength division multiplexed system. Fabry–Perot resonator was utilized to produce up to 43 Brillouin Stokes signals that can be tuned within 10.56 nm from 1547.40 to 1557.96 nm [81].

The higher number of output channels was attributed to the carefully optimized laser cavity parameters and due to the double-pass amplification in the Erbium and Brillouin gain medium in the linear cavity itself. In order to enhance the performance of the BEFL configuration, the impact of the output coupling ratio is demonstrated by [82]. Different coupling ratio of 40 % to 60% was chosen to find its effect on the numbers of the generated Stokes signals, the band in which the cavity work without self lasing modes, and the power of the output signals. Up to 40 stable Brillouin Stokes signals with 10 GHz frequency shifting were achieved at BP of 2.5 mW and 980 nm pump power of 100 mW. This proposed linear BEFL structure can be used in an inexpensive WDM system.

Y. Huang at el. demonstrated a widely tunable MBEFL structure utilizing self-excited pumping technique [83]. By adjusting the polarization controllers which conducted inside the Sagnac loop mirror, higher numbers of generated Stokes were obtained. This highest output channels were achieved using two of 980 nm pump power in bidirectional. The generated Stokes signal can be tuned over a wide band of 45-nm from 1546.5 nm to 1591.4 nm, which represent the gain band of the EDFA sections, at a fixed 980 nm pump power of 160 mW. In order to optimize the numbers of the output channels, the impact of the pump power was experimentally studied.

The impact of the EDFA location inside a ring laser cavity structure was investigated by [84]. The first EDFA was located before the DCF, the second located in which the EDFA was after the DCF, and the output was measured before the EDFA at the last position. The result of this study shows the generated Stokes power and tuning range are mainly dependent on the position of the amplifier section, EDFA, inside the cavity. In the first location, the injected BP power is amplified firstly then it was lunched to the DCF in order to generate higher power of the line Stokes. This technique was able to enhance the tuning range by eliminating the self lasing modes which was produced from the EDFA. Only one-output channels with maximum power of 25.1 mW were achieved by this configuration at 1480 nm pump power of 135 mW, while a lower Stokes power of 1.4 mW from second location and 15.5 mW from last position was recorded. the pre-amplification technique shows a wide tuning range of 50 nm (1525 nm to 1575 nm), while only 28 nm and 3 nm were achieved from BEFL-2 and BEFL-3 respectively.

A high nonlinearity optical fiber (HNLF) was used to initiate a four wave mixing phenomenon inside the MBEFL ring cavity [85]. Fiber length of 135 m was utilized to produce higher numbers of Stokes and anti-Stokes signals. Up to 150 Brillouin Stokes with very narrow wavelength width of 0.075 nm was achieved. A 1480 nm pump power of 165 mW used to pump the Erbium section and high BP of 12 dBm was used to produce this output channels in this experiment. A good method to increase the number of the generated Stokes was experimentally presented in this work. The laser comb was tuned over 6 nm band from 1562 nm to 1568 nm with a good stability of the amplitude of the Stokes signal. M. H. Al-Mansoori et al. 2008, demonstrated experimentally a multiple wavelength L-band Brillouin-erbium fiber laser [86]. A pre-amplified Brillouin pump power technique was used to achieve a low threshold power. High number of output channels of 33 at low 1480 nm pumping powers of 50 mW was observed. The number of the generated Stokes and the tuning range were enhanced using pre-amplification technique in which the BP firstly amplified then lunched to the gain medium. Internally pre-amplification of BP and Brillouin Stokes signals in EDFA section and bidirectional generation of Brillouin Stokes channels in SMF increase the efficiency of generating multiple Brillouin Stokes lines.

The same technique, pre-amplification method, within a BEFL linear structure was presented by [12]. Generally, in order to enhance the tuning range, high BP is required. Using such pre-amplification technique in proposed cavity avoids the requirement for high external BP power. The tuning range was improved by 4.5 nm for the proposed technique compared with BP direct-injection structure with the same experimental parameters. Up to 17-19 Brillouin Stokes signals can be tuned during 9 nm of L-band wavelength from 1600 nm to 1609 nm

To improve the multiple Brillouin Stokes signals generation, a reverse-S-shaped fiber section used as a coupling mechanism was used by [87] . The enhancement can be made by locating a common section of EDF next to the Brillouin gain medium (SMF) to amplify the BP and the oscillating Stokes lines. A tuning range of 14.8 nm is achieved since the mode competitions arise from the self-lasing cavity modes of the fiber laser are efficiently suppressed by the stronger pre-amplified Brillouin pump power before entering the single mode fiber section. The maximum output power of 20 mW is obtained from the proposed fiber laser with 10 laser lines. Up to 27 single space Brillouin Stokes was achieved utilizing nonlinear amplifying loop mirror [88]. The EDF section in the fiber loop mirror provided efficient amplification of Brillouin pump (BP) to generate the stimulated Brillouin scattering in the single mode fiber coil. The laser structure achieved symmetry breaking of the loop without requirements to an asymmetric coupler or polarization controller. The first Stokes was recorded at low threshold of 10 mW. The output channels can be tuned over 11 nm in L-band from 1600 to 1611 nm. Broadly tuning range of 14 nm was presented by M.H. Al-Mansoori et al [89]. The double-pass pre-amplifier technique in the linear cavity was used to generate up to 30 Stokes signals at 40 mW of pump power and 0.035 mW of Bp. Low threshold power of 15.9 mW was observed for the first Stokes signal. The double- pass preamplification of BP shifted the unstable operation of the laser to a higher pump power, therefor high- power laser signals was achieved.

M. N. Mohd Nasir et al., proposed a widely tunable low stimulated Brillouin scattering MBEFL [29]. A photonic crystal fiber of 100 m and a tunable band-pass filter within the pre-amplified BP configuration was used in order to obtain 14 output channels. The Brillouin Stokes lines can be tuned over 29 nm from 1540 nm to 1569 nm. this

wide tunability was only limited by the bandwidth of the tunable band-pass filter. The signal to noise ratio of more than 20 dB for each channel were also recorded from the proposed design.

A MBEFL linear cavity structure was experimentally demonstrated by [90]. The laser's output coupler can be initiated by using A power-symmetric nonlinear optical loop mirror (NOLM). The gain induced increase in transmission (IIT) that leads to higher cavity loss for oscillating wavelengths with higher power. The IIT feature of the NOLM eliminates the free running modes which produced from the EDFA section and ensures stable multiwavelength operation at room temperature. Up to 16-output channels within 3 dB bandwidth have been achieved. The generated Stokes showed a good stability fluctuation within 0.7 dB over 1 h. Both the wavelength number and the output power of the output comb can be controlled by adjusting the NOLM via a quarter wave plate and/or a polarization controller.

The reverse-S-shaped fiber section was used to produce a widely tunable multiwavelength Brillouin Stokes [91]. The enhancement is done by locating the amplifier and the Brillouin pump into the reverse-S-shaped fiber section. The free running modes in the cavity are directly influenced solely by the Brillouin gain. By adjusting the cavity loss, an average of 11 laser lines can be tuned over 45 nm wavelengths (1520-1565 nm) at 40% optimum output coupling ratio.

An L- band multiple- wavelength in a linear cavity resonator was reported by [92]. The cavity ends relate to high- reflectivity optical mirror on one side and an amplified fiber loop mirror on the other. Up to 55 stable output channels was observed at low Brillouin and laser pump powers of -8.54 dBm and 33 mW, respectively. The laser structure permitted preamplification of the BP signal in the laser cavity before being transmitted into the Brillouin gain medium A.W. Al-alimi et al. developed an efficient multiwavelength Brillouin–Erbium fiber laser (BEFL) [93]. The development was done by improving the feedback mechanism of Brillouin Stokes lines. A double pass amplification technique was utilized to improve the BEFL performance in terms of threshold power and wavelengths count. A variable optical coupler (VOA) was used to form a fiber loop mirror that reduces the number of optical components, thus, only

three optical components were needed. At the conditions, up to 41 and 26 Brillouin Stokes were recorded utilizing 0.6 km and 0.3 length of standard SMF respectively.

The Four Wave Mixing phenomena was utilized by [94] to generate higher numbers of the Brillouin Stokes signal. Based on inducing FWM and cascading SBS in HNLF, more than 150 Stokes lines with wavelength spacing of the 0.078 nm was achieved at Brillouin pump power of 3 dBm and EDF pump power of 100 mW. Rayleigh back scattering was suppressed, and the generated laser comb wavelengths were in the absence of self lasing cavity modes over a wide tuning range. This was due to an optimizing BP and 1480 nm pump powers. Wide tuning range of 40 nm were achieved. however, only 8 Stokes lines with Stokes power variations from 2.6 dBm to -18 dBm were generated due to the SBS effect inside the fiber in the absence four wave mixing. The multiwavelength Brillouin-erbium fiber laser was enhanced by using virtual mirror concept [95]. Three linear amplifier structures were investigated and optimized in terms of schemes performance. Eight stable channels are produced which can be tuned across a span of 39 nm (from 1524 to 1562 nm) at 915 nm pump laser of 616 mW pump power without any self-lasing cavity modes. This output number is double the previous achievement with the same range of tunability. The wide tuning range is contributed by the weak reflectivity of Rayleigh scattering effect.

T. F. Al-Mashhadani et al., presented the influence of the residual BP pump power on the Brillouin Stokes signal threshold inside the BFL linear cavity [23]. The resonator reflectors were done by using two high reflective optical mirrors which allow bidirectional residual BP pump power that causes bidirectional Brillouin gains. The SBS threshold reduced as the Brillouin Stokes power goes up due to this circulation. Under the same parameters such as SMF length the SBS threshold reduced by the ratio of 50 % compared with recycling Brillouin threshold reduction techniques and up to 75 % according to conventional structure. In addition, the effect of Brillouin gains on the Brillouin Stokes power was investigated and shows no additional gain in the laser cavity as compared with the recycling technique, especially for long SMF greater than 8 km. A two-matching ring-loops of EDF lasers combined through using of a 25-km-long SMF to implement a self-seeded MBEFL dual-cavity system [96]. The self-seeded signal was generated by the oscillating waves from EDFs which cause

spontaneous scattering and backscattered Stokes wave in the fiber. Up to 67 Brillouin Stokes signals with ultra-narrow width of 0.088 nm were achieved at 1480 nm pump power of 100 mW. The stable laser comb can be tuned over 5.64 nm wavelength band from 1528.19 to 1533.83 nm with high OSNR of 13.2 dB

A four-wave mixing phenomenon was utilized by [97] in order to enhance the numbers of the generated Stokes signal in MBEFL cavity. A Brillouin mirror with feedback and a ring configuration was used to implement the proposed setup. A flat laser comb and widely tuning range was investigated experimentally. The efficiency of output channels generation was improved by the feedback-based Brillouin mirror structure. Up to 200 output Stokes can be tuned over 16 nm band from 1534 to 1550 nm with wavelength channel spacing of 0.08 nm. The difference between the Stokes of 4.65 dB and optical signal-to-noise ratio of 15 dB were recorded. The laser can also be tuned over 32 nm and is stable with power fluctuations of 0.7 dB over 1-hour duration.

W. AL-Alimi et al. demonstrated a wide MBEFL with improved flatness by using a micro-air cavity [98]. This air-gap presents a cavity loss to eliminate the gain saturation as well as providing efficient pump recycling scheme through Fresnel back-reflection. The FWM in the highly nonlinear fiber presents a contribution to the self-flattening of the output spectra. During operation, the optimized pumping values are set at 13 dBm Brillouin power and 600 mW erbium-ytterbium doped fiber amplifier when the air-gap length is fixed at 10 μm. Up to 180 Brillouin Stokes signals with frequency shift of 10 GHz were obtained. The flat output comb bandwidth was 14 nm from 1557 to 1571 nm wavelengths within 3-dB range. The average OSNR was 18 dB with high maximum power of −8 dBm. In addition, the laser comb exhibits a good stability of 0.76 dB order during 45-minute durations makes it suitable in optical fiber sensing and communications.

An enhanced multiwavelength Brillouin-Erbium fiber laser by utilizing double linear cavity based on a double-pass pre-amplification technique was demonstrated by [99]. This simple structure was composed of two 24 km and 24.2 km single mode fiber (SMF) coils and two segments 13-m Erbium doped fibers (EDF). In order to obtain the Brillouin gain under low external injection Brillouin pump power, the BP is amplified in the linear cavity before entering the SMF. In this experiment, so as to

obtain the most Stokes lines, the optimization of 980 nm pump power and tunable laser source (TLS) power together with its corresponding wavelengths is very important. When setting the TLS power as 7.4 dBm and 980 nm pump power as 300 mW, a total of 51 Brillouin Stokes lines with frequency spacing of 0.089 nm are produced. Many techniques have been implemented to accomplish broad tuning range. High Brillouin pump (Bp) power was utilized in [9], in this work, tunable tuning range of 60 nm was achieved in the expense of number of generated Stokes signals. Thus only 2 Stokes signals was produced. An optical filter like Sagnac loop mirrors [77] and bandpass filter [29] were used for the same purpose. However, using such optical filters can be resulted into two setbacks in terms of complexity and cost issues. Avoiding using such optical filters [12,89] presented an acceptable tuning range using single and double pass pre-amplification for the inserted Bp power. Tuning range of 10 nm with 20 Stokes channels were produced in [12] while up to 14 nm tuning range with 17 Stokes signals were produced by [89].

Four ring cavity structures have been implemented by [100]–[103]. In [100] the end face of the Brillouin gain medium, 11 km of dispersion compensation fiber (DCF), was isolated as depicted in Figure 2.6a. Up to 39 nm tuning range from 1527 nm to 1566 nm with only 4 output Stokes signals ,as illustrate in Figure 2.7a and Figure 2.8a respectively, were achieved. For Brillouin pump wavelength of 1550 nm and 1480 nm laser pump and Brillouin pump powers of 130 mW and 2 mW respectively, all the generated output channels have peak power above 0 dBm, with the first output channel having a peak power of 8.52 dBm.

On the other hand, the effect of the EDFA directivity on the laser cavity performance was illustrated by [101] as shown in Figure 2.6b. with bidirectional configuration a tuning range of 23 nm and 13 Stokes channels were presented while with unidirectional structure, the tuning range and the number of Stokes were 46.8 nm, 6 as illustrated in Figure 2.8b and Figure 2.7b respectively. MBEFL configuration depicted in Figure 2.6c, in which the self lasing cavity modes was totally suppressed by virtual mirror, was presented by [102]. Up to 7 Stokes signals as shown in Figure 2.7c and tuning range of 35 nm from 1530 nm to 1565 nm as illustrated in Figure 2.8c were observed at a Brillouin pump power of 2 mW and 130 mW of 1480 nm pump power.

The first four channels have an output power each above 1.6 dBm with the first and the seventh channels having a peak power of 8.19 dBm and −8.30 dBm.

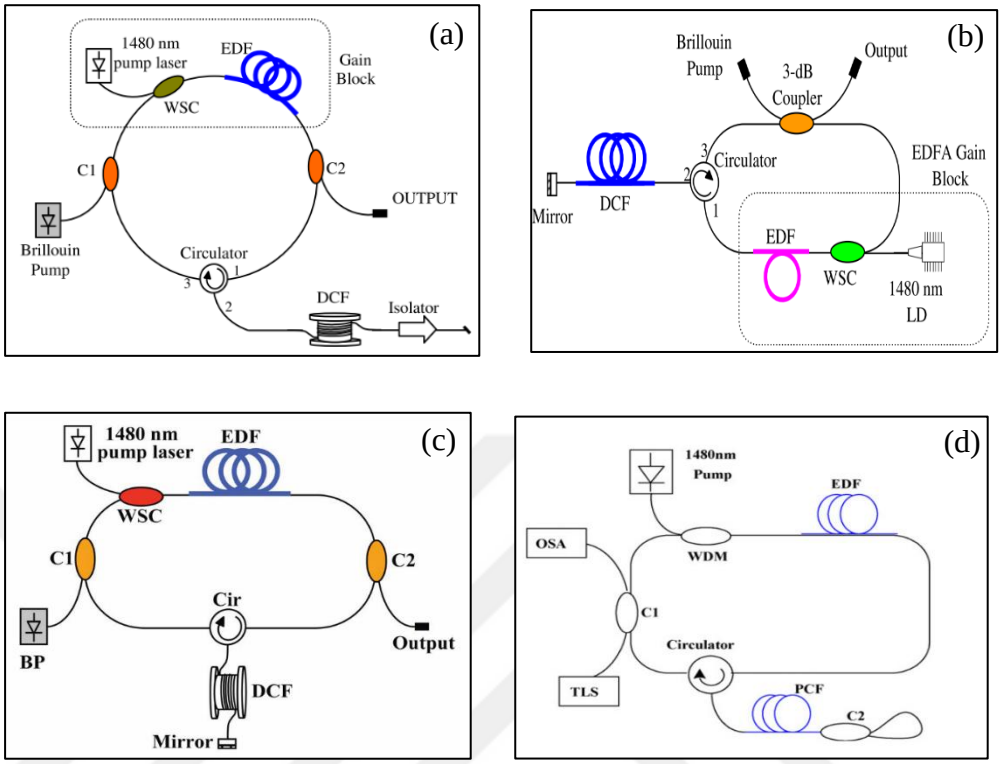


Figure 2.6 Experimental setup which reported by (a) [100] (b) [101] (c) [102] (d) [103]

The stimulated Brillouin scattering (SBS) threshold was reduced utilizing 70 m of high nonlinear photonic crystal fiber (PCF) [103]. The fiber laser shown in Figure 2.6d utilized recycling mechanism to enhance stimulated Brillouin scattering (SBS). The configuration that consists of only 3 optical components is easy to be integrated and improves the practicality. Due to the threshold reduction, higher Stokes number of 10 with more than 10 dB optical signal to noise ratio (OSNR) as depicted in Figure 2.7d were presented but the tuning range was limited to 10 nm only as shown in Figure 2.8d.

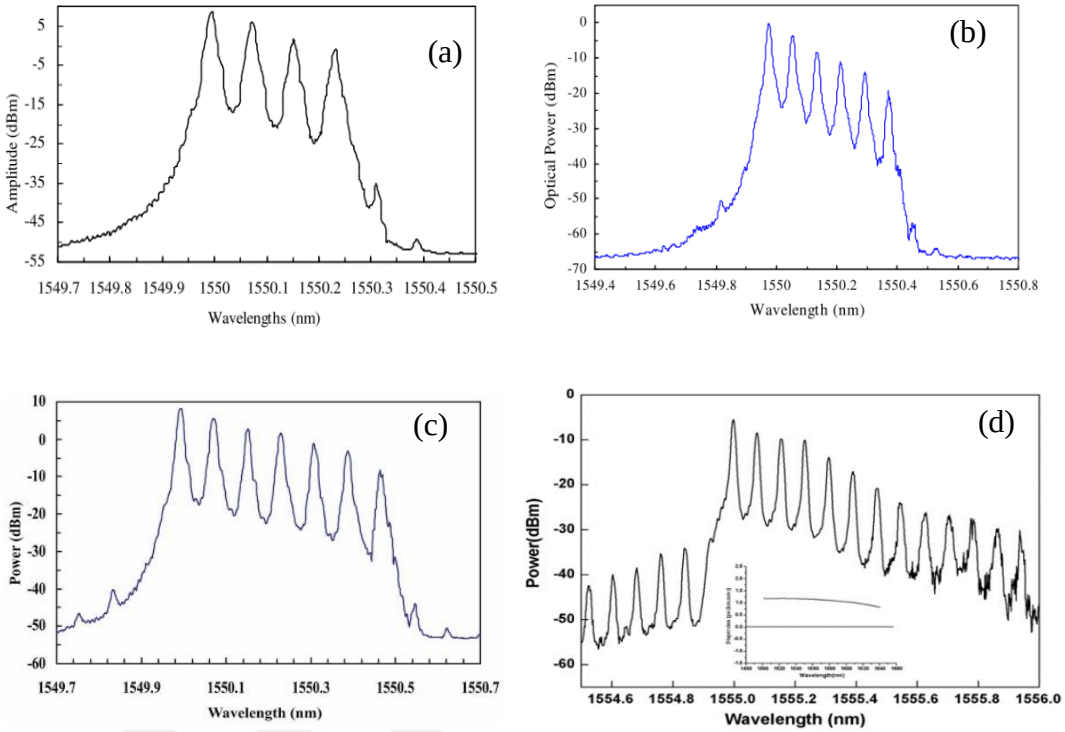


Figure 2.7 Output spectrum of the structures which presented by (a) [100] (b) [101] (c) [102] (d) [103]

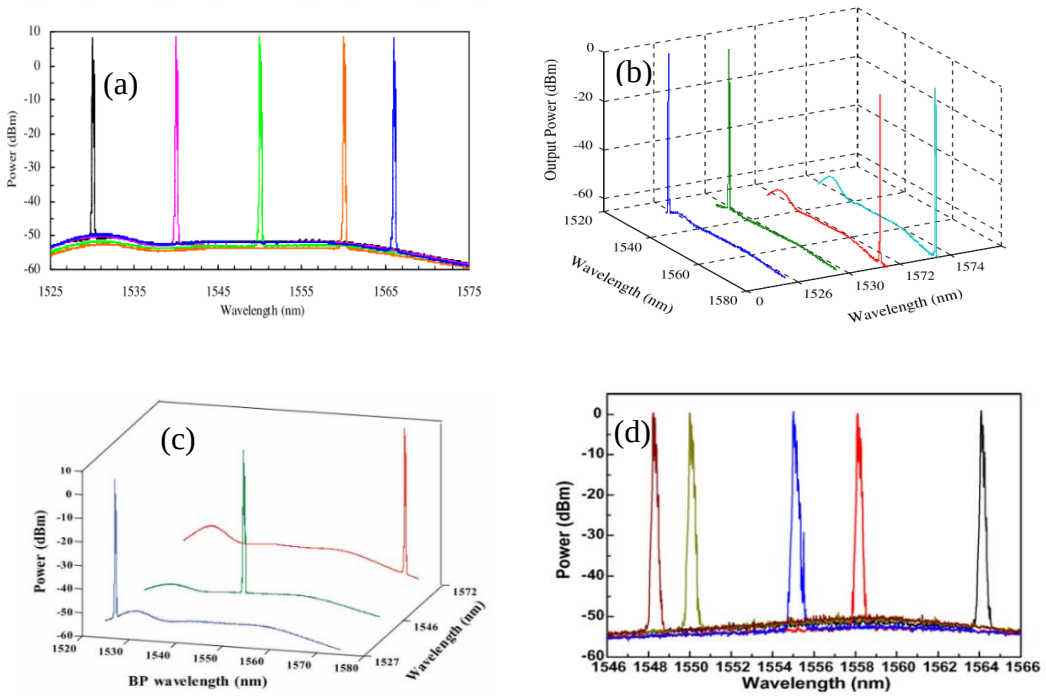


Figure 2.8 The output spectra at different BP wavelengths of the cavities which proposed by (a) [100] (b) [101] (c) [102] (d) [103]

Passive Erbium doped fiber (PEDF) was implemented to enlarge the number of the generated Stokes signals [104]. In this work the number of the generated Stokes was enhanced by 33% compared to the same setup without including such PEDF. However, this study did not show the effect of such PEDF on the other cavity parameters like cavity tunability.

The study that show the impact of inclusion PEDF on the tuning range was presented by [105]. The influence on the performance of MBEFL in term of number of generated Stokes lines, tuning range and lasing threshold were investigated. It shows that increasing the pump power can be reduced the cavity tunability even the number of the Stokes was increased. At fixed BP power and 100mW of 1480 pump power, longer passive EDF length of 5m exhibits the highest average number of Stokes lines of 23 with tuning range of 14 nm. In contrast, shorter passive EDF length of 1m shows the highest tuning range of 17nm and an average number of 21 Stokes lines.

Bo Dong et al., in 2010, proposed a new linear cavity BEFL configuration by inserting both a passive EDF gain section and an VOA inside the cavity. Using such proposed configuration can help in further expand the tunable multiwavelength range of the BEFL and effectively suppress the cavity modes competition. A tunable cavity modes oscillation range of 19.4 nm and a tunable multiwavelength range of 23 nm was obtained [14]. However, although the proposed configuration is success in tunability increasing by using VOA inside the cavity but due to the presence of such attenuator, the generated Stokes number was limited only to 11 Stokes signals and at the same time very low Stokes power. A tunable L-band MBEFL that uses PEDF as an absorber section was presented by [106]. In this work, a comparison between with and without PEDF was illustrated. Inclusion PEDF enhanced the cavity tunability by 31% and up to 16 Stokes signals were tuned over 24.4 nm. However, the number of the generated Stokes signals were a bit decreased via PEDF due to the small Brillouin gain absorption within it. The Summary of tunability enhancement technique in a single Brilloiun frequency shift MBEFL is tableted in table 2.1.

Table 2.1 Summary of tunability enhancement technique in a single Brilloiun frequency shift MBEFL

Ref. No.	Tuning range (nm)	No. of Stokes	Tunability Enhancement Technique
[9]	60	2	• High BP power
[14]	23	11	• Using 5 m passive EDF gain section and an VOA
[29]	29	14	• Tunable band-pass filter • Pre-amplified BP configuration
[89]	14	30	• Double-pass pre-amplifier technique
[91]	45	11	• The reverse-S-shaped fiber section
[95]	39	8	• virtual mirror concept
[100]	39	4	• End face of DCF was isolated
[101]	46.8	6	• Recycling technique (by mirror)
[102]	35	7	• virtual mirror
[103]	10	10	• utilizing 70 m PCF
[105]	14	23	• Using PEDF (Booster section)
[106]	24.4	16	• using 1 m PEDF (absorber section)

2.4.2 Previous Works of Double Channel Spacing (0.16 nm, 20 GHz)

The de-multiplexing problem that could be caused in the receiver side of the optical communication system due to the very small channel spacing of 0.08 nm in single space multiwavelength fiber laser. Wider channel spacing is required to overcome such problem. Therefore, many researchers were concerned on achieving double channel spacing of 0.16 nm. In this section a review of double-spacing Brillouin frequency shift is presented.

A novel operation scheme of a Brillouin/erbium fiber laser (BEFL) whose cavity consists of two metal-coated fiber planar mirrors (FPMs) and a Sagnac reflector was presented by [107]. Optical comb generation of both 10 and 20 GHz spacings was demonstrated by discrimination of the even order Stokes waves and the odd order

Stokes waves. Theoretical analysis based on the reflection properties of the Sagnac reflector yielded a good description of the multi-wavelength BEFL characteristics. Up to 3, and 4 was obtained for odd and even double-spacing Stokes signal respectively.

Multiwavelength fiber laser configuration based on SBS phenomenon in SMF as illustrated in Figure 2.9a was proposed by [108]. Both of Stokes and anti-Stokes signal with a wavelength spacing of 0.16 nm were achieved using high BP power of 23 mW as illustrated in Figure 2.9b. A 3-dB (50:50) coupler was used to achieve largest Stokes number with a maximum Stokes power of 8dBm. The bi-directional cavity structure can assist with the help of the four-wave mixing to generate the anti-Stokes signals in this configuration.

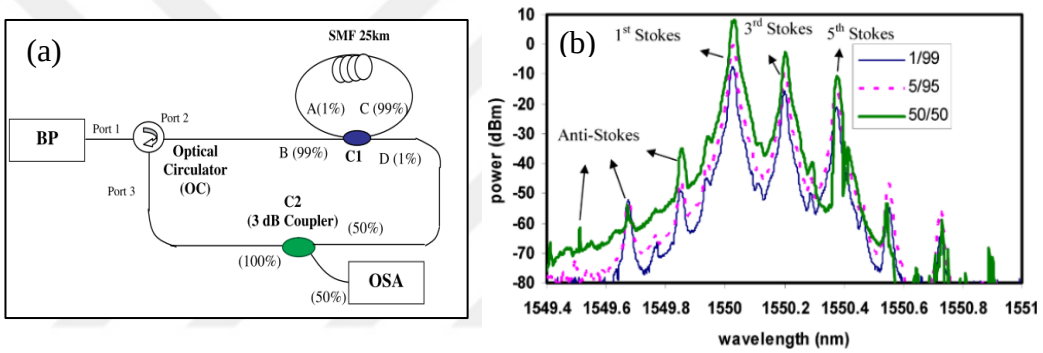


Figure 2.9 MBFL reported by [108] (a) Experimental setup (b) output spectrum

The proposed setup by [108] shows high tuning range related to the BP wavelength produced by the tunable laser source (TLS). In another word, no tunability limitation caused by an additional gain inside the cavity was observed. In addition, the Brillouin gain medium of SMF can be easily replaced with another optical fiber type with higher nonlinearity to achieve higher Brillouin gain and to make the system more compact. Bi-directional ring Brillouin fiber laser cavity in which both of Odd and Even-order Stokes signals were achieved in the forward and backward direction related to the BP signal direction was presented by [35]. Long SMF of 25 km was utilized in this setup to achieve up to 4 Brillouin Stokes signals in each output port. The channel spacing of the all generated Even, and Odd Stokes signals was 0.16 nm (20 GHz) that represent double Brillouin frequency shift of 0.08 nm (10 GHz). In addition, the authors claimed that the produced Even and Odd Stokes signals can be tuned over the range of the BP

wavelength tunability and by combined the double Brillouin frequency shift signals from these two outputs, single spacing Brillouin frequency shift of 0.08 nm can be obtained.

In the same context, SBS was demonstrated in SMF to achieve multiwavelength BFL [109]. A bi-directional ring cavity structure that consists of two optical couplers and one optical circulator was proposed. Since there was no additional Erbium gain was used in this configuration, the output laser comb can tune within the BP wavelengths band used. Up to 8 and 10 Stokes signals with double Brillouin frequency shift of 0.16 nm were produced at BP power of 14 dBm in the forward and backward direction respectively. Thanks to both couplers (99:1 and 50:50) that contributes highest Stokes power of 8 dBm and highest Stokes numbers. In addition, due to the bi-directional circulation and the four wave-mixing concepts, the anti-Stokes were also observed in the output laser comb.

The circulation of the Odd-order Stokes lines within the BFL cavity shown in Figure 2.10 was incorporated to achieve the Even-order Stokes signals which have double Brillouin frequency shift of 0.16 nm as proposed by [110]. The idea is by circulating the successive SBS into the Brillouin gain medium via four port optical circulator. In this setup, the generated Odd-order Stokes signals were forced to be circulated inside the cavity while the Even-order Stokes lines were permitted to be monitored as an output laser comb. Using 5km SMF and the amplified BP power of 14 dBm, two output Stokes channels with high optical signal to noise ratio of more than 30 dB were recorded as illustrated in Figure 2.11.



Figure 2.10 Experimental setup of MBFL reported by [110]

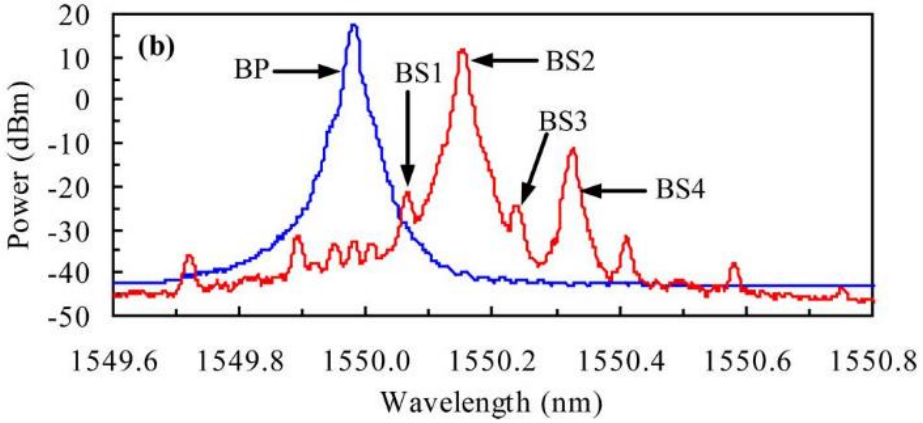


Figure 2.11 Output spectrum of MBFL reported by [110]

Same authors have proposed a MBEFL that generate 10 Stokes signals with Brillouin frequency shift of 0.174 nm [111]. This double Brillouin frequency shift was gathered by circulating of the Odd-order Stokes lines via four-port circulator. Through the circulation of the Odd-order Stokes lines, the Even Stokes signals were generated. Then the new Even Stokes signals will experience a gain in the EDFA block to generate the higher order Odd-Stokes lines. Up to 8 nm tuning range from 1556 nm to 1664 nm were obtained at BP and 1480nm pump powers of 0.5 and 150 mW. Good maximum power variation within ±0.5 dB and high OSNR of more than 30 dB were achieved.

A simple tunable multiwavelength BFL that implemented dual pass structure was reported by [112]. The Brillouin gain medium was represented by 10 km non-zero dispersion shifted fiber (NZ-DSF). In this setup, an Odd-order Stokes signals with a Brillouin frequency shift of 0.16 nm (20 GHz) was observed. On the other side, the Even-order Stokes lines were forced to be circulated inside the cavity and not allowed to be monitor in the output laser comb. Up to 15 output Brillouin Stokes and anti-Stokes channels that can be tuned over a 50 nm range and with high OSNR of about 30 dB were generated. This 50 nm tuning range can be expanded depending on the BP wavelength range used since there was no additional Erbium gain included in this configuration. A stable output BFL comb with 0.16 nm channel spacing was demonstrated by [34] by exploiting the cascade SBS in 2.5 km SMF. The Odd-order Stokes signals (first and third Stokes) inside the cavity have the ability to excite both

of higher order Stokes line and in the same time the higher order anti-Stokes were excited by the FWM phenomenon. Using high amplified BP power of 160 mW, up to 10 Stokes and 9 anti-Stokes signals that separated by 20 GHz channel spacing were recorded. In addition, low maximum signals power variation of about 1dB was monitored at room temperature and within a period of 1.5 hour.

A 100 m of photonic crystal fiber (PCF) was implemented in a figure of eight structure to achieve a compact multiwavelength BFL design [113]. Up to 7 Brillouin Stokes lines with a double frequency shift of 0.16 nm were recoded using high amplified BP power of 15.3 dBm. In this design, the generated Odd-order Stokes lines were forced to be circulated inside the cavity and due to this circulation, the output laser comb was consisting only the Odd-order Stokes signals. FWM process was also implemented in this design, so the anti-Stokes signals were observed at the output laser comb. This structure was compared with multiwavelength BEFL. The comparison showed that the BFL exhibits an advantage related to the laser cavity tunability since the BEFL has an Erbium gain inside the cavity that limit the output laser comb due to the self lasing cavity modes oscillations. Therefore, up to 80 nm tuning range which depends on the BP wavelength's band source. In addition, up to 0.5 dB maximum Stokes power fluctuation was obtained. A multiwavelength BEFL was implemented to generate the optical signal of milli-meter wave signal as reported by [114]. Up to 4 Brillouin Stokes signals with a double frequency shift (21.5 GHz) via adjusting the Brillouin gain inside the cavity structure were produced. Then by eliminating the two middle Stokes lines utilized two fiber brag grating (FBG), two Brillouin Stokes lines with a frequency shift of 0.516 nm (64.17 GHz) were recognized.

Two parted EDFA blocks were implemented in multiwavelength BEFL in the linear cavity to achieve Brillouin frequency shift of 0.176 nm that can tuned over a wide tuning range of 50 nm [115]. Such wide laser cavity tunability was obtained due to free running modes elimination, which are responsible for tuning range limitation in conventional linear cavity BEFL, by utilizing physical mirrors at the end of the cavity resonators. In this setup, the BP was firstly amplified by EDFA block then inserted to the Brillouin gain medium. This technique can beneficially reduce the Stokes signal threshold and enhance the number of the generated Stokes lines. Up to 4 output Stokes

signals with a double Brillouin frequency shift spacing which has a range of 50 nm (1525-1575 nm) were recorded.

A new configuration at which 2km of special high nonlinear fiber (HNLF) was used as a Brillouin gain medium and Raman pump as a cavity pump unit were utilized in multiwavelength BEFL to generate double Brillouin frequency shift [116]. In this new design, double ring cavity structures were employed via four-port optical circulator to achieve double Brillouin frequency shift. By incorporation of four-port optical circulator, the Odd-order Brillouin Stokes lines were removed and the double channel spacing was recorded only by the Even-order Stokes signals. Up to 27 and 17 of Stokes and anti-Stokes lines which a high OSNR of more than 15 dB were monitored at Brillouin frequency shift of 0.16 nm. In this structure, the optimal BP and the Raman pump powers were 8 dBm and 40 mW respectively. In addition, the generated Stokes signal can be tuned over a 27 nm in the L-band region from 1591 nm to 1618 nm. The idea in this proposed design is to enhance both of the number of the generated Stokes lines its OSNR and also to make such laser cavity more compact to be used in real time system application.

In the same context, another compact multiwavelength BFL was demonstrated by [117] using HNLF as well as a Brillouin gain medium. Both of Odd and Even-order Stokes signals were observed in this setup by using bi-directional ring cavity structure. At BP power of 16.7 dBm, up to 36 Odd-order Stokes lines and 15 Even-order Stokes channel which both have double Brillouin frequency shift of 0.15 nm were recorded. This design was compared with the same structure that utilizes SMF as a Brillouin gain medium, and the proposed setup illustrated higher number of generated Stokes number and higher Stokes signals power. In addition, they concluded that the Even-order Stokes lines power were less than the Odd-order Stokes signals power since they are produced by lowest Odd-order Stokes signals.

A liner cavity multiwavelength Brillouin Raman fiber laser (BRFL) was demonstrated by [33] to achieve 20 GHz Brillouin frequency shift. Special 30 cm of Bismuth-Oxide EDF was utilized. In addition, two DCF length of 7.2 and 11 km were implemented as a Brillouin and Raman gain media. In order to increase the number of the Brillouin Stokes lines, both of BP and Raman pump power were optimized in terms of power

and wavelengths. The results showed that with longer DCF length or 11 km and under the optimization conditions, higher number of generated Stokes channels with higher OSNR can observed. If this the case, and at -2 dBm BP and 1W Raman pump power, up to 195 Stokes lines with a 26 dB OSNR that can be tuned over 28 nm were achieved.

A multiwavelength BEFL cavity that produced both of double Brillouin frequency shift in addition to the Q-switching characteristics utilizing figure of eight ring cavity structure was proposed by [118]. The double signal spacing was achieved via a four-port circulator which circulated and prevented the Odd-order Stokes signal within NZ-DSF that acts as a Brillouin gain medium. Using two NZ-DSF length of 2 and 10 km, up to 8 and 14 Brillouin Stokes signals with a double frequency shift of 0.16 nm were generated respectively. At 1480 nm pump power of 29-40 mW in the proposed design, a Q-switched pulse with a repetition rate of 20.4 and 104.2 kHz were achieved. In addition, the pulse width of these two repetition rates using both of NZ-DSF and DCF were 3.84 and 1.03 μs respectively.

A simple BEFL cavity that produced double Brillouin Stokes signal spacing at the room temperature was presented by [119]. The inserted BP power was firstly amplified by the EDFA block before it inserted to the Brillouin gain medium though pre-amplification technique. As a result, to the bi-directional cavity structure, both of Even and Odd-order Stokes signals can experiences gain in two opposite directions. Because of the gain provided by the EDFA block to the generated Brillouin Stokes lines, a homogenous gain saturation was occurred. Up to 12 and 13 of Even and Odd-order Brillouin Stokes channels that have a wavelength spacing of 0.172 were recorded at BP and 980 nm pump powers of 6dBm and 120 mW respectively. In addition, the effect of the BP and the EDF pump powers variations on the laser cavity tunability were studied. A broadband tuning range multiwavelength BEFL of about 110 nm that generated Brillouin Stokes lines with double frequency shift of 0.172 nm was reported by [120]. The proposed structure consists of simple ring cavity design in which the Odd-order Brillouin Stokes lines were confined within the right ring cavity and permitted both of initial BP and Even-order Brillouin Stokes signal to be an output laser comb. The wide tuning range was achieved due to the using of broadband tunable

optical band-pass filter (TBF) which controlled the position of the free running modes oscillation inside the cavity.

A multiwavelength Brillouin-Raman fiber laser (BRFL) that produced L-band Brillouin Stokes lines with 20 GHz frequency spacing was demonstrated by [121] using bi-directional cavity structure as depicted in Figure 2.12. A DCF which pumped by a co-pumped Raman pump unit was used as Brillouin and Raman gain medium. Up to 12 Brillouin Stokes lines with a double frequency shift of 016 nm with a high OSNR more than 20 dB were recorded as shown in Figure 2.13a. The generated Brillouin Stokes signals can be tuned within a 35 nm in L-band region with no optical filter used as illustrated in Figure 2.13b.

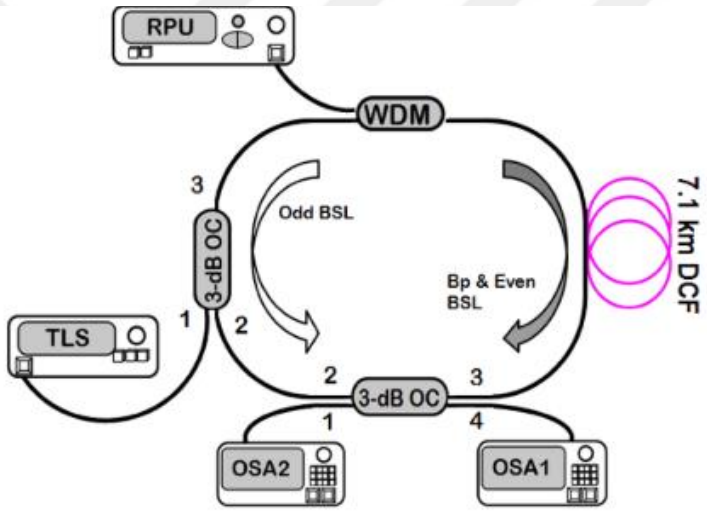


Figure 2.12 Experimental setup of MBFL reported by [121]

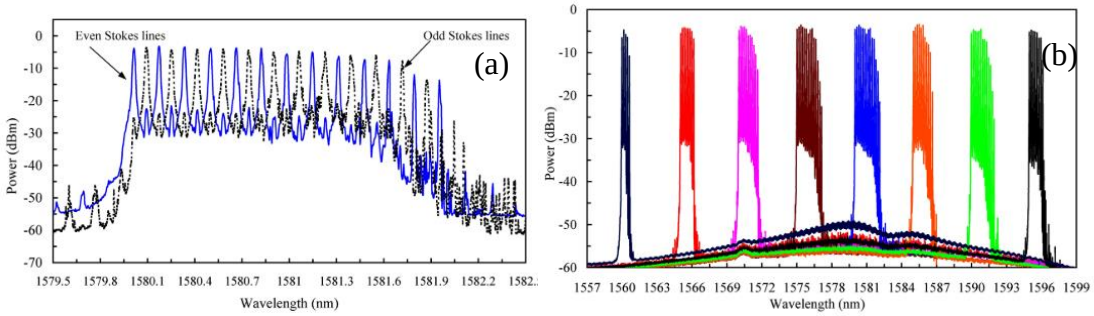


Figure 2.13 MBFL reported by [121] (a) Output spectrum of odd and even Stokes lines (b) Tuning range

A ring cavity BEFL with a double Brillouin frequency shift that utilized a nonlinear amplified fiber loop mirror (AFLMF) as an optical filter was presented by [122]. Up to 12 Brillouin Stokes lines with channel spacing of 0.16 nm at the centre wavelength of 1563 nm and at 980 nm pump power of 10.29 dBm were achieved. In addition, the impact of the BP wavelength, polarization controller, and the 980 nm pump power on the generated Brillouin Stokes signals was investigated.

A reflection property of the optical isolator and the fiber loop mirror were implanted in unique and simple multiwavelength Brillouin fiber laser cavity structure [123]. Instead of more than one loop in the previous cavity structures, only one loop was used so it can isolate the generated Even and Odd-order Brillouin Stokes signals in this design. In one round trip, the inserted optical signal will be absorbed two times in the Brillouin gain medium to generate the double Brillouin frequency shift signals. Therefore, a multiwavelength double frequency spacing lines can be monitored at the output laser comb. In addition, the experimental results showed that by using two different cavity structures, two different Brillouin frequency shifts of 0.1745 and 0.1734 nm were recorded. Micro-air gap was implemented in double and single Brillouin frequency shift multiwavelength BEFL cavity [124]. The idea is to produce high Fresnel reflection caused by micro-air gap cavity that can change the Brillouin frequency from double to single frequency signal spacing. Under the condition of the BP and the utilized pump power of 13 dBm and 300 mW respectively, up to five Brillouin Stokes lines with a double frequency shift of 0.16 nm and six output Stokes channels with frequency shift of 0.084 were recorded. A flat output laser comb in the range of 3dB Stokes power variation were recorded for both double and single Brillouin frequency shift within a period of 60 minutes. In addition, less than 1.2 dB was observed as cavity efficiency variation between the double- and single-spacing systems.

Two ring cavities was suggested and presented by [36] as a novel multiwavelength BEFL structure. In this new design, the optical switch was used to switch the Brillouin frequency spacing from single to double frequency shift. Under 4 mW BP with a wavelength of 1599.4 nm and 980 pump power of 600 mW, up to 5 Brillouin Stokes lines under double frequency shift of 0.178 nm and 16 single spacing Stokes lines with

a frequency shift of 0.89 nm were achieved. Both Brillouin frequency shift signals illustrated same tuning range of 15 nm from 1539 to 1608 nm. In addition, both systems showed low Stokes power fluctuation less than 1.5 dB within a period of 30 minutes. Table 2.2 shows the summary of tunability enhancement technique in a double Brillouin frequency shift MBEFL.

Table 2.2 Summary of tunability enhancement technique in a double Brillouin frequency shift MBEFL.

Ref No	No. of Stokes	Tunning Range	Description
[107]	3	NA	• Sagnac reflector yields • Two EDFA sections • polarization controllers (PCs)
[108]	3	NA	• Ring cavity • Brillouin Fiber Laser
[35]	4	NA	• Ring cavity • Brillouin Fiber Laser • Long SMF of 25 km
[109]	4	NA	• Ring cavity • Brillouin Fiber Laser
[110]	2	NA	• Ring cavity • Brillouin Fiber Laser
[111]	10	8 nm 1556 nm to 1664 nm	• Brillouin-erbium fiber laser • Figure of eight
[112]	15 St and anti-St	50 nm 1525 nm to 1575 nm	• Brillouin-erbium fiber laser • Figure of eight • High variation between the Stokes around 30 dB
[34]	10 St 9 anti-St	NA	• Ring cavity • Brillouin Fiber Laser • four-wave mixing processes • High variation between the Stokes around 30 dB
[113]	3	NA	• figure-of-eight configuration • Brillouin Fiber Laser • high amplified BP power of 15.3 dBm
[114]	4	NA	• figure-of-eight configuration • Brillouin-erbium fiber laser
[115]	4	50 nm (1525-1575 nm)	• Brillouin-erbium fiber laser • Two gain mediums (SMF) • Two DFA sections
[116]	27 and 17 of St and anti-St	NA	• Brillouin-erbium fiber laser • double ring cavity structures • 2km of HNLF • The variation between the Stokes around 40 dB

Table 2.2 (continued) Summary of tunability enhancement technique in a double Brillouin frequency shift MBEFL.

[117]	36 Odd 15 Even	NA	• BFL • bi-directional ring cavity structure • HNLF • The variation between the Stokes around 35 dB
[33]	195	28 nm	• Brillouin-Raman fiber laser • linear cavity • Special 30 cm of Bismuth-Oxide EDF • RPU power = 1 W
[118]	8	NA	• Brillouin-erbium fiber laser • figure of eight ring cavity structure
[119]	12	7nm 1558.1 to 1565.1 nm	• Brillouin-erbium fiber laser • Ring
[120]	5	110 nm	• Brillouin-erbium fiber laser • figure of eight ring cavity structure • broadband tunable optical band-pass filter (TBF)
[121]	12	35 nm	• Brillouin-Raman fiber laser • Raman pump of 425 mW
[122]	12	NA	• Brillouin-erbium fiber laser • A ring cavity
[123]	3	NA	• Brillouin-erbium fiber laser • Double ring cavity • Two HNLF
[124]	5	35 nm 1530 nm to 1565 nm	• Brillouin Erbium Fiber Laser • Micro-Air Gap Cavity
[36]	5	15 nm (1593 nm − 1608 nm)	• Brillouin Erbium Fiber Laser • Two ring cavities • switchable frequency spacing

2.4.3 Previous Works of Triple Channel Spacing (0.25 nm, 33 GHz)

Referring to the previous section, using double Brillouin frequency spacing in the receiver side of the optical communication system, the de-multiplexing problem still considered as a challenge. Thus, many researchers were tried to enlarge the Brillouin frequency signal spacing by proposing MBEFLs with triple frequency shift of 33 GHz that recently proposed by few researchers [37, 38, 40–42, 125].

A novel multiwavelength BEFL structure in which switchable Brillouin frequency shift was achieved utilizing both of gain and absorption through SBS phenomenon was propose and experimentally demonstrated by [37] as depicted in Figure 2.14a. the switchable Brillouin frequency shift were observed only by changing the BP power.

In this structure, at low BP power, up to 16 Brillouin Stokes lines with single frequency shift were recorded. While at high BP power and by exploiting BP absorption, only 7 double Brillouin frequency spacing signals were observed. Therefore, they used three cascades of SMF spools. On the other side, only two Brillouin Stokes signals with triple frequency shift spacing and at low Stokes power of -3.5 dBm were generated as depicted in Figure 2.15a. In addition, the recorded Stokes lines were limited to the tuning range of 22 nm from 1547 to 1569 nm. Xuefang Zhou et al., proposed a triple Brillouin frequency spacing, multi-wavelength Brillouin laser combined with two cavities: a single Brillouin frequency spacing cavity and a double Brillouin frequency spacing cavity as illustrated in Figure 2.14b [38]. In this structure, the optimization of multi-wavelength lasing was done with proper adjustments of Brillouin pump (BP) power and 980-nm pump power. However, up to 50 km SMF as a Brillouin gain medium was used. Besides that, low generated Brillouin Stokes power of -4 dBm was measured as depicted in Figure 2.15b and limited tuning range of 35 nm were monitored.

A hybrid Brillouin erbium fiber laser scheme that employs cascaded multiple Brillouin gain fibers in a ring cavity to realize multiwavelength laser output with switchable frequency spacing was proposed and experimentally investigated by [125] as shown in Figure 2.14c. In this cavity, the cascades SBS effects in a round-trip, resulted in different Brillouin frequency shift processes. Therefore, an integer multiple of Brillouin Stokes frequency shift can be realized as a multiwavelength output laser comb. Using only two SMF cascades and by controlling the BP power, both of single and double Brillouin frequency shift signals were recorded. However, three SMFs with total length of 70 km and large pump power of about 1.2 W were utilized to generate only 4 Brillouin Stokes lines with triple frequency spacing as illustrated in Figure 2.15c. the long fiber length and the high pump power used in this structure may made this cavity not applicable in real time system applications. In addition, the tuning range was not covered.

M H Al-Mansoori et al., demonstrated a multi-wavelength Brillouin-erbium fiber laser (BEFL) with ~33 GHz frequency spacing using cascaded stimulated Brillouin scattering effects in optical fiber as depicted in Figure 2.14d [40]. The proposed laser

structure exhibited a stable output channel with a tuning range of 19 nm, from 1549 nm to 1568 nm. The number of stable output channels produced is six channels with a triple-Brillouin frequency spacing as shown in Figure 2.15d. The output channels exhibit high output power and high optical signal-to-noise ratios (OSNRs). However, the proposed structure at pump power of 100 mW exhibited only 4 Stokes channels which tuned over low tuning range of 19 nm. In addition, long DCF length of 20 km was used.

In the same year, ZHEN WANG et al., proposed a multiwavelength BFL that produced Brillouin Stokes lines with triple frequency shift through a modular structure as shown in Figure 2.14e [41] . Up to 9 Stokes signals with triple frequency shift of 0.259 nm were observed as depicted in Figure 2.15e. Low Stokes signal peak power of -15 dBm were recorded and the tuning range was limited to self lasing cavity modes oscillations frequency band. Therefore, by tuned the BP away from these central frequency band, the free running modes oscillations were monitored at the output spectrum. In this design, the switchable Brillouin frequency shift (single, double, and triple) was obtained by the using of modular configuration. The influence of EDFA output power, BP wavelength, and the BP power on the cavity performance was studied. In addition, a beating microwave signals with different Brillouin frequency spacing (10.5 GHz, 21.48 GHz, and 31.77 GHz) within the 3 dB linewidth (16.4, 15.2, and 12.8 MHz) were obtained.

Recently, up to 3 Brillouin Stokes lines with a triple Brillouin frequency spacing were presented by [42] as illustrated in Figure 2.15f. The advantage of the proposed design that shown in Figure 2.14f that the recorded Brillouin Stokes signals was limited only to the EDFA section emission band from 1530nm to 1550 nm rang. However, two SBS fiber spools (10 km SMF and 12 km DCF) and high EDF pump power of 370 mW were utilized. Utilization of long DCF length, more absorption could take place as a result to the SBS threshold saturation with longer fiber length. Table 2.3 illustrate the summary of the triple Brillouin frequency shift in MBEFL

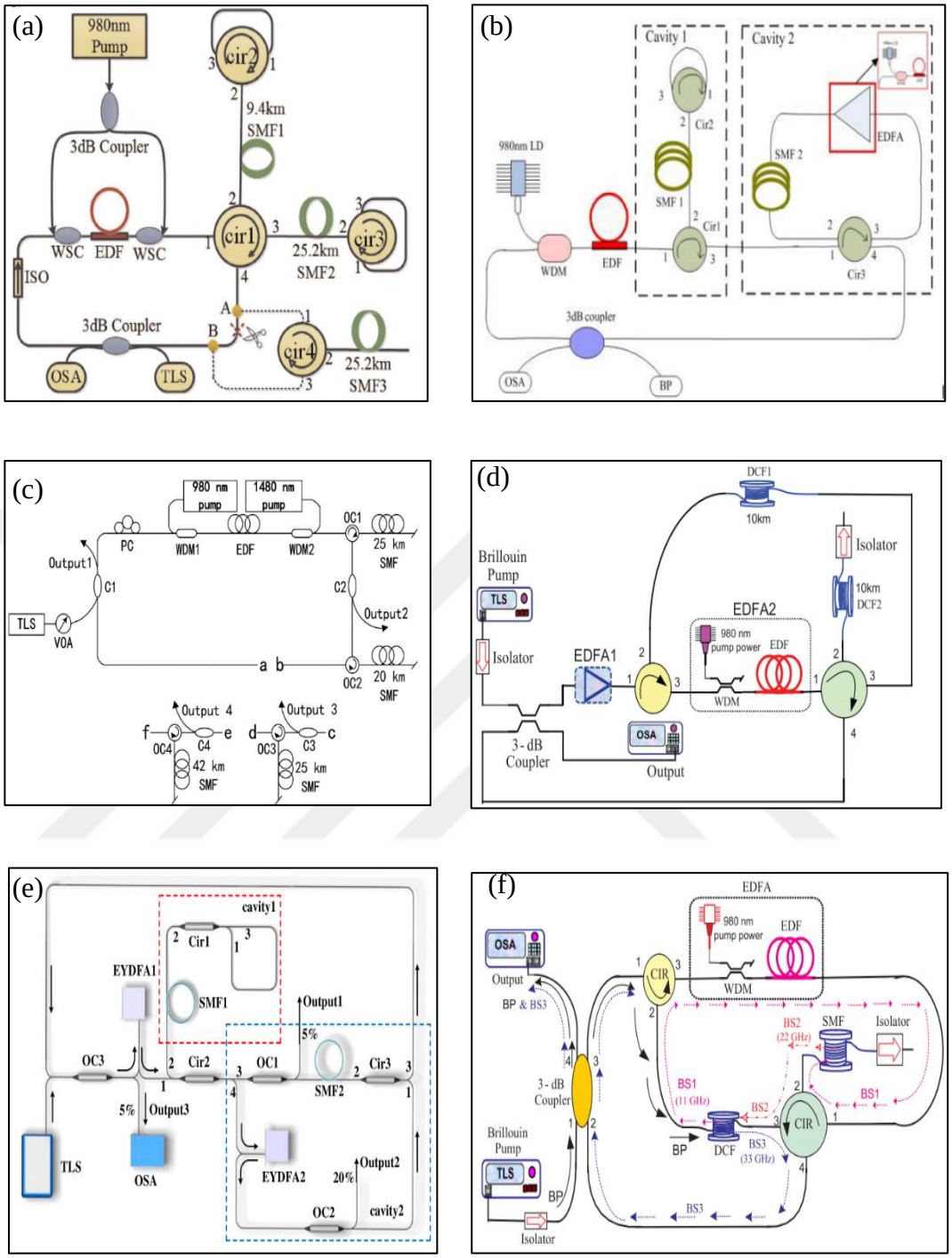


Figure 2.14 Experimental setup which reported by (a) [37] (b) [38] (c) [125] (d) [40] (e) [41] (f) [42]

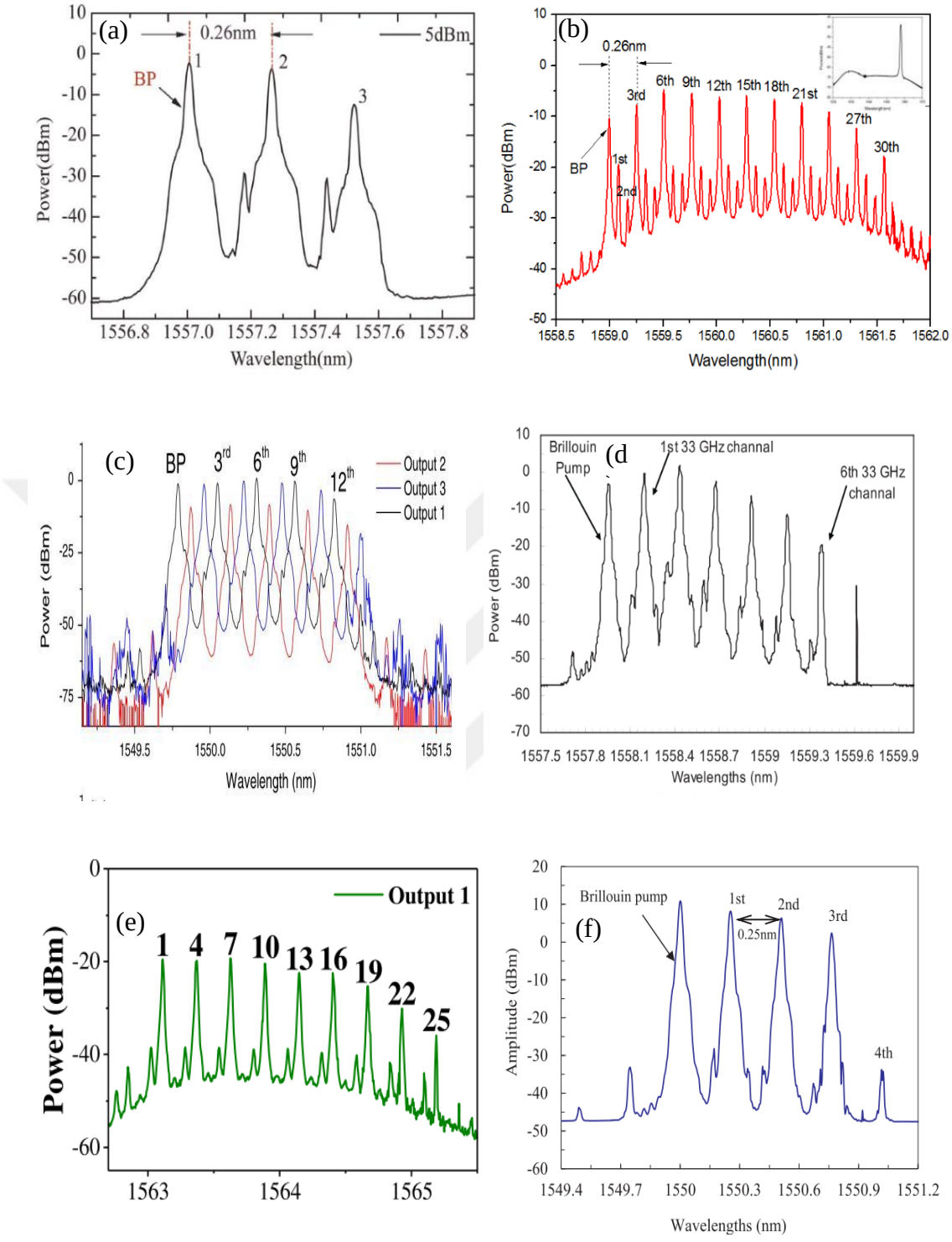


Figure 2.15 output spectrum of the structures proposed by (a) [37] (b) [38] (c) [125] (d) [40] (e) [41] (f) [42]

Table 2.3 Summary of the triple Brillouin frequency shift in MBEFL

Ref. No.	No. of Stokes	Tuning range (nm)	Description
[37]	2	22	• three cascades long single mode fiber • change the cavity manually • low output Stokes power of -3.5 dBm
[38]	10	35	• long SMF length of 50 km • high pump power of 600 mW • low Stokes power of -4 dBm
[125]	4	not covered	• 70 km SMFs length • 1.2 W pump power
[40]	6	19	
[41]	9	only at the center wavelength	• two sections of erbium-ytterbium-doped fiber amplifier (EYDFA) • long two SMF spool with length of 45 km
[42]	3	40	• long DCF spool with length of 12 km added an additional loss inside the cavity

2.4.4 Previous Works of Quadruple Channel Spacing (0.33 nm, 40 GHz)

So far, to the best of our knowledge, limited researches had reported quadruple wavelength spacing of ~0.33 nm (~40 GHz) [43, 125–127]. generating quadruple wavelength spacing was reported by [125] as illustrated in Figure 2.16a. Four 40 GHz Stokes signal was presented using four cascade SMFs for long length of 112 km and high EDF pump power of 1.1 W for two EDF pump units of 980nm and 1480nm. Relatively low Stokes power lower than -2 dBm, as depicted in Figure 2.17a, was exhibited in addition the tuning range was not covered in this work. However, using such long fiber length and consuming such high pump power led to make this design hard to be applicable. A novel high finesse ring filter was incorporated to achieve both of switchable single longitudinal mode (SLM) and dual-frequency erbium-doped fiber laser (EDFL) as shown in Figure 2.16b [126]. Two couplers and an active EDFA section are consisting in the proposed ring filter. Due to the gain provided by EDFA section, a spectral response with a high finesse was recorded. By including the ring filter, the unwanted oscillations modes in the dual-frequency EDFL were suppressed Up to 50dB. In addition, two SLM wavelengths were generated as illustrated in Figure 2.17b. The frequency shift of these two signal's wavelengths was tuned with a frequency shift tuning of ~10 GHz. Up to ~10 to ~40 GHz switchable microwave signal was recorded as photodetector (PD) beat the other two wavelengths. Lower than

5 kHz spectral width was measured for the generated microwave signal. Xuefang Zhou et al., proposed a multiwavelength BEFL with a 40 GHz Brillouin frequency shift using two ring cavity structures as shown in Figure 2.16c [127]. A Brillouin gain medium was formed in these two cavities by using 25 km SMF. EDFA section consists of 8m EDF that pumped by 980 nm pump power unit. At BP power of 8.3 dBm centered at 1550 nm and 600 mW maximum pump power, up to 7 Stokes lines with quadruple frequency spacing were achieved as depicted in Figure 2.17c. However, the laser cavity tunability was limited only to 15 nm (1545-560 nm). The experimental novel study that generate 40 GHz Brillouin frequency shift was presented by [43] as shown in Figure 2.16d. Dual wavelength lasers were produced by two ring cavity and passive EDF. An FBG was used to choose the frequency shift of the generated Brillouin Stokes lines. In addition, both of passive EDF and dual ring cavity structure were proposed to select SLF laser mode. Two lasers' frequencies are beaten by a PD and resulted in different microwave signals frequencies of 10.66, 21.39, 32.12, or 42.85 GHz. However, only single longitudinal Stokes signal with a quadruple wavelength spacing was achieved as illustrated in Figure 2.17d. Table 2.4 shows the summary of the quadrable Brillouin frequency shift in MBEFL

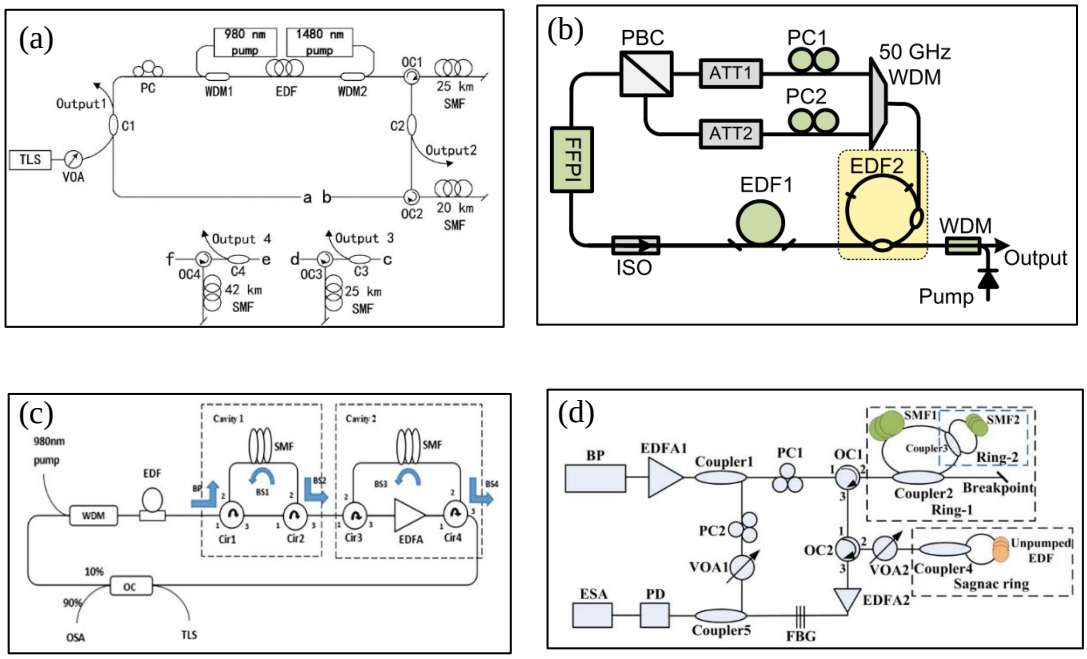


Figure 2.16 Experimental schemes which reported by (a) [125] (b) [126] (c) [127] (d) [43]

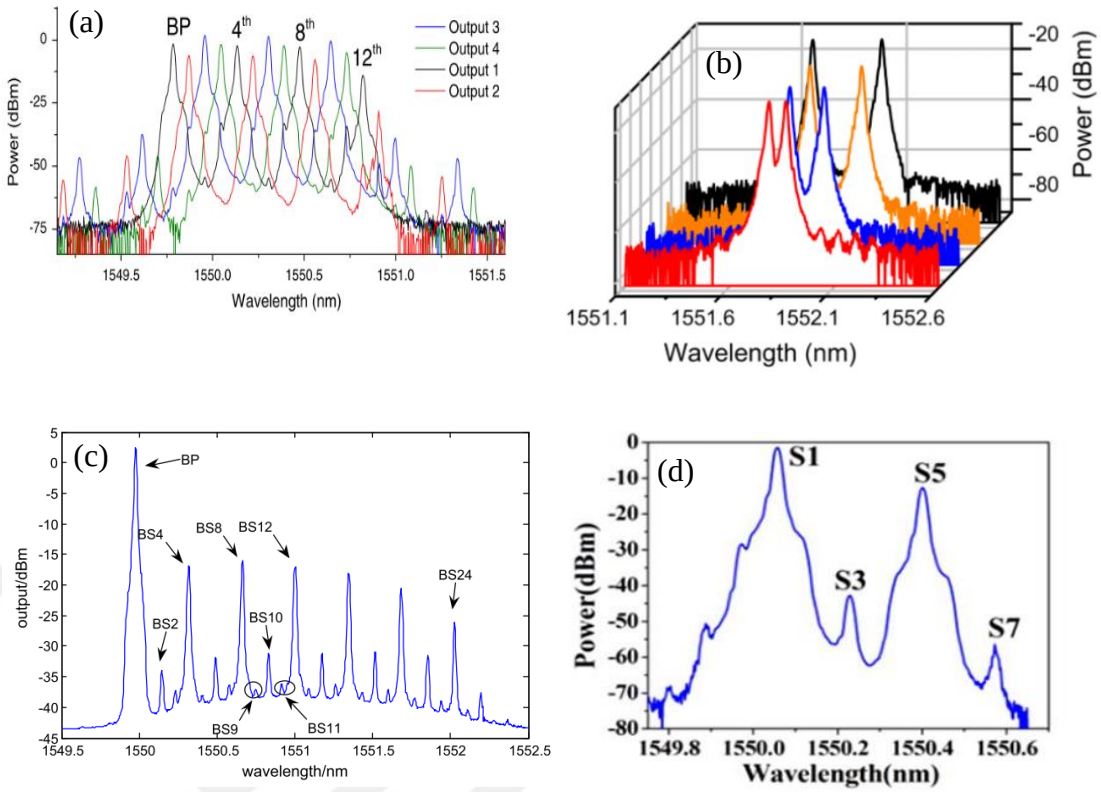


Figure 2.17 Output spectrum of the generated Stokes for the cavities proposed by (a) [125] (b) [126] (c) [127] (d) [43]

Table 2.4 Summary of the quadrable Brillouin frequency shift in MBEFL

Ref. No.	No. of Stokes	Tuning range (nm)	Description
[125]	3	not covered	• four cascade SMFs for long length of 112 km • high EDF pump power of 1.1 W
[126]	1	not covered	• high- finesse ring filter
[127]	6	15	• two cascaded double Brillouin- frequency-spacing cavities
[43]	1	not covered	• different Brillouin frequency shifts are selected by FBG

CHAPTER 3

RESEARCH METHODOLOGY

3.1 Introduction

The experimental results and the measurements related to all Brillouin frequency shift spacing methodology are presented in this chapter. To explain the entire conducted methodology, a flow charts styles are utilized. Firstly, the overall research processes flowchart is discussed and the whole components used in this study are illustrated. All the input parameters and the structure's variables that considered in different laser cavities (Uni-directional and Bi-directional ring cavities) are measured carefully. The illustrations begin with the experimental study of Uni-directional setup (single ring cavity structure) to generate signal Brillouin frequency shift. Then, a Bi-directional structure is utilized to achieve double Brillouin frequency spacing. Again, Uni-directional designed are involved to obtain triple frequency shift using double ring cavity design. On the other hand, a triple ring cavity configuration is implemented to generate both of quadruple and quintuple Brillouin frequency shifting.

3.2 General Research Flow

The general experimental flow of the entire study is depicted in Figure 3.1. In this thesis, a multiwavelength fiber laser structures based on different Brillouin frequency shift spacing are discussed. Different ring fiber laser cavities based on SBS phenomenon are explained in the first stage. Mainly the Brillouin frequency shift is about 0.08 nm (10 GHz) which represent a single Brillouin frequency shift from the inserted optical signal's wavelength to the Brillouin gain medium (optical fiber). So, the work is started with improving the laser cavity parameters related to cavity tunability. In order to expand the channel spacing to be 20 GHz (0.16 nm), a Bi-directional ring cavity structure is utilized. No more frequency expansion can be achieved in such cavity structure. Therefore, a double Uni-directional ring cavity setup is involved to increase the signal spacing from 0.16 nm to 0.25 nm (30 GHz). Further Brillouin frequency shift is required in the DWDM communication system. Thus, a

new cavity structure that consists triple ring cavity configurations are implemented. In these new configurations both of quadruple and quintuple Brillouin signals spacing are achieved. Finally, the input parameters of all proposed cavity structures are optimized and the output parameters such as number of generated Stokes, tuning rang, threshold power, and the stability of the generated signals are recorded.

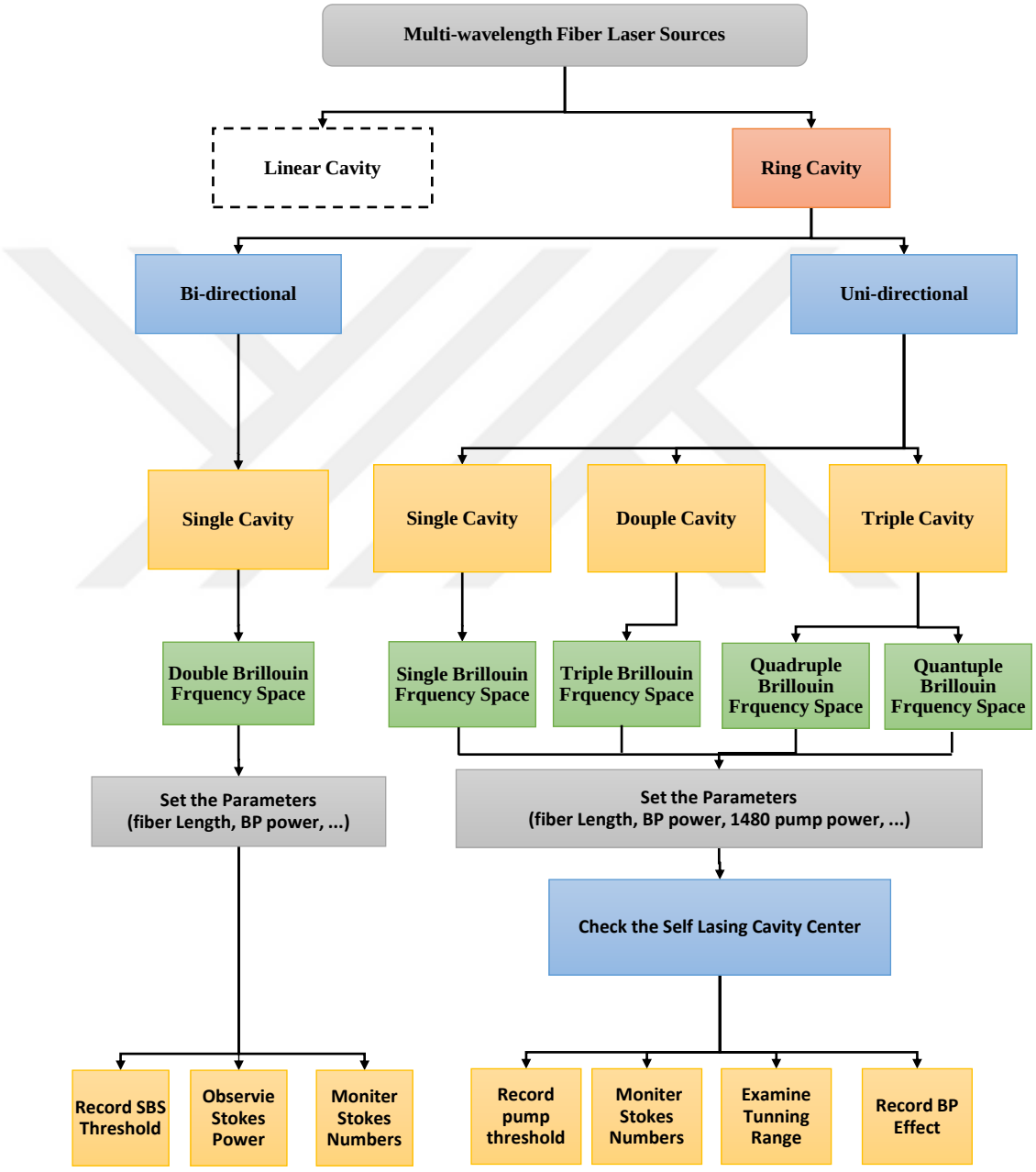


Figure 3.1 Research Process Flowchart.

3.3 Equipment and components

During the experimental results, a Tunable laser source (TLS) was used as a BP signal power source. Optical isolator was used to prevent any optical feedback into the TLS in order to protect it. Different single mode fiber (SMF) lengths and different dispersion compensation fiber (DCF) spools are tested as a Brillouin gain medium. Various EDF types are used as an EDFA section and as a passive EDF section. An optical spectrum analyzer (OSA) was used to record the output spectrum of the generated output Stokes signal power and the required threshold power. Table 3.1 illustrates all the optical equipment and components used in the experimental setups, measurements, observation and data collection.

Table 3.1 Components and equipment used in the experimental and theoretical study

No.	Equipment and Components	Specification
1.	Tunable laser source (TLS)	Resolution accuracy ± 5% Wavelength resolution 0.001 nm Maximum power wavelength +14.5 dBm Relative wavelength accuracy ≤ ± 0.01 nm Wavelength range 1480-1620 nm
2.	Optical Spectrum Analyzer (OSA)	Measurement wavelength range 600 to 1750 nm Wavelength linearity ± 0.01 nm (1520-1580 nm) Wavelength reproducibility ±0.005 (for one minute) Maximum wavelength resolution 0.03nm
3.	LD and Temperature Controller (CLD1015)	Current Limit 1 mA to 1.5 A Resolution 100 µA 50 µA
4.	Dispersion Compensation Fiber (DCF)	Model number DCM-40 Designed for SMF-28, (ITU G.652) Chromatic Dispersion -680 ± 10 ps/nm Fiber Length 1.7km Insertion Loss 4.5 ± 0.5dB
5.	Dispersion Compensation Fiber (DCF)	Model number DCM-80 Designed for SMF-28, (ITU G.652) Chromatic Dispersion -1360±10 ps/nm Fiber Length 6.8km Insertion Loss 9.0 ± 0.5dB
6.	Different single mode fiber (SMF) lengths	Model (ITU-T G.625. D Effective area 80µm Attenuation @ 1310 nm <=0.33 dB/km Attenuation @ 1550 nm <=0.19 dB/km

Table 3.1 (continued) Components and equipment used in the experimental and theoretical study

7.	Laser pump diode	Wavelength: 1480nm Output power: 500mW 14 pin Butterfly
8.	2x2 Optical Coupler	Coupling Ratio 50:50 Center Wavelength 1550 nm Minimum Bandwidth ±40 nm
9.	1x2 Optical Coupler	Coupling Ratio 10:90 Center Wavelength 1550 nm Minimum Bandwidth ±40 nm
10.	Erbium Doped Fiber-M12 (EDF)	Numerical Aperture 0.21 - 0.24 Absorption (dB/m) 11.0 – 13.0 @980nm 16.0 – 20.0 @1531nm Attenuation (dB/km) ≤10 @1200nm
11.	Erbium Doped Fiber-ER80-8/125 (EDF)	Mode Field Diameter at 1550 nm μm 9.5 ± 0.8 Peak Core Absorption at 1530 nm dB/m 80.0 ± 8.0 Core Numerical Aperture (nominal) 0.13 Cut-off Wavelength nm 1250 ± 150 Cladding Diameter (flat-to-flat) μm 125 ± 2 Coating Diameter 245 ± 15
12.	Optical Fiber Isolators	Center wavelength: 1550nm Isolation bandwidth: $\pm 30nm$ insertion loss: 0.6dB
13.	Wave Division Multiplexing (WDM)	Input Fiber [2] Wavelength 1300nm - 1515nm Input Fiber [3] Wavelength 1520nm - 1620nm Output Fiber [1] 1300-1515nm / 1520-1620nm Insertion Loss: [1] to [3] 0.30dB typical Insertion Loss: [1] to [2] 0.30dB typical Isolation: [1] to [2] (dB) N/A Isolation: [1] to [3] (dB) N/A Return Loss (dB) 50 dB Input and output Fiber Type SMF-28, 250um
14.	4-Ports Circulator	Wavelength Range 1550± 40nm Transmission direction 1 to 2, 2 to 3, 3 to 4 Insertion loss <0.8 dB Channel isolation >40 dB
15.	3-Ports Circulator	Operating Wavelength 1460nm-1620nm Isolation (dB) Port 2 to Port 1: 50dB minimum Insertion Loss (dB) Port 1 to Port 2: 0.8dB maximum Return Loss (dB) 55dB minimum
16.	Optical mirror	Operating wavelength 1520-1630 nm Maximum insertion loss 0.40 dB Fiber type SMF-28 Fiber length 1m Connector type FC/PC

3.4 Single Brillouin Frequency Shift Generation Flowcharts

It can be easily understood the procedure of the generated signal space Brillouin Stokes signal from Figure 3.2. The study starts with design and investigates the Uni-directional ring cavity structure depicted in Figure 4.1. Then the passive EDF was inserted into the same design and both two structures were compared. Many parameters like threshold power, number of generated Stokes signals, and the tuning range are recorded. Same optical components were used in these two setups except that the PEDF was included in our proposed scheme. In addition, the structures were examined under the same input parameters conditions.

According to the cavity structure, at first, the oscillation frequency band of the free running modes under the optimum 1480 pump power at which these modes were saturated is determined. Then in the next step, the optimal BP signal's wavelength which is suitable for these oscillation band is selected. Then, the BP power at which the optimal laser performance is set. Also, the BP signal wavelength is varied, and both number of the generated Stokes signals and the tuning range is measured. At the fixed BP power, the 1480nm pump power was varied and the pump power, at which the first Brillouin Stokes signal is observed, is recorded as a threshold power for the cavity.

In the next step, the BP signal power is varied and the output cavity performance such as the number of generated Stokes signals, threshold power, and the laser cavity tunability is recorded. It is well known that there is a trade-off between the number of the generated Stokes signals and the achieved tuning range at certain BP power. Therefore, the type of application will determine which BP can be used. In another world. The application that needs high tuning range, high BP power is required.

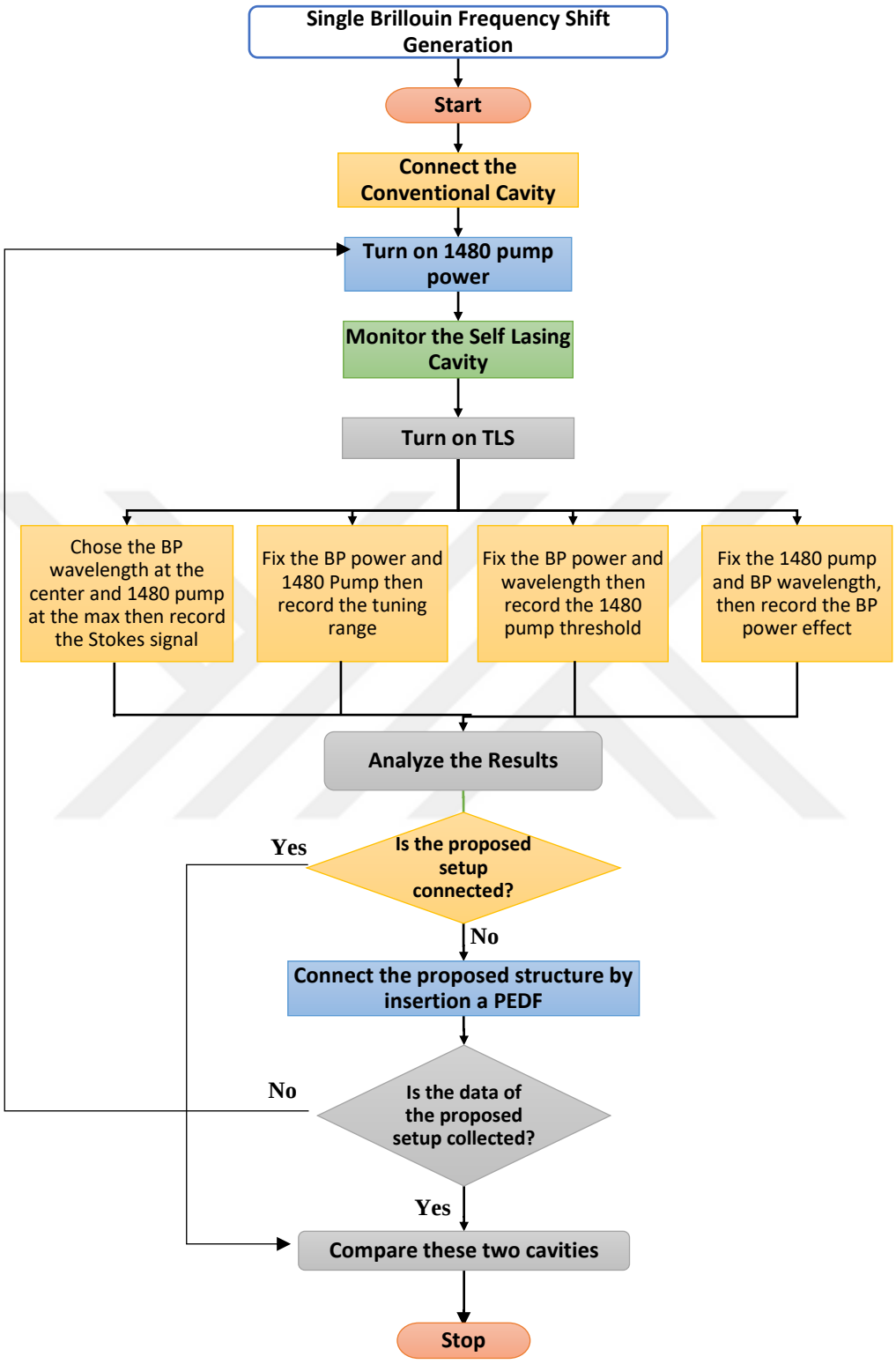


Figure 3.2 Single Brillouin frequency shift generation flowchart.

3.5 Double Brillouin Frequency Shift Generation Flowcharts

From Figure 3.3, the procedure of the generated double space Brillouin Stokes signal can be easily explained. The methodology begins with design and investigates both of conventional fiber laser and Bi-directional ring cavity structures (Figure 4.10). Then different SMF lengths were varied in these two setups. Similar optical elements were used and the only different between these configurations was the second edge of the SMF was connected in ring cavity while it was opened in the convectional setup. In addition, both cavities are tested under the same BP signal power and wavelength. Also, the same output parameters such as number of generated Stokes channels and the SBS threshold were recorded.

In the first step, the conventional setup is tested under the variation of the BP power for certain SMF length. In this stage, the required BP power to achieve the first Stokes signals is recorded as a threshold power. At the same time, the generated stokes signal power is also recorded with the variation of the BP power. This procedure is repeated for the next SMF spool length in order to monitor both of threshold and Stokes variations power. All the SMF length is tested within the conventional setup within the step of 2 km length.

Now the methodology is transferring to Bi-directional ring cavity structure in which the other terminal of the SMF is connected. Same steps which used in the conventional setup will be used in the new design under the same BP wavelength and power in addition to the SMF length variation.

In the next step, a comparison between these two different cavity structures in terms of threshold power and the maximum Stokes power at certain SMF length is presented. In addition, the output laser comb spectrum at the low SMF length of 5 km and long SMF of 18 km is recorded in order to show the effect of saturated transmitted power on the performance of the laser cavity.

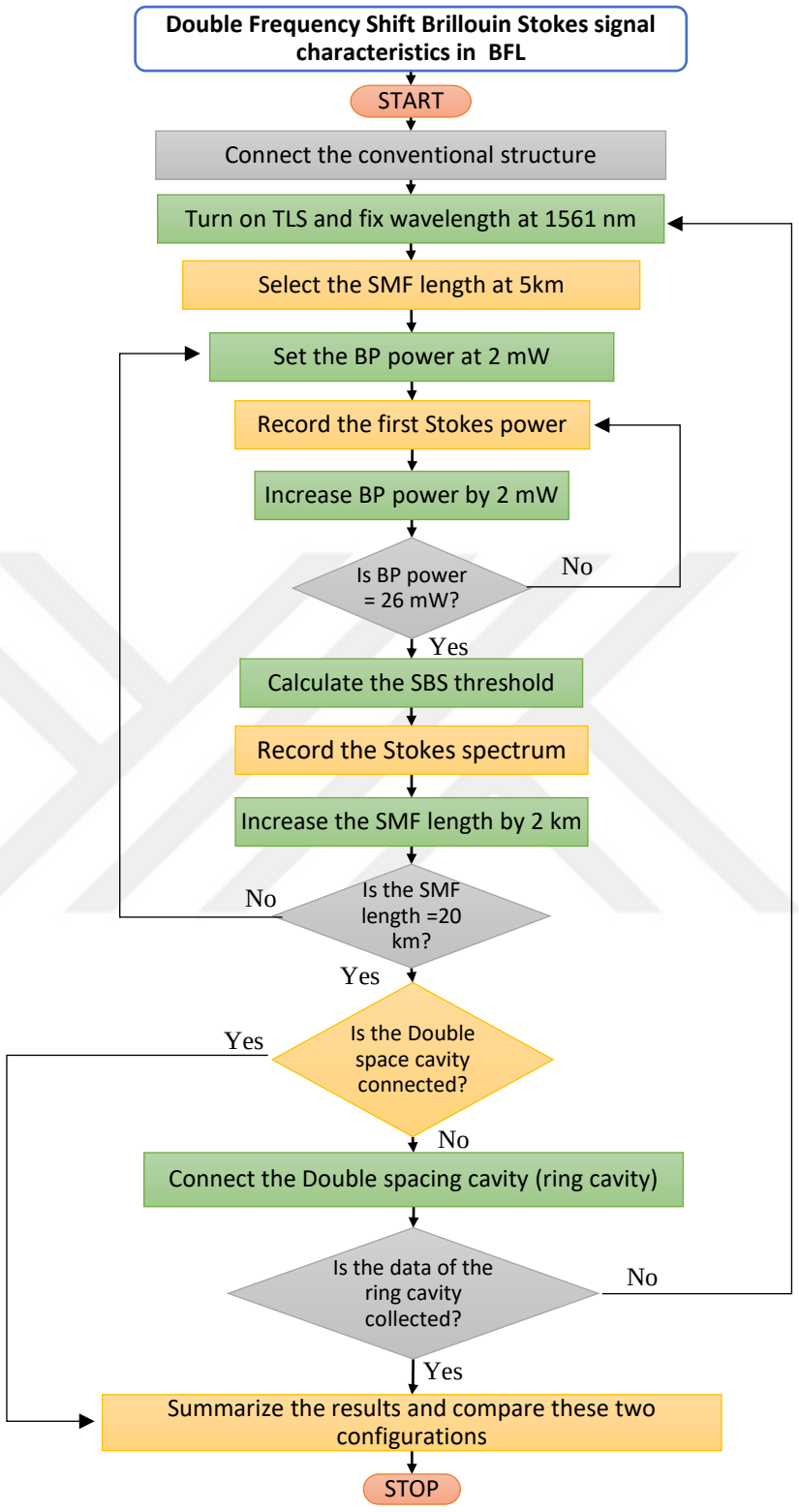


Figure 3.3 Double Frequency Shift Brillouin Stokes signal characteristics flowchart.

3.6 Triple, Quadruple, and Quintuple Brillouin Frequency Shift Generation Flowcharts

The methodology of generating triple, quadruple, and quintuple Brillouin frequency signal spacing is depicted in Figure 3.4. At first, different Uni-directional ring cavity structures (Figure 4.16, Figure 4.22, and Figure 4.31 respectively) are designed and investigated. Triple Brillouin frequency spacing can be achieved using Figure 4.16. in this design two ring cavities are utilized. While three ring cavities are involved in Figure 4.22 and Figure 4.31.

Various output parameters like number of generated Stokes signals, threshold power, and the laser cavity tunability are recorded. Almost same optical components were utilized for these different cavities. The different is either by optimize the EDFA section location inside the cavity or by using a different optical component in some cavity location. In general, these three different structures are used to expand the Brillouin frequency shift which is necessary to avoid de-multiplexing problem in the receiver side of the optical communication system.

As usual in such of cavity design that has both of BP and EDF pump power, at first, the self lasing cavity modes wavelength band should be determined in order to specify the optimum BP signal wavelength which is prober for this band. Then the maximum1480 pump power that saturate the self lasing modes is recorded. Then, the BP power at which the optimal laser performance was observed is set. The next step is to change the BP power at the optimal 1480 nm pump power in order to see the effect of the BP power variation on the output laser performance like threshold power, number of Stokes signals, and the tuning range. Here the threshold power is the pump power at which the first triple, quadruple, and quintuple Stokes signal is observed at certain BP power.

In order to measure the tuning range, the output laser comb was measured at different BP wavelengths and the in the optimal power for both of BP and 1480 nm pump power. In addition, the stability of the output Stokes channels spectrum is monitored within the period of one hour in order to make sure that these generated Stokes can be applicable for real time system.

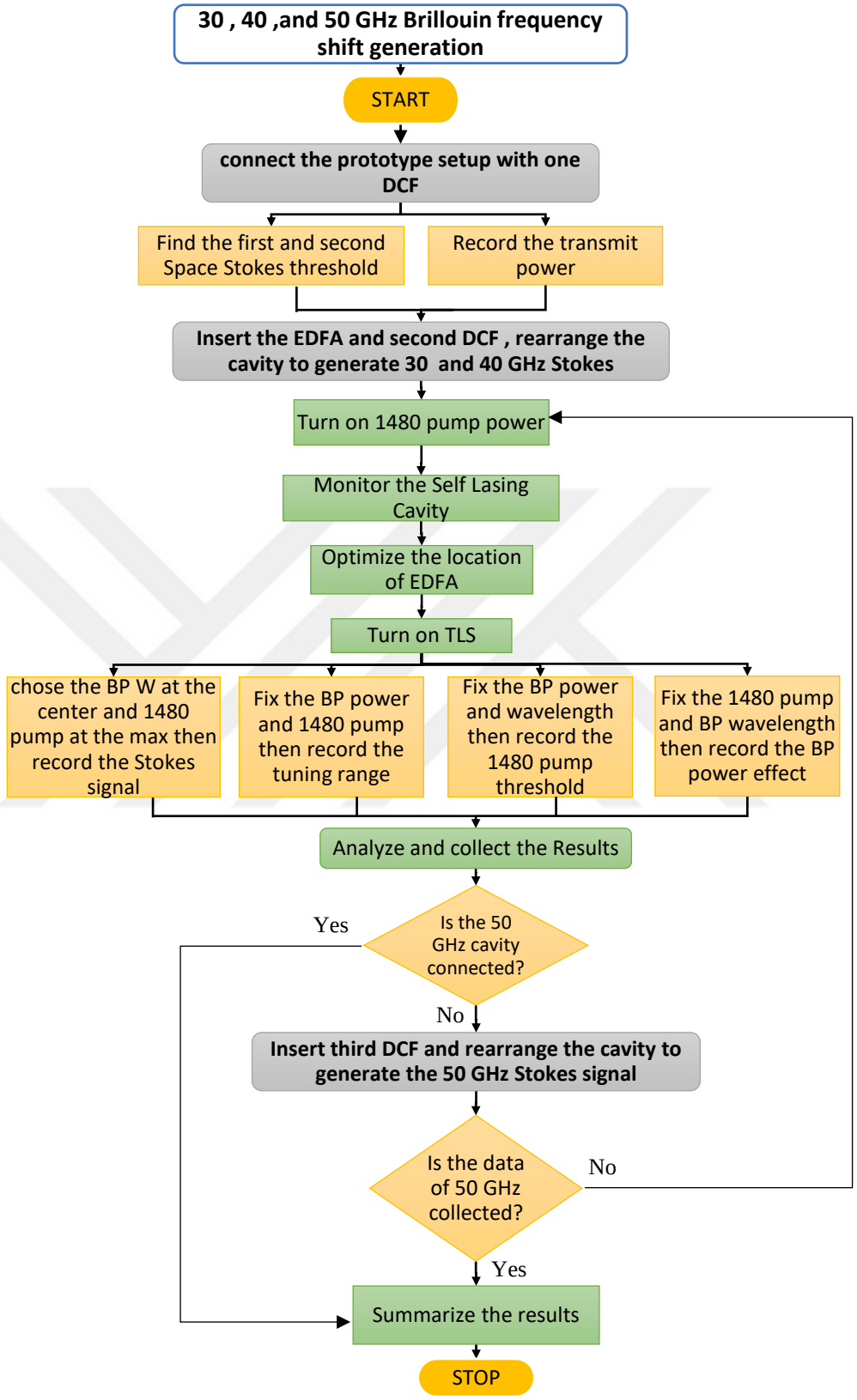


Figure 3.4 Generation of 30, 40, and 50 GHz Brillouin frequency shift flowchart.

CHAPTER 4

RESULTS AND DISCUSSION

4.1 Introduction

This chapter focuses on the experimental results that conducted for different ring fiber laser cavities. The results are classified into five sections according to the Brillouin frequency shift. Starting with single Brillouin frequency shift, the experimental implementation of the unidirectional BEFL cavity is presented and the cavity tunability is enhanced using simple PEDF. Then the experimental investigation study on the bidirectional BFL is illustrated. Within the study, the SBS threshold equation is experimentally estimated by comparing the experimental threshold values between conventional and laser cavity. This chapter is also concerned on the enhancement of the triple Brillouin frequency shift in MBEFL cavity performance. Finally, a generation of wide Brillouin frequency shift of 40 and 50 GHz (quadruple and quintuple channel spacing) is covered in this chapter. To the best of our knowledge a MBEFL with such wide channel spacing is presented for the first time.

4.2 Single Brillouin Frequency Shift (10 GHz)

4.2.1 Experimental Setup

The structural setup of MBEFL is depicted in Figure 4.1. Two cavities are included in this setup: the amplification cavity and the Brillouin Stokes (BS) cavity. The BS resonator, which is like the recycling technique, consists of two units of optical circulator (Cir1 and Cir2), DCF of 6 km as a Brillouin gain medium, and two connection points (a and b) that either connected directly or connected to the two ends of the PEDF. on the other side, amplification cavity includes EDF amplifier (EDFA) block that consists of 10 m of EDF type M12 and 1480 nm pump power with maximum pump power of 500 mW, 2x2 3-dB coupler, and tunable laser source (TLS) which maximum power of 14 dBm and 150 nm range (from 1480 to 1630 nm). Optical spectrum analyzer (OSA) with a resolution of 0.03 nm was used to record the generated Stokes powers.

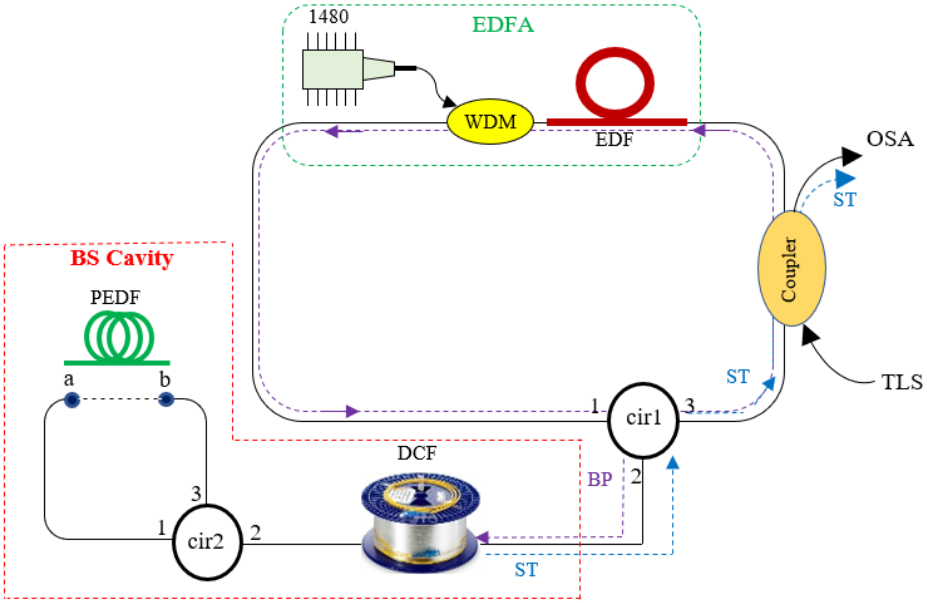


Figure 4.1 Experimental setup of both configurations with and without PEDF.

The Bp power is firstly injected into the amplification cavity through 3-dB coupler to experience an additional Brillouin gain within EDFA block. Then the amplified Bp power is inserted to the BS resonator through Cir1 (port 1 to port 2). Brillouin gain can be initiated in the forward and backward direction through DCF and since there is no additional gain within the BS cavity, the Brillouin threshold is constant and mainly depends on the amplified Bp power comes from the amplification cavity. In this context, in case of with and without PEDF in BS cavity, the threshold power will increase by inclusion such absorber section at the end of cavity resonator [106]. Thus, high amplified Bp is required to generate the Brillouin Stokes lines. Once the amplified Bp power reaches the SBS threshold power, the first order Stokes signal can be generated and propagated in opposite direction to the inserted signal power. Same procedure is taken place for the generated first order Stokes signal and the higher order Stokes signals can be only generated if the total gain is equal to the threshold power value.

4.2.2 Free Running Modes

Free running modes of both configurations, with and without PEDF, are depicted in Figure 4.2. Same 1480 nm pump power of 220 mW was provided to the cavities in

order to examine the impact of the PEDF, that inserted between the connection's points a and b, on the behavior of self lasing cavity modes.

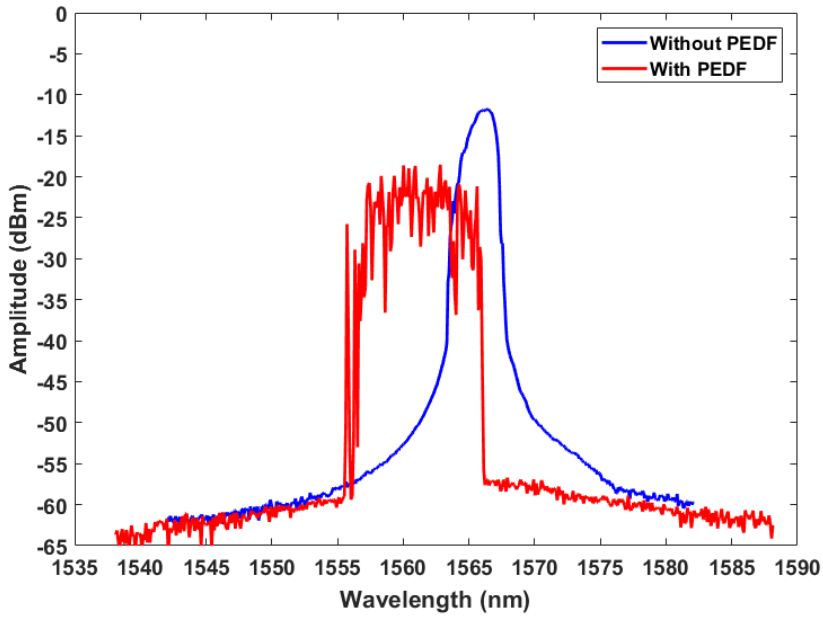


Figure 4.2 Peak gain of the free running cavity modes at 230mW of 1480 pump power with and without PEDF.

The center wavelength of these oscillations for the scheme without PEDF was at 1567 nm with a peak power of -12 dBm while for the setup with PEDF the center was at 1560 nm with maximum power of -20 dBm. In addition, these modes have bands of 5 nm and 10 nm for with and without PEDF respectively. It can be noted that by including such PEDF in the setup, the self lasing oscillations were shifted to the lower wavelength band and became more wider. In addition, the peak power was also reduced. This is because the fact that the PEDF can adds more losses inside the cavity. This performance is like studies presented by [14,106] in which the VOA and PEDF were conducted in order to manage the self lasing cavity modes inside the cavity.

4.2.3 Pump Powers Required for the First Brillouin Stokes.

The required pump powers for these two different setups (with and without PEDF), at which the first order Brillouin Stokes signal was oscillated, was firstly recorded and depicted in Figure 4.3 by varying Brillouin signal wavelength from (1540-1605 nm) with step of 5 nm at fixed TLS power of 10 mW. It is quite clear that by including

PEDF, high pump power is required for all wavelengths range compared to the pump power values required in the same wavelengths in the setup in which PEDF was not included. This can attribute to the PEDF that absorbed some of the transmitted Brillouin gain inside the BS cavity. The Brillouin Stokes threshold is mainly depending on the inserted amplified BP power into the Brillouin gain medium [128].

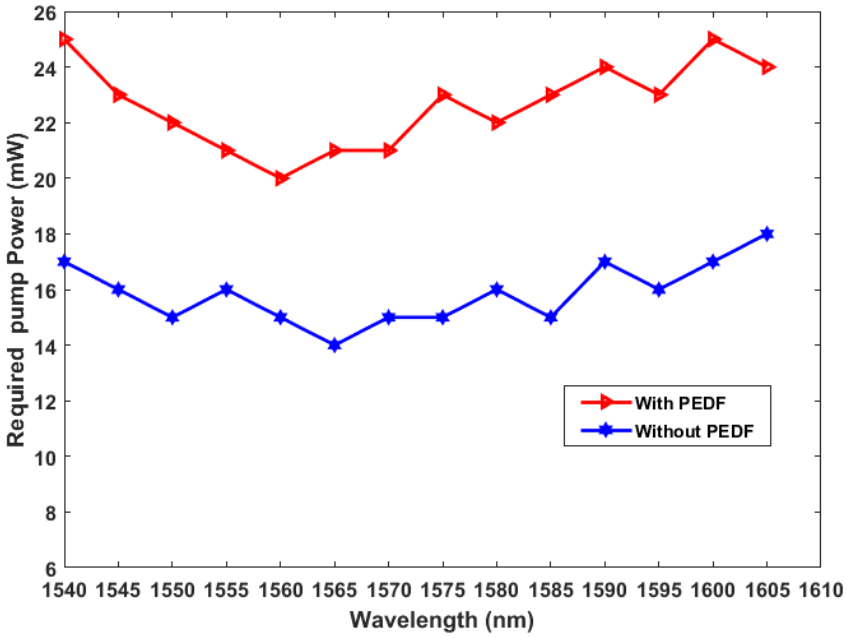


Figure 4.3 Required pump power for generating the 1st Stokes signal of the two configurations.

Also, the amplified BP power is mainly depending on the 1480 pump since the TLS value was fixed. Thus, high pump power is required in order to increase the inserted amplified signal to be able to generate the Stokes signal. Lowest pump powers of 20 and 15 mW were observed at 1560 and 1565 nm, the center wavelength of the free running modes of these two cavities. On the other side, highest pump powers of 25 and 18 mW were recorded when the Bp wavelength was tuned far from the Erbium gain center.

4.2.4 Output Spectrum for the Generated Stokes at Threshold Pump Power.

More experimental results were conducted and the required 1480 nm pump powers for all generated Stokes signals were monitored at the central wavelengths (1560, 1565 nm) for the two cavities as shown in Figure 4.4. It can be seen from Figure 4.4a, where

no PEDF was included, that the first Brillouin Stokes (S1) was generated at 1480 nm pump power of 15 mW, while 20 mW pump power was needed to obtain S1 in Figure 4.4b in which PEDF was included. Further increasing the pump power until 20 and 30 mW for these two cavities, S1 became an effective and enough to generate the second order Stokes signal (S2).

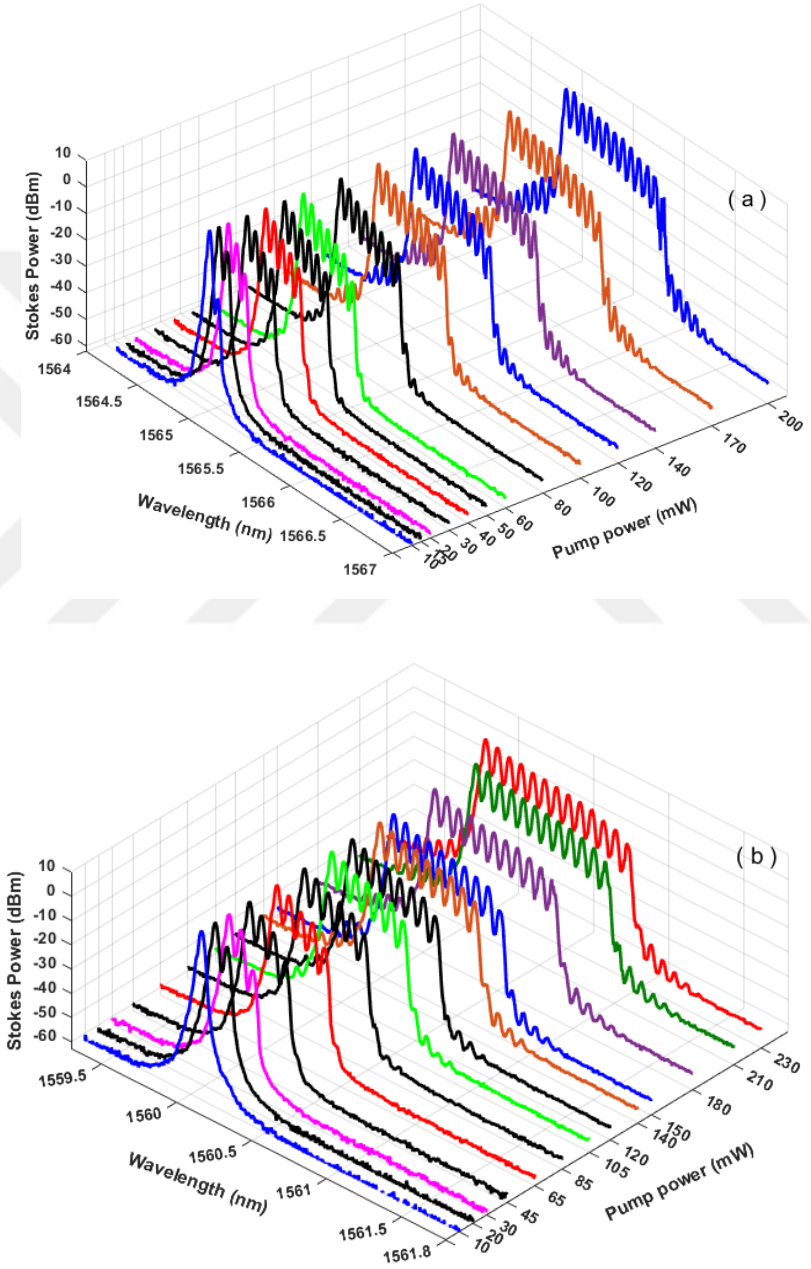


Figure 4.4 Output Spectrum for the generated Stokes signals of proposed structure at the threshold power (a) without PEDF (b) with PEDF.

In the same way, higher pump powers were necessary by including PEDF for all generated Stokes signals. Successive higher order Stokes channels were obtained in the same behaviour. In other word, the 1480 nm pump power needed to generate a certain Brillouin Stokes in the cavity without PEDF was lower than that was required in proposed structure. Beyond 200 and 230 mW pump power of conventional and proposed setups respectively, the numbers of the generated Brillouin were fixed at 13 channels. The reason behind this, that the EDFA was saturated due to the high pump power saturation phenomena in the certain cavity.

Figure 4.5 (a, b) shows the output spectrum of the laser comb for both schematics, with and without PEDF respectively, at the maximum pump power of 200 and 230 mW respectively. It is clearly observed that the numbers and the average power of the Brillouin Stokes signals were similar for both MBEFL configurations. This can be attributed to the different threshold powers required for these structures.

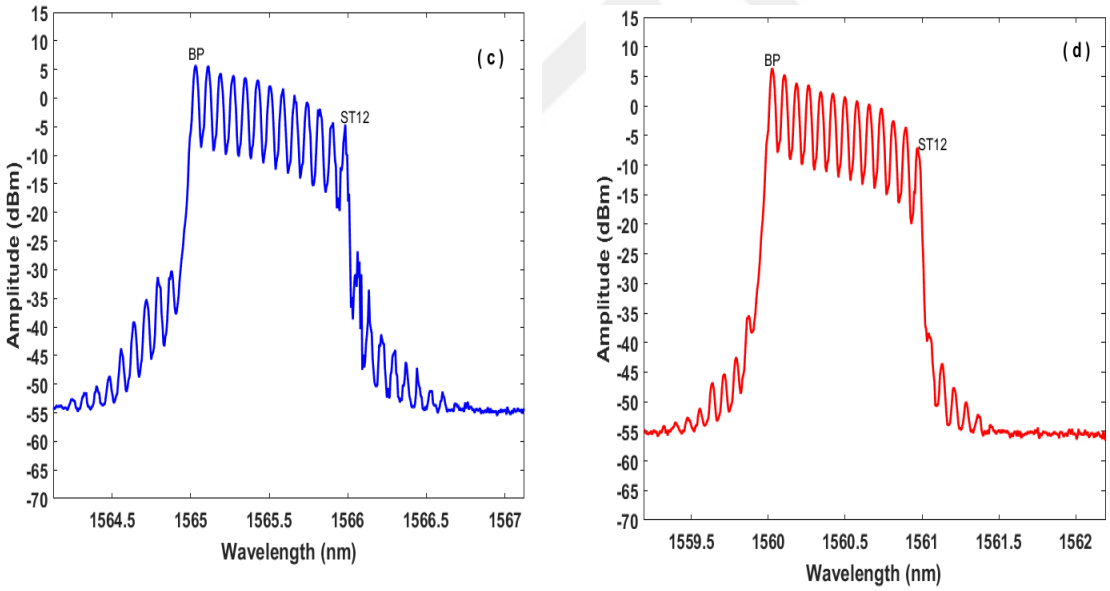


Figure 4.5 Output Spectrum for the generated Stokes signals at the maximum pump power (a) without PEDF (b) with PEDF

Higher SBS threshold will led to generate lower Stokes power since the Stokes power is mainly depends on the difference between the inserted optical power (the amplified optical signal power at port 2 of circulator 1) to the Brillouin gain medium and the

SBS threshold for DCF [58]. Thus, higher EDFA gain can be achieved in our proposed setup, which has larger threshold, compared to the Erbium gain obtained for conventional setup due to that lowest Stokes signal can experience higher gain in EDFA section [129]. Up to 13 Brillouin Stokes signals greater than -5 dBm peak power were achieved for both cavities. Comparing our generated Stokes numbers and powers with other results presented by [100–103] that they utilized almost the same cavity, 13 channels were obtained in our setup while 4, 6, 7,and 10 were achieved by them respectively.

4.2.5 Tunability of the Output Laser Comb

Figure 4.6 illustrates the tunability of the output laser comb at fixed BP of 10 dBm and 1480 nm pump powers of 200 mW and 230 mW for with and without PEDF configurations respectively. The tuning range was examined within 75 nm band from 1535 to 1610 nm with an increment of 5 nm. The laser comb of the proposed structure with PEDF exhibits a broadly tuning range of 65 nm within both of C and L-band (from 1540 nm to 1605 nm) in the absence of cavity modes oscillations, whereas the conventional cavity produced only 40 nm band (from 1555 to 1595 nm). With an enhancement of 62.5 % compared with the setup in which PEDF was not included.

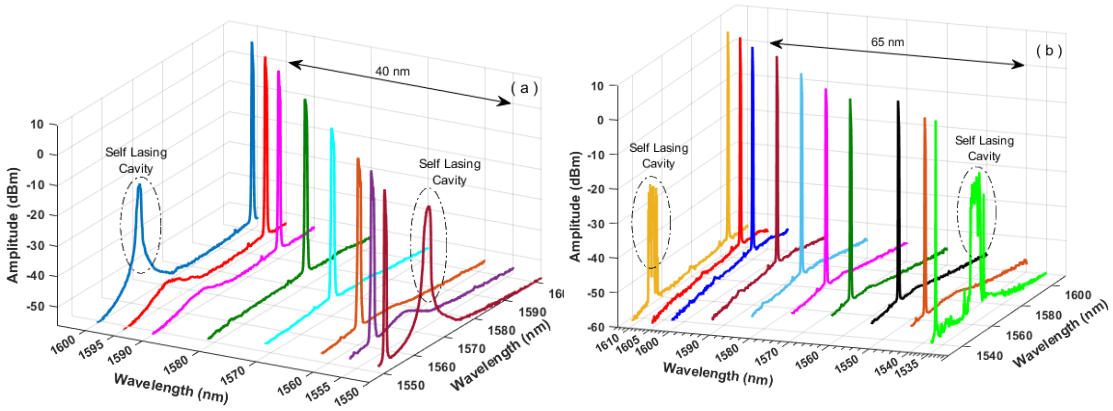


Figure 4.6 Output channels tunability of MBEFL cavity at different wavelengths at maximum of BP and 1480 nm powers of 10 dBm and 230 mW respectively (a) without PEDF (b) with PEDF

Widely tuning range was achieved via utilizing four techniques; conducting EDFA section outside the BS cavity, using PEDF as an absorber segment in order to absorb

the backward ASE, which was produced from EDFA, pre-amplification technique, and high Bp. In addition, no complex components were used like optical filters [77] or VOA [14] in our proposed cavity to obtain such wide range. These findings show better tuning range improvement than recently reported; 39 nm [100], 46.8 nm [101], 35 nm [102] and 10 nm [103].

4.2.6 Spectrum of the Brillouin Stokes at Different BP Wavelengths

The output spectrum of the Brillouin Stokes lines at different Bp wavelengths within the entire tuning range of both different configurations was depicted in Figure 4.7. Maximum pump powers of 200 and 230 mW for the setups without and with PEDF respectively in addition to fixed Bp power of 10 dBm were used. Both cavities illustrate maximum numbers of 13 Stokes signals when the BP wavelength was tuned over and near the center of the free running modes. Once the BP wavelengths were tuned far from the center, the number of the generated Stokes was reduced as a result to low EDFA gain provided. Referring to Figure 4.7a, 13 Stokes signals were produced at 1560 and 1570 nm, it was reduced to 11 Stokes signals at 1555 and 1580nm. Tuned the BP further away from the centre, the number of the generated Stokes signal was limited to 9 and 8 for the BP wavelength of 1590 and 1595 nm respectively. While in the cavity in which PEDF was involved, a highest number of 13 Stokes channels were recorded at 1550 and 1560 nm. Up to 11 Stokes were presented at 1570 nm. Further BP wavelength shift to the long band (L-band) region, a number of 9, 8, 8, and 8 Stokes signals were monitored at BP wavelength of 1580, 1590, 1600, and 1605 nm respectively. At BP wavelength of 1540 nm, the number of the generated Stokes signal was limited to 6 only that is because the PEDF absorption band was near to this wavelength and resulted in such low number limitation.

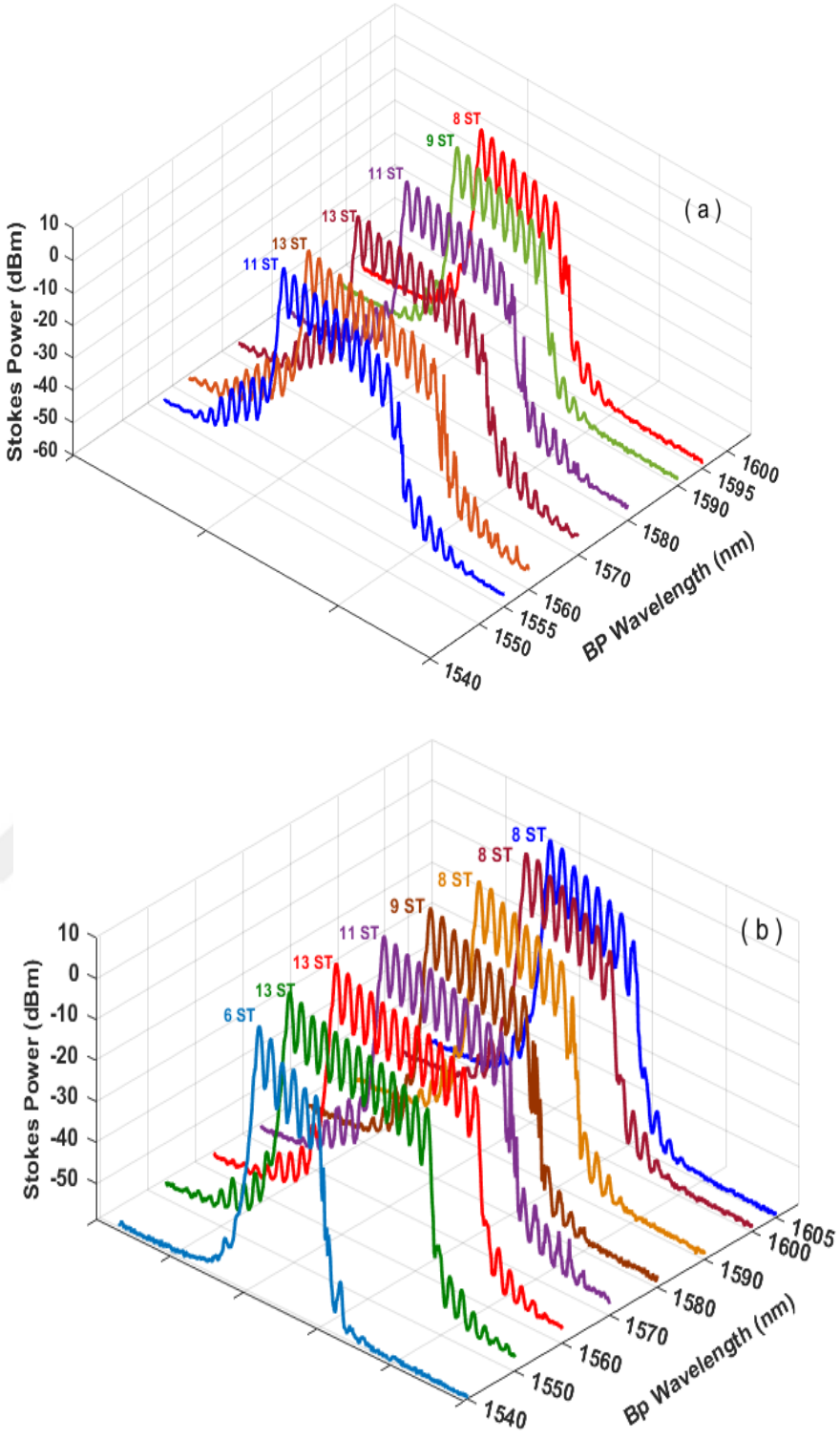


Figure 4.7 Output spectrum of Stokes signals generated at different BP wavelength within the entire tuning range(a) without PEDF (b) with PEDF

4.2.7 Effect of the 1480 Pump Power on the Numbers of the Generated Stokes Signals and Tuning Range

Figure 4.8 summarizes the effect of the 1480 pump power on the numbers of the generated Stokes signals and tuning range of the proposed structure. The Bp power was chosen to be constant at 10 dBm and its wavelength was varied within the tuning range. The pump power was changed from 10 to 270 mW with step of 10 mW. As the 1480 nm pump power increases, the laser comb tunability decreases, while the opposite behaviour occurred to the numbers of generated channels. This is due to that the free running modes energy increases at high pump power which is increased the mode competition with the Brillouin gain. On the other side, at high pump power, EDFA provided an additional gain to the generated Stokes which will be able to generate the N-order of the channels. The Stokes generation process continues till the total provided gain in the cavity became less than the cavity loss.

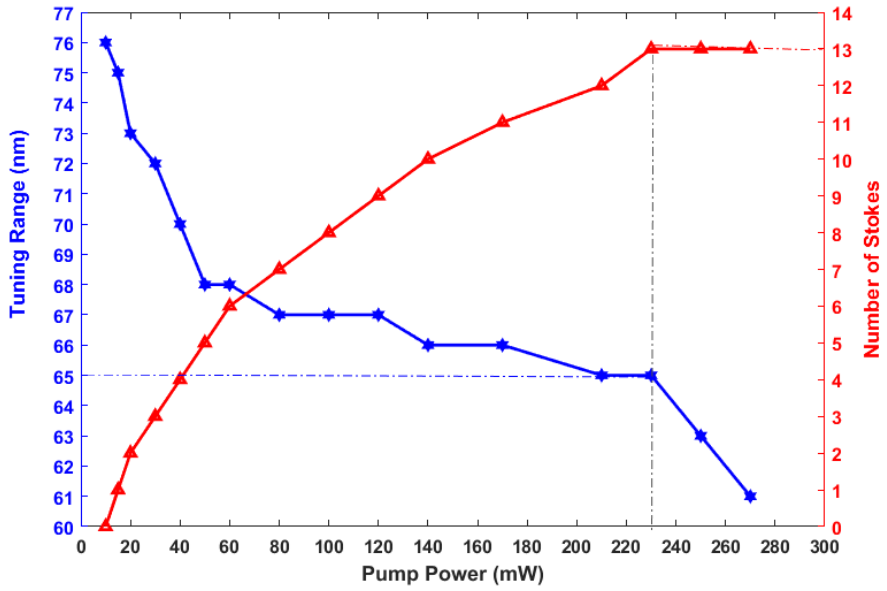


Figure 4.8 Tuning range and numbers of output channels of proposed cavity as a function of 1480 nm pump power.

In context, at low pump power the Stokes signals can be tuned over a wide band since the unwanted oscillation was at low level and the Brillouin gain was able to suppress it. Whereas the numbers of the generated channels were limited because the low gain

provided by EDFA section at such low pump power. Only 2 Stokes were recorded at low 1480 nm pump power of 20 mW, but it can be tuned over high tuning range of 73 nm. As the pump power was increased the number of the generated Stokes was increased until it was saturated at 230 mW at 13 Stokes lines. At this point, the cavity tunability was 65 nm. The value of 230 mW was chosen since beyond it, the number of the generated Stokes signals was saturated, and the tuning range was rapidly decreased.

4.2.8 Impact of BP Power Variation on the Tuning Range and the Number of the Generated Stokes

The impact of BP power variation on the tuning range and the number of the generated Stokes signals of our proposed structure was illustrated in Figure 4.9. The pump power was kept fixed at 230 mW while the BP power was changed from 0 to 14 dBm with 1 dBm steps in this experiment. It can be clearly noted that the tuning range increases by increasing the BP power. The reason can be attributed to the fact that the high Bp was able to suppress the unwanted modes oscillations inside the cavity.

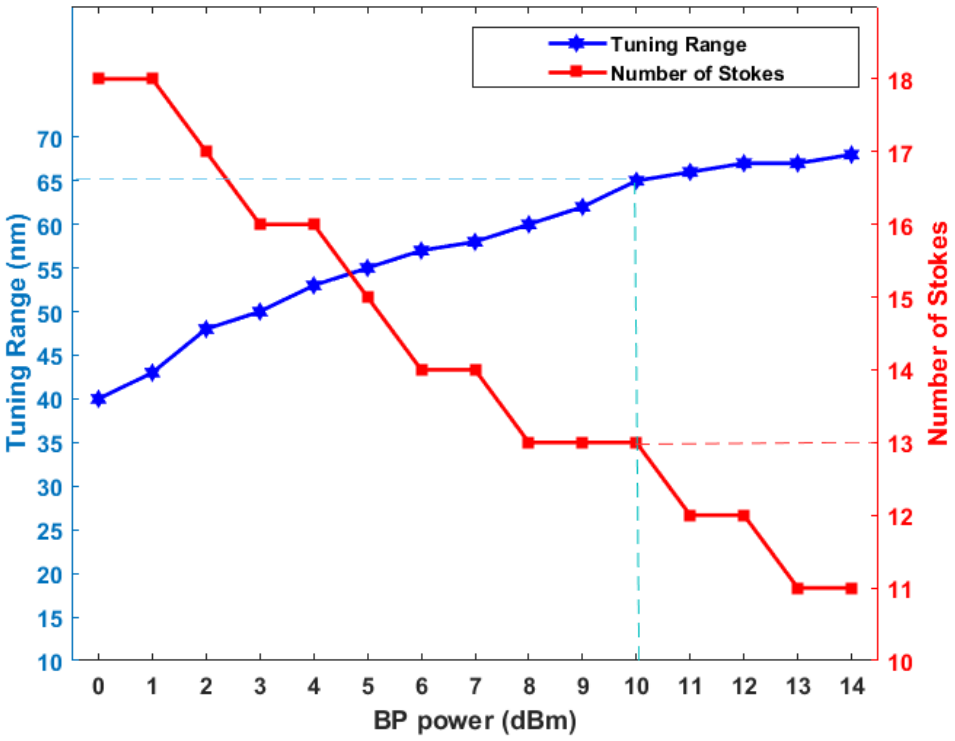


Figure 4.9 Tuning range and number of output channels for proposed configuration as a function of BP power.

On the other hand, the trade-off was happened to the number of the output channels which decreased as the BP power was raised up. This is because at high Bp power, EDFA section tends to be saturated due to high input signal power saturation mechanism, thus, no additional gain can provide from the amplifier to the subsequent Stokes signals. On the other side, higher gain can be achieved for lower BP power and higher number of Stokes signals was obtained. Our goal is to achieve wide tuning range with an acceptable number of Stokes lines. Therefore, BP of 10 dBm was chosen since beyond this power the tuning range was almost constant at 65 nm, and the number of Stokes signals was decreased from 13 to 11 Stokes channels.

4.3 Double Brillouin frequency spacing (20 GHz)

4.3.1 Experimental Setup

Within the entire study, two configuration structures are tested. Ring BFL cavity and conventional technique as depicted in Figure 4.10. Same optical components were used in these two configurations, tunable laser source (TLS) that achieve Brillouin pump (BP) power. An Erbium doped fiber amplifier (EDFA) is performed by EDF of 124.5 µm fiber diameter, 0.22 numerical aperture, 946nm cut off wavelength, 18.79/m absorption@1531nm and length of 10m and a maximum 1480 pump power of 130mW. The BP power is amplified to its maximum power of 50mW. 3-dB optical coupler, optical circulator and two optical spectrum analyzer (OSA).

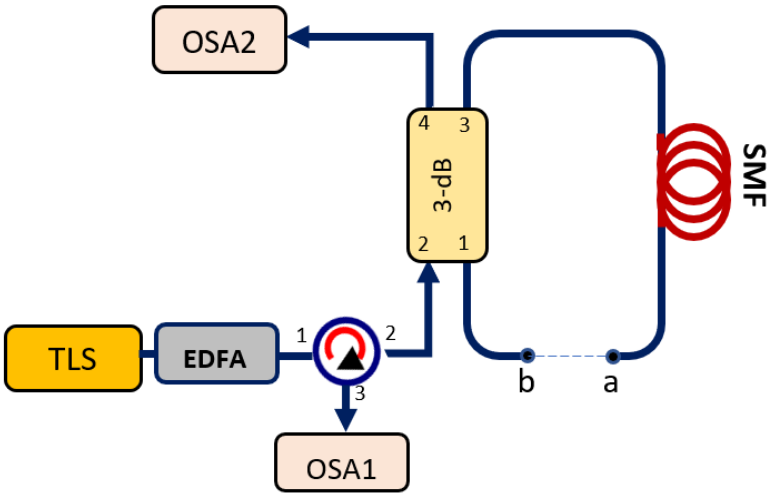


Figure 4.10 Ring BFL cavity and conventional technique structures.

OSA1 was connected to the Port 3 of an optical circulator to measure the odd Stokes signals power as well as even Stokes signals threshold. The threshold power for the even Stokes signals is measured by OSA1 which represented by low order odd Stokes signals power at which high order even Stokes signal is appeared (the required low order odd Stokes signal power that generate high order even Stokes signal). On the other side OSA2 was connected to the port 4 of an optical coupler to measure the even Stokes signals power and threshold power of the odd Stokes signals. In the same way the threshold of the odd Stokes signal is represented by the low order even Stokes power at which high order Stokes signals is generated (the required low order even Stokes signal power that generate high order odd Stokes signal). Various SMF lengths (5, 8, 10, 13, 15, and 18) km is conducted in this study as a Brillouin gain medium.

As depicted in Figure 4.10 at first, points a and b are connected to achieve ring BFL cavity. The BP power is amplified by an EDFA and varied from 0 mW to reach its maximum value of 50 mW. Then it will pass through an optical circulator (port 1 to port 2) to be inserted into the SMF though an optical coupler (port 2 to port 3). Once the amplified BP power reach the threshold value, the 1^{st} Stokes signal start to appear at OSA_1. At this point the threshold is measured at OSA2 which represent the required BP to generate 1st stokes which represents the inserted BP power to the SMF. By increasing BP power 1^{st} Stokes power getting higher until its reach the threshold value of the 2nd Stokes signal at this point, 2nd Stokes signal start to observe at OSA_2. At the same time OSA_1 recorded the threshold value for 2nd stokes signal which represents the amount of 1^{st} Stokes power that inserted to the SMF. High order Stokes signal will be generated, and this behaviour will continue until the total gain equal to the total loss inside the cavity. Again, same procedure will continue to generate the high order Stokes signal until the total gain and the total loss tends to be equal inside the cavity. On the other side, conventional technique can be achieved be connecting points a and b with an optical isolator to prevent any feedback or circulation inside the cavity. At the same way Ps1 will be generated to be observed at OSA_1. Also, the threshold for ps_1 is measured at OSA_2. The only different that ps1 is prevented to be oscillated inside the cavity to generate ps_2.

4.3.2 First Stokes Power at Different BP power

Ring BFL cavity and conventional configuration were tested using same parameter conditions. An input power at 1560nm with a maximum power of 50mw was used for all SMF spools. Figure 4.11 shows the 1st Stokes signal power as a function to the BP power using 5km SMF length in ring BFL cavity and conventional technique. From the figure, the 1st Stokes signal was starts to oscillate at 16.2mW in conventional technique while it starts to appear at 1.67mW in ring BFL cavity. In other word, the Stokes signal threshold (the required BP power) was reduced up to 90% in laser cavity as comparing to the conventional technique.

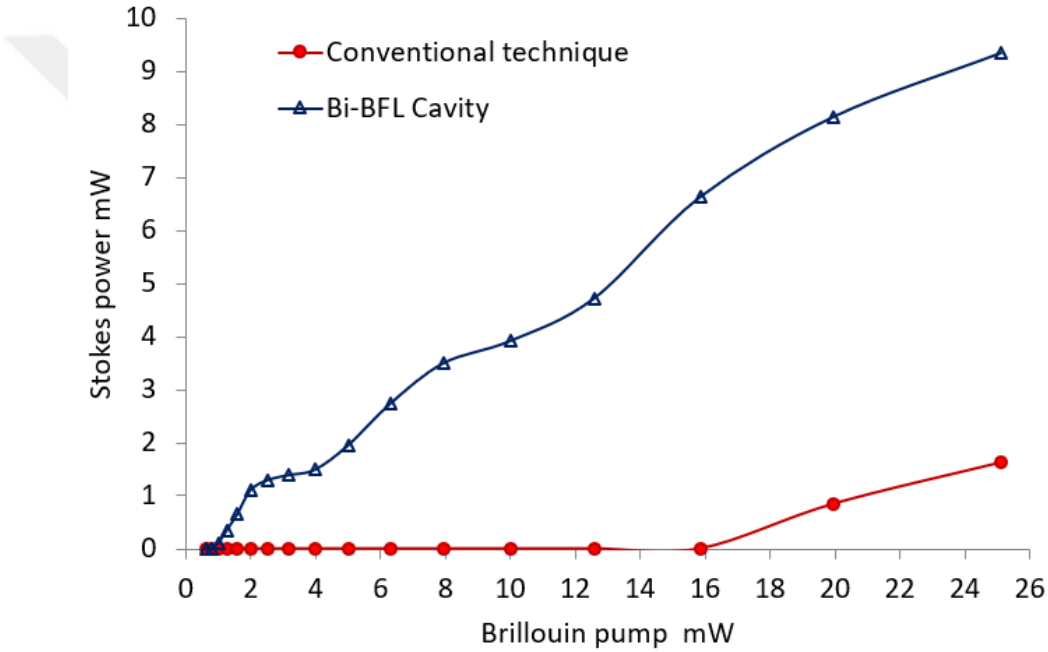


Figure 4.11 First Stokes signal variation as a function of BP power in 5km SMF for ring BFL cavity and conventional technique.

4.3.3 First Stokes Threshold as a Function of SMF Length

Further results were conducted using different SMF lengths to prove this reduction ratio. Figure 4.12 illustrates the 1st Stokes threshold for these two different setups. All the selected fiber spools were experimentally examined and exhibits the same Stokes threshold reduction ratio. In addition, both configurations show saturation in the threshold value as the SMF length exceeds 10 km. This can be attributed to the

effective length (L_{eff}) saturation as a result of the SMF length increases. For further justification, the SBS threshold in conventional technique was presented by [24] as:

$$\frac{g_B P_{cr} L_{eff}}{A_{eff}} = 21 \qquad (\mathbf{4.1})$$

where P_{cr} represents the critical power (SBS threshold power). L_{eff} can be expressed as:

$$L_{eff} = \frac{1 - e^{-\propto L}}{\propto} \qquad (\mathbf{4.2})$$

where $\propto$ represents the attenuation coefficient for certain fiber type. Once the SMF length increased more than 10 km, the second terms of the nominator $e^{-\propto L}$ will become very small value and tends to be approximately 0. Thus L_{eff} can be written as:

$$L_{eff} = \frac{1}{\propto} \qquad (\mathbf{4.3})$$

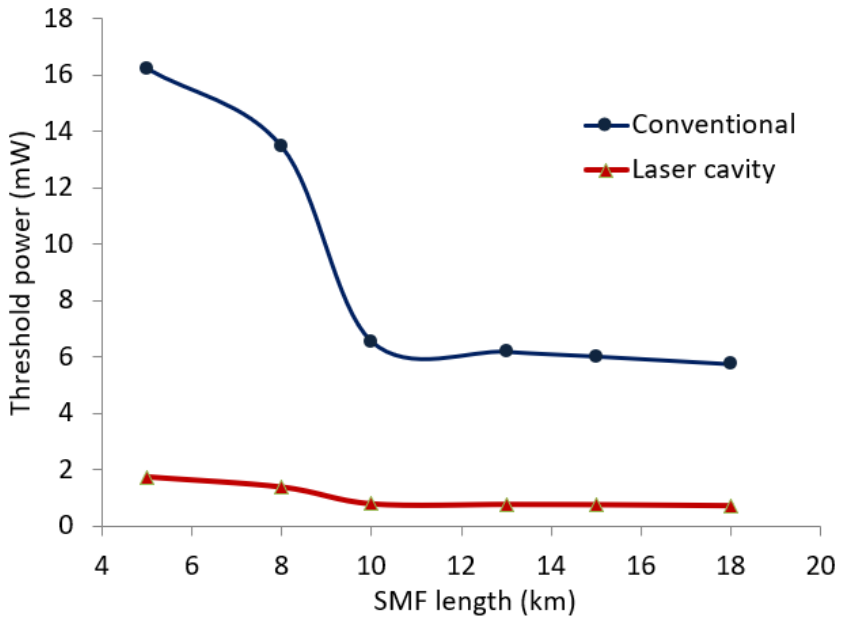


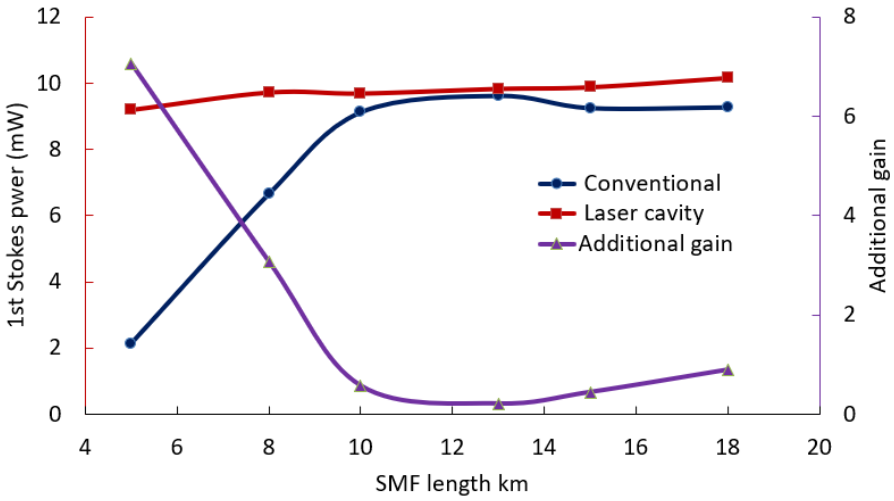
Figure 4.12 First Stokes threshold power as a function of SMF length for both Structures.

equation (4.2) shows fixed effective length after 10 km fiber length and will led to saturate SBS threshold in equation (4.1). Also, it can be easily seen from the result that the optimal SMF length for these two cavities is 10km that is because there is no SBS threshold reduction after this length. In other word, increasing the length beyond 10km led to increase the losses caused by α. According to the results presented in Figure 4.11, the SBS threshold equation in ring laser cavity can be obtained corresponding to the conventional threshold equation as:

$$P_{Th(Ring\ laser\ cavity)} \cong \frac{P_{Th(conventional)}}{10} \cong \frac{2.1A_{eff}}{g_B L_{eff}} \qquad (\mathbf{4.4})$$

4.3.4 Maximum First Stokes power and the addition gain vs SMF length

Figure 4.13 illustrates the maximum 1st Stokes power and the additional Brillouin gain at the maximum BP power of 50mW using different fiber lengths. It can be easily noticed from the results that ring laser cavity shows higher Stokes power in relatively short fiber length (3 to 10 km).



.

Figure 4.13 Maximum 1st Stokes power and the addition gain vs SMF length in both structures.

As the length was increased form 3 km to 10 km, the gain was reduced from 7dB to 1dB. Further increment in fiber length beyond 10km, both setups show almost same Stokes power although there was an additional Brillouin gain provided by the laser cavity. The reason behind this behavior can be attributed to the highly gain attenuation

in long SMF length. Therefore, for long SMF length, the main contribution of the additional Brillouin gain is to reduce the SBS threshold power as depicted in Figure 4.12. In addition, in laser cavity, even all the SMF lengths exhibited same Stokes power but still 10km length can be considered as an optimal length since it has lower saturated SBS threshold value. Therefore, high Stokes number can be generated using 10 km compared to SMF lengths of 3, 5 and 8 km.

4.3.5 Output Optical Spectrum

Figure 4.14 exhibits the output Stokes spectrum for these two different techniques in short and long fiber length of 5km and 18km. This figure clearly shows the additional gain provided by the laser cavity compared to conventional technique in 5 km fiber length and how this gain was highly attenuated in 18 km fiber length. In other word, these results prove the result depicted in Figure 4.13 in which the generated stokes power was almost saturation in laser cavity due to the high gain attenuation in long fiber length

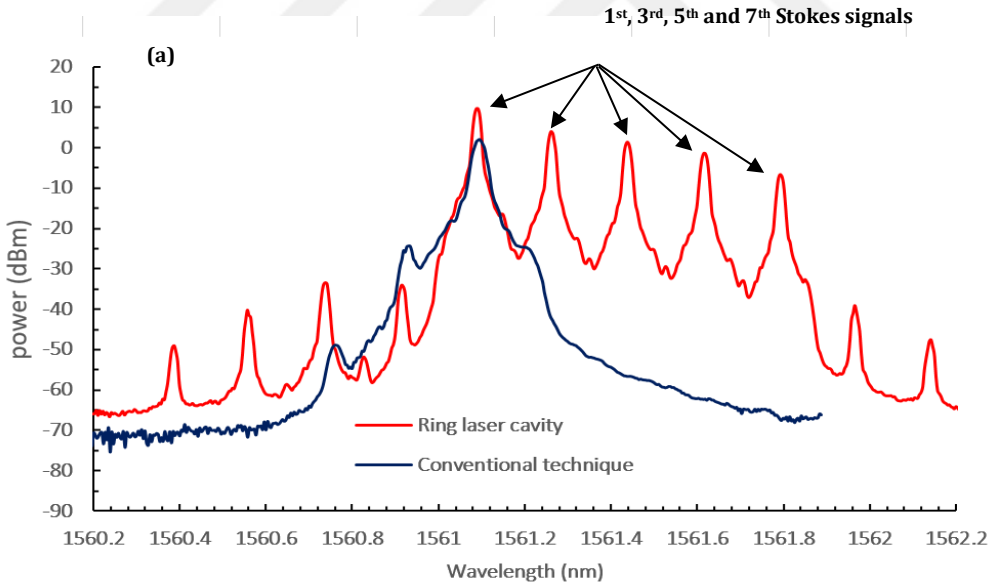


Figure 4.14 Output optical spectrum for the conventional technique, and ring BFL cavity at a) 5 km SMF length and (b) 18 km fiber length.

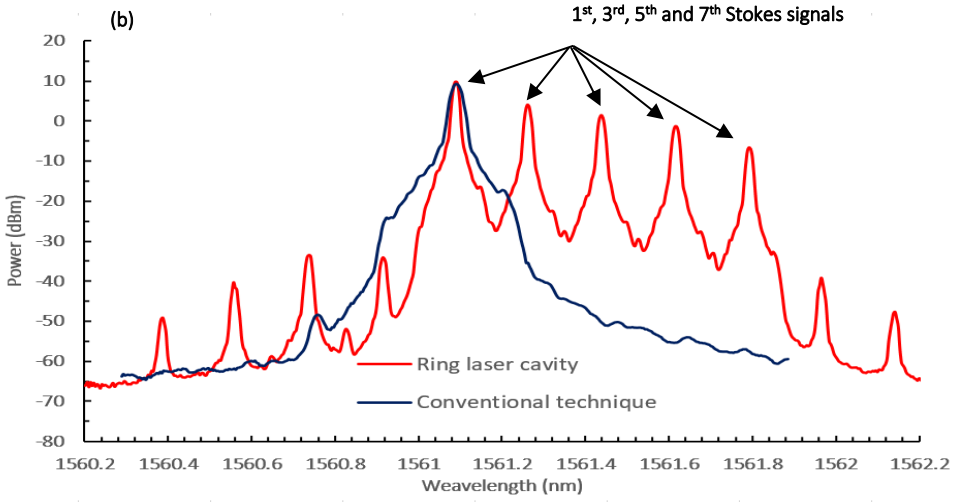


Figure 4.14 (continued) Output optical spectrum for the conventional technique, and ring BFL cavity at a) 5 km SMF length and (b) 18 km fiber length.

4.3.6 First Stokes Power and Threshold Comparison in Different Cavities

Ring BFL cavity and linear BFL cavity presented in our previous work [130] was compered in terms of maximum 1st stokes power and 1st Stokes threshold power as depicted in Figure 4.15. In term of Stokes threshold power, ring BFL cavity shows lower threshold values as compared to the threshold values in linear BFL cavity for all selected fiber lengths. That is because the generated Stokes signal in ring cavity is directly injected to the far end of SMF at z=L through an optical coupler. While the generated Stokes signal will pass two times through an optical coupler to be passed through SMF at z=0 then to be reflected by the optical mirror and reinserted again to the SMF at z=L. In other word, higher gain can be provided in Ring laser cavity due to lower loss path compared to linear BFL cavity. On other side, linear BFL cavity illustrates highest 1st Stokes signals power for all selected SMF lengths as compared to ring BFL cavity even though that both cavities were tested under same conditions in term of BP power and component specifications. Also ring BFL cavity shows lower threshold powers compared to the linear BFL. The reason can be attributed to the fact that 1st Stokes signal saturates once the 2nd starts to oscillate. Therefore 1st stokes signal in ring BFL cavity was saturated faster due to the lower 2nd stokes signal threshold compared to the higher 1st Stokes signal saturation in linear BFL cavity due to the higher threshold for the 2nd Stokes signal.

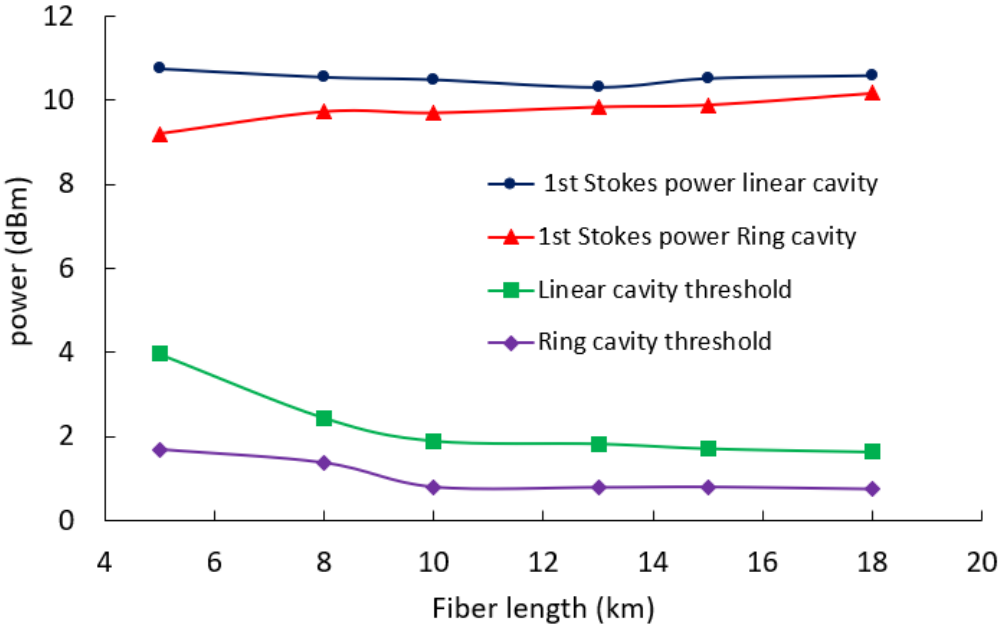


Figure 4.15 Maximum of 1st Stokes signal power and threshold for linear and ring BFL cavities as a function of SMF length.

4.4 Triple Brillouin Frequency Shift (30 GHz)

4.4.1 Experimental Setup

Figure 4.16 illustrates the experimental setup of the proposed MBEFL cavity. The cavity structure consists of three 3-ports Circulators (Cir1, Cir2 and Cir3), 50:50 coupler, two dispersion-compensating fibers (DCF1 and DCF2) as a Brillouin gain medium with a length of 6 km for each one, EDFA section consist of an erbium-doped fiber (EDF) with a length of 10 m type M12, 1480 nm pump power unit, wave division multiplexer (WDM), and wave selective coupler (WSC) to extract the residual pump power outside the cavity. A Brillouin signal is provided by an external tunable laser source (TLS) with a maximum power of 14 dBm and wavelength range of 150 nm (1480–1630 nm). An optical isolator is connected directly to the TLS and to DCF2 to prevent any reflection signal back.

Firstly, BP signal is injected to DCF1 though 3-dB coupler and port 2 of Cir1. Once the BP signal reach the threshold power, 1st Stokes signal (S1) with down shift frequency of 0.08 nm is generated and propagated in opposite direction of the BP

signal to be inserted to another end of the DCF1 via port 2 of Cir2. The S1 signals starts to be circulated between Cir1 and Cir2 due to the unidirectional propagation of these two circulators. In this time once S1 exceed the threshold, 2nd order Stokes signal (S2) with a down shift frequency of 0.17 nm is generated. The S2 signal is injected to EDFA section for accumulating more gain. The amplified S2 signal is directed through Cir3 port 2 to be inserted to DCF2. Now the 3rd order Stokes signal (S3) with a wavelength spacing of 0.25 nm can be generated if the inserted amplified S2 signal exceeds the threshold power. In this stage, the transmit- ted power of S2 signal can be observed at the other end of DCF2. The produced S3 signal travel through Cir3 (port2 to port3) and 3-dB coupler to complete one round trip. Higher order Stokes signal with 0.25 nm wavelength spacing can be generated in the same way until the total gain become below the threshold value. Optical spectrum analyzer (OSA) with a resolution of 0.03 nm was connected to the optical coupler to monitor the induced triple Brillouin Stokes signals.

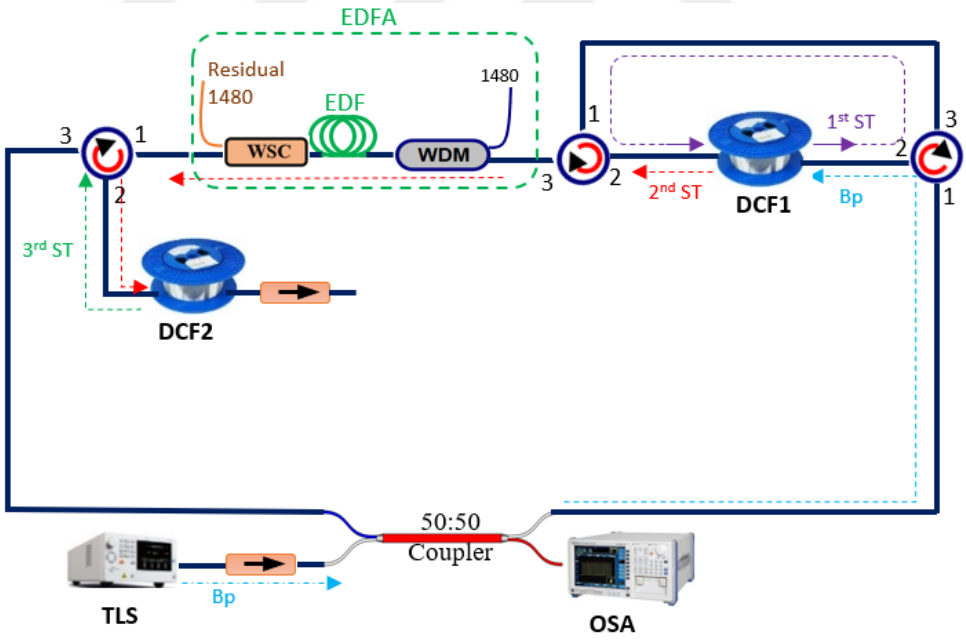


Figure 4.16 Experimental setup of the proposed MBEFL cavity.

4.4.2 Self Lasing Cavity Mode Oscillations

Figure 4.17 shows the self lasing cavity mode oscillations (Erbium gain) in case that BP is off and at the maximum 1480 nm pump power of 220 mW. The spectrum was

measured within 60 nm span (1535–1595 nm). The free running mode has 10 nm band (1560–1570 nm) at the centre wavelength of 1562 nm. Determination of these oscillation modes were necessary to select the optimal BP wavelength to achieve an optimal gain in the cavity. The free running modes are basically depending on two parameters; emission spectrum of the Erbium ions and the total gain provided by the cavity structure. On the other hand, Erbium ions emission is related to the physical properties of the Erbium types that already used in EDFA section and these emission bands are lies usually between 1535 to 1565 nm (C-band region) for M12 type. These modes can be shifted towards L-band region or to the C-band region depending on whether strong or weak feedback inside the cavity is achieved.

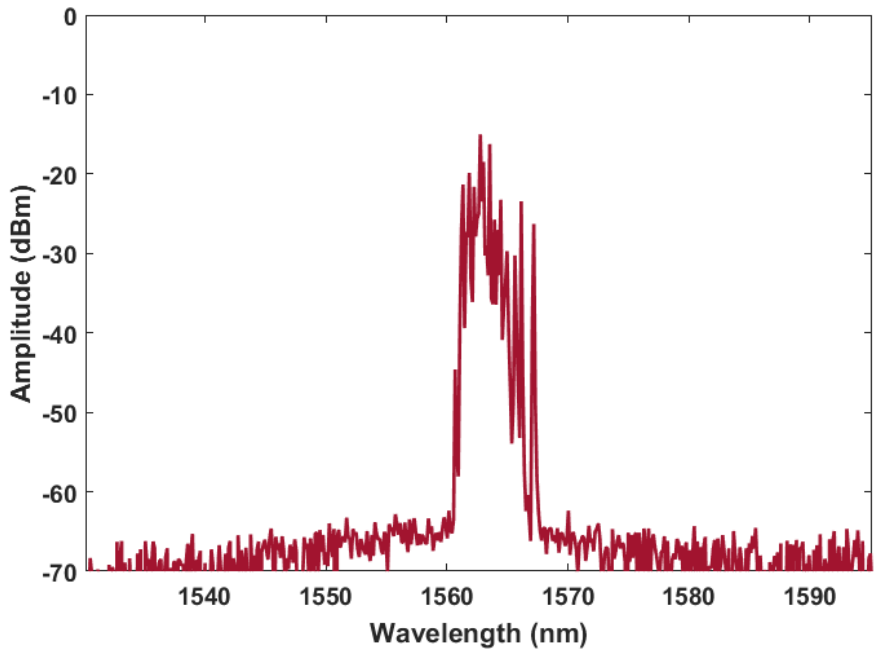


Figure 4.17 Self lasing cavity modes Erbium gain without BP at the maximum pump power of 220 mW.

4.4.3 Stokes Spectrum at Threshold Power

At the BP power of 13 mW, firstly, the threshold power (required 1480 nm pump power) for all generated triple Stokes signals S3, S6, S9, S12, and S15 was depicted in Figure 4.18.

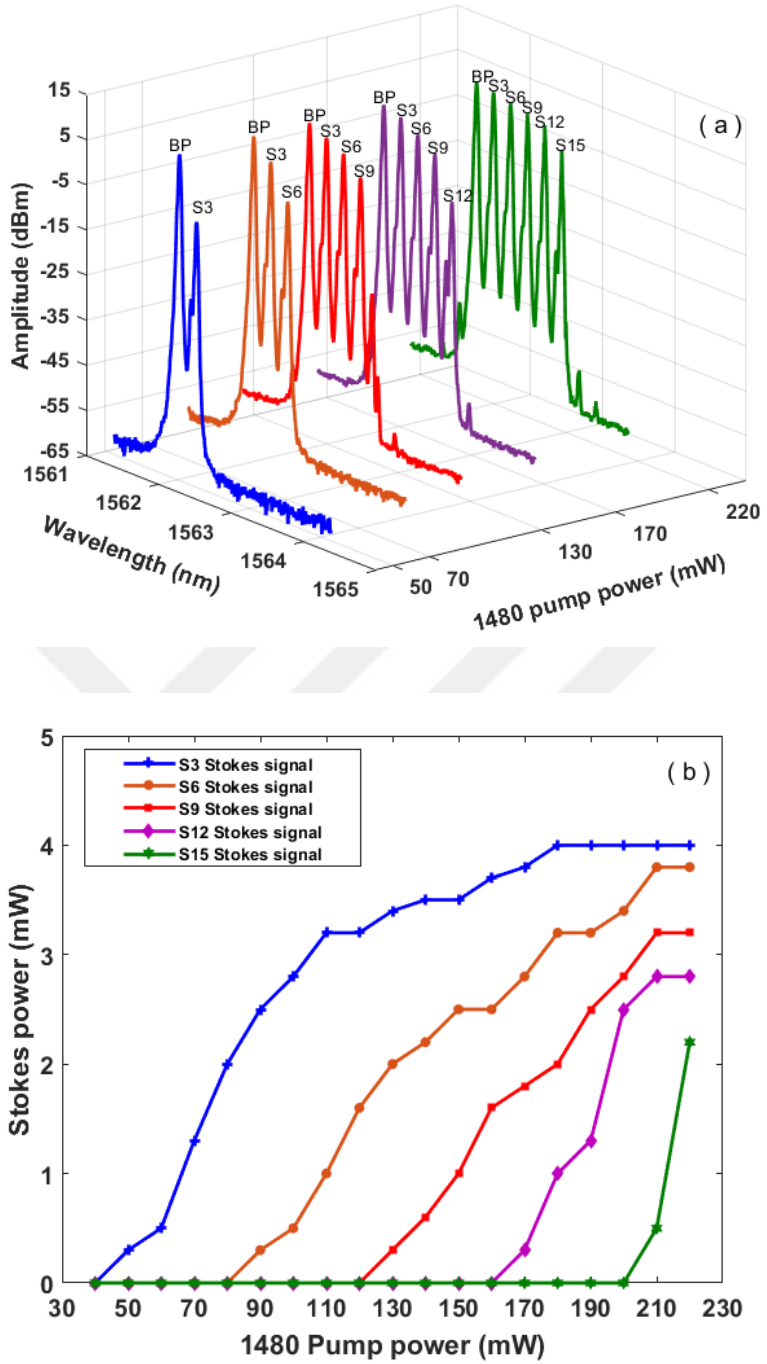


Figure 4.18 (a) Stokes spectrum at threshold power. (b) Stokes power variation versus pump power.

Referring to Figure 4.17, the BP wavelength was selected to be in the center of the free running mode oscillations at 1562 nm. Figure 4.18a shows the values of the pump power at which the certain triple Stokes signals were generated. The 1st triple Stokes signal (S3) was oscillated at pump power of 50 mW. Further increment of the pump

power to the point at which the 1st Stokes power was effective, the 2nd triple Stokes signal (S6) was appeared at pump power value of 90 mW. In the same way, the pump power was more increased, and the 3rd triple stokes signal (S9) was observed at 130 mW pump power. When the valued of the pump power was 170 mW, the 4th triple Stokes signal (S12) was generated. On the other side, the 5th Stokes signal (S15) required high pump power of 220 mW to be oscillated. Figure 4.18b was conducted for further improvement that shows the effect 1480 nm pump power on the generated Stokes signals. First triple Stokes signal was clearly appeared at 50 mW and rapidly increased with the increment of the pump power until it was saturated at the point in which S6 signals was appeared at 90 mW. Same behavior was recorded for S6 signal, and it was saturated once the S9 signal was oscillated at 170 mW. The last triple Stokes signal was generated at the pump power of 220 mW and resulted in S6 signal saturation. Compare our results with the results conducted by [42], 6 triple Stokes lines were generated while only 4 triple Stokes signals obtained by them.

4.4.4 Output Channels Tunability

MBEFL cavity tunability is showed in Figure 4.19 at a 220 mW and 13 mW for 1480 nm and BP, respectively. The proposed setup illustrates broadly tunability about 50 nm (1530–1580 nm). Two parameters were utilized that achieving this broad range. The first is using high BP power that can achieve an additional Brillouin gain more than the threshold power required for generating the Stokes signal. This additional Brillouin gain allowed the Brillouin Stokes signal to be tuned for a wider range [131]. Secondly, using WSC to extract the residual pump power outside the cavity, using such high pump power of 220 mW, the residual pump power at the end of EDFA section is effective that can cause high competition with BP power and highly impact the tunability [132]. By comparing our finding with other tunability offered by [83] [31,133,134] that they used different filtering technique for enhancing free running mode oscillation, our results illustrate wider tuning range with no filtering technique is needed. In addition, the tunability presented by [135] that they used high BP power but without residual pump power capturing out of the cavity was limited to 40 nm.

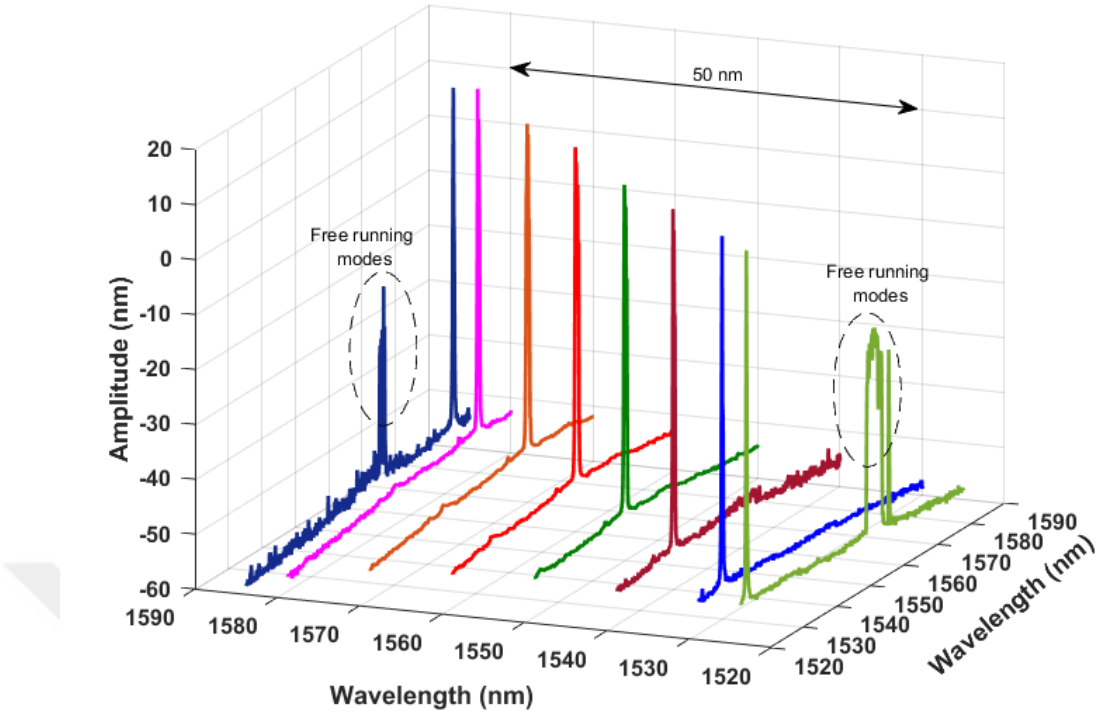


Figure 4.19 Output channels tunability of MBEFL cavity.

4.4.5 Spectrum of the Output Laser Comb at Various BP Wavelengths

Figure 4.20 illustrates the spectrum of the output laser comb at various wavelengths of BP within the tuning range wavelengths; 1530, 1540, 1550, 1562, 1570, and 1580 nm. 13 mW and 220 mW were used for BP and 1480 nm respectively. When the BP wavelength was tuned near to the free running modes oscillation center, 1550 to 1570 nm, six triple Stokes signals were recorded as shown in Figure 4.20 b–e. While at BP wavelengths of 1530 nm and 1580 nm (a bit far from the Erbium gain center), five triple Stokes channels were observed as shown in Figure 4.20a, f. It can be noticed that the number of the generated Stokes signals were not reduced much. That is due to using high BP power which is able to compensate the free running oscillation modes and to achieve high Stokes gain inside the cavity. At the center of the free running mode oscillations of 1562 nm, at which the maximum gain can be gotten, the best Stokes performance in terms of gain difference between BP and the 1st triple Stokes signal and OSNR was achieved. In this context, no gain difference was recorded and the highest OSNR of 45.5 dB was observed. While a gain difference range of 0.4 to

1.7 dB was noticed at different BP wavelengths. In addition, high OSNRs of more than 44 dB were presented at all different BP wavelengths.

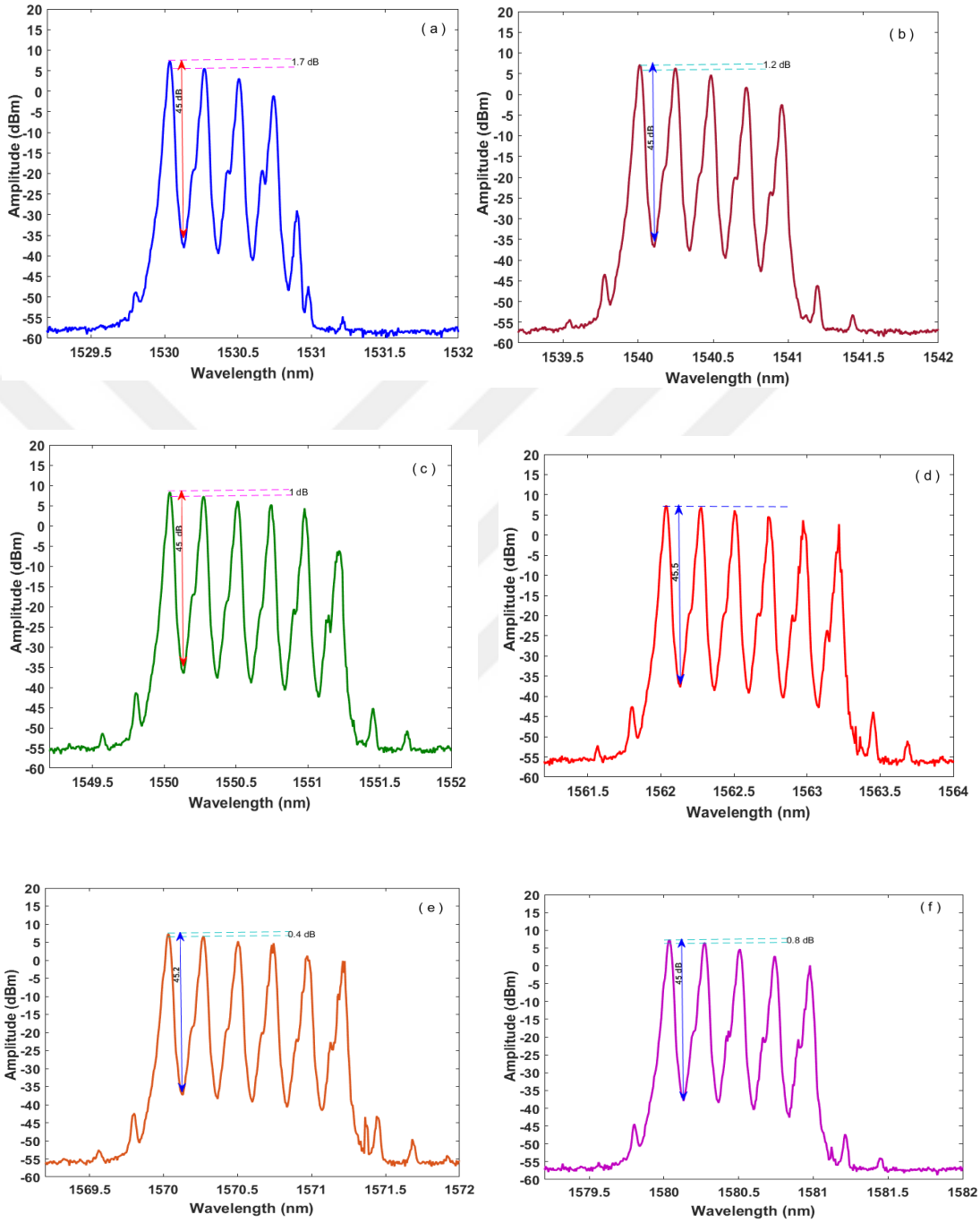


Figure 4.20 Output spectrum of Stokes signals generated at different BP wavelength (a) 1530, (b) 1540, (c) 1550, (d) 1562, (e) 1570, (f) 1580 nm.

4.4.6 Stokes Signals Power Stability

Figure 4.21 illustrates the maximum Stokes power oscillation for the generated 33 GHz signals within a duration of one hour. The output Stokes powers stability were recorded at each 5 minutes until 60 minutes.

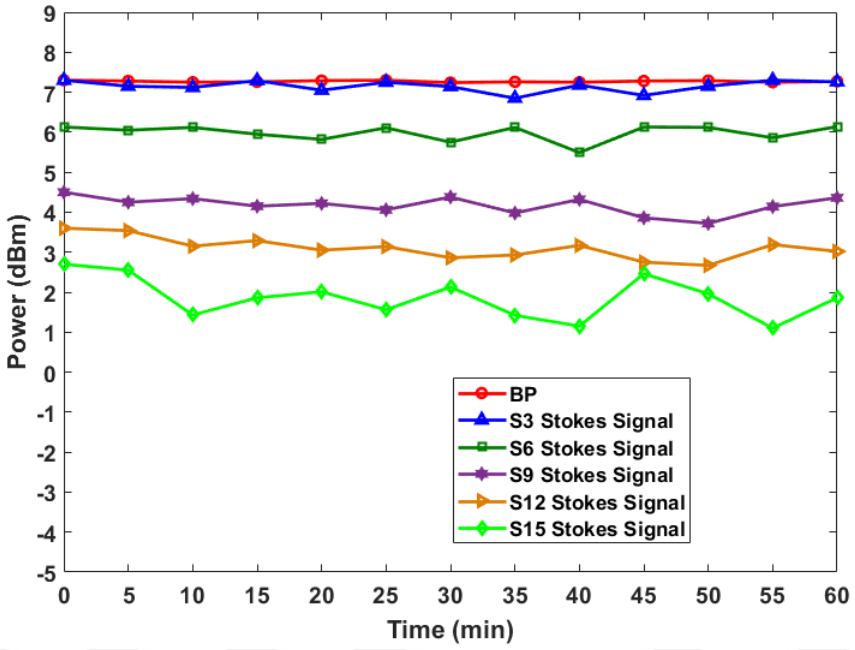


Figure 4.21 Peak power stability of Brillouin Stokes signals at a pump power of 220 mW.

The maximum power of 13 mW and 220 mW were used for both of BP and 1480 nm pump power respectively. High stability less than 1 dB was recorded for BP (0.06 dB), S3 (0.5 dB), S6 (0.65 dB), S9 (0.78 dB), and S12 (0.93 dB) signals. Higher variation of 1.6 dB was recorded for S15 due to that this Stokes power is always below the saturation power level and it will by largely affected within the cavity.

4.5 Quadruple Brillouin frequency shift (40 GHz)

4.5.1 Experimental setup

The experimental setup of the proposed MBEFL cavity is shown in Figure 4.22. The cavity structure consists of Cir1 (3-port circulator), Cir2 (4-port circulator), Cir3 (3-port circulator) 3-dB 2 × 2 coupler, three couplers with coupling ratio of (90:10), two dispersion-compensating fibers (DCF1 and DCF2) as a Brillouin gain medium with a

length of 6 km for each of them, and two EDFA gain blocks (EDFA1 and EDFA2). The EDFA1 section consist of an erbium-doped fiber (EDF) with a length of 5 m type M12, 1480 nm pump power unit, wave division multiplexer (WDM), and wave selective coupler (WSC) to extract the residual pump power to be used as a pump for EDFA2. The EDFA2 section consist of EDF length of 5 m, WDM coupler to inject the residual pump power comes from EDFA1 and WSC to capture the residual pump outside the cavity. Laser signal is provided by an external tunable laser source (TLS) with a maximum power of 14 dBm and wavelength range of 150 nm (1480–1630) nm. An optical isolator is connected directly to the TLS to prevent any reflection signal back to TLS. At first, BP signal is injected to EDFA1 though 3-dB coupler to get a pre-amplification before it inserted to the first Brillouin gain media (DCF1) though port 2 of Cir1. Once the amplified BP signal reach the threshold power, 1st Stokes signal (S1) that has down shift frequency of 0.08 nm is generated and propagated in opposite direction to the inserted BP signal to be inserted to another end of the DCF1 via port 2 of Cir2. Most of the inserted BP power is transferred to S1 signal due to the high Brillouin gain coefficient of DCF1 [32].

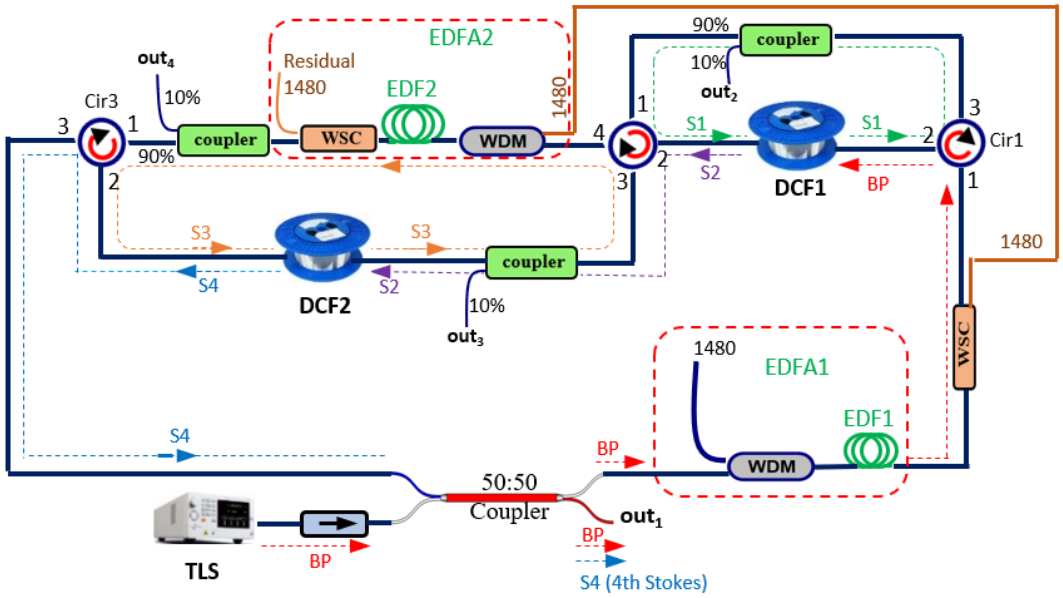


Figure 4.22 Experimental setup of the proposed MBEFL cavity.

On the other side, the transmitted BP power is totally attenuated through DCF1 due to the high absorption coefficient. The generated S1 signal is circulated between Cir1 and

Cir2 due to the unidirectional propagation of these two circulators and it can only be monitored at out2. Once the circulated S1 power exceeds the threshold, 2nd order Stokes signal (S2) with a down frequency shift of 0.17 nm is generated which can be observed by out3 before it inserted to DCF2 through port 3 of Cir2. In DCF2, 3rd order Stokes signal (S3) with a wavelength spacing of 0.25 nm will be generated once the inserted S2 power reach the threshold value. Since DCF2 has the same DCF1 specifications, S2 power is transferred to S3 signal and the transmitted power of S2 signal is totally attenuated. The generated S3 signal is injected to EDFA2 section for accumulating more gain. The amplified S3 signal is directed through Cir3 port 2 to be inserted to DCF2 at the far end. Again, due to the unidirectional propagation of Cir2 and Cir3, S3 signal forced to be circulated between these two circulators and it can only be recorded at out4. If the circulated S3 signal reached the threshold power, the 4th order Stokes signal (S4) with a wavelength spacing of 0.33 nm can be generated. The produced S4 signal travel through Cir3 (port 2 to port 3) and 3-dB coupler to get more gain in EDFA1 section before completing one round trip. Higher order Stokes signal with 0.33 nm wavelength spacing can be generated until the total gain become below the threshold value. Optical spectrum analyzer (OSA) with 0.03 nm resolution was used at four output ports out1 (BP, S4, S8, S12), out2 (S1, S5, S9, S13), out3 (S2, S6, S10), and out4 (S3, S7, S11) for monitoring the induced 0.33 nm Brillouin Stokes signals.

4.5.2 Free Running Cavity Modes (Erbium Gain)

Figure 4.23 shows the free running cavity modes (Erbium gain) in the absence of BP power at 225 mW of 1480 nm pump power within 65 nm span (1525–1590) nm. It can be noticed that the self lasing cavity mode has 8 nm band (1557–1565 nm) at the center wavelength of 1560 nm. The oscillation modes were recorded in order to choose the BP wavelength that can get the maximum gain inside the cavity.

4.5.3 Threshold Power (1480 nm Pump Power Required)

The required 1480 nm pump power that generate quadruple spacing (0.33 nm) Stokes signals S4, S8 and S12 at fixed BP power of 20 mW was firstly recorded as depicted Figure 4.24. BP wavelength of 1560 nm was used to be at the center wavelength of the free running cavity modes.

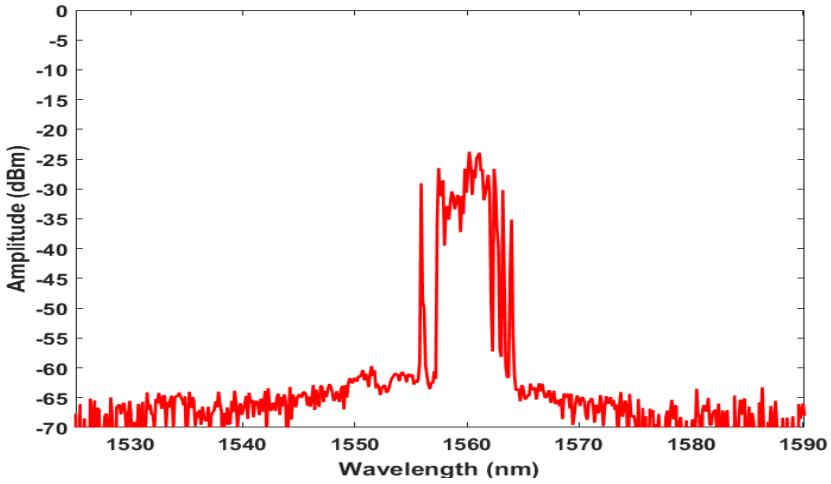


Figure 4.23 Self lasing cavity modes (Erbium gain) at the maximum pump power of 225 mW.

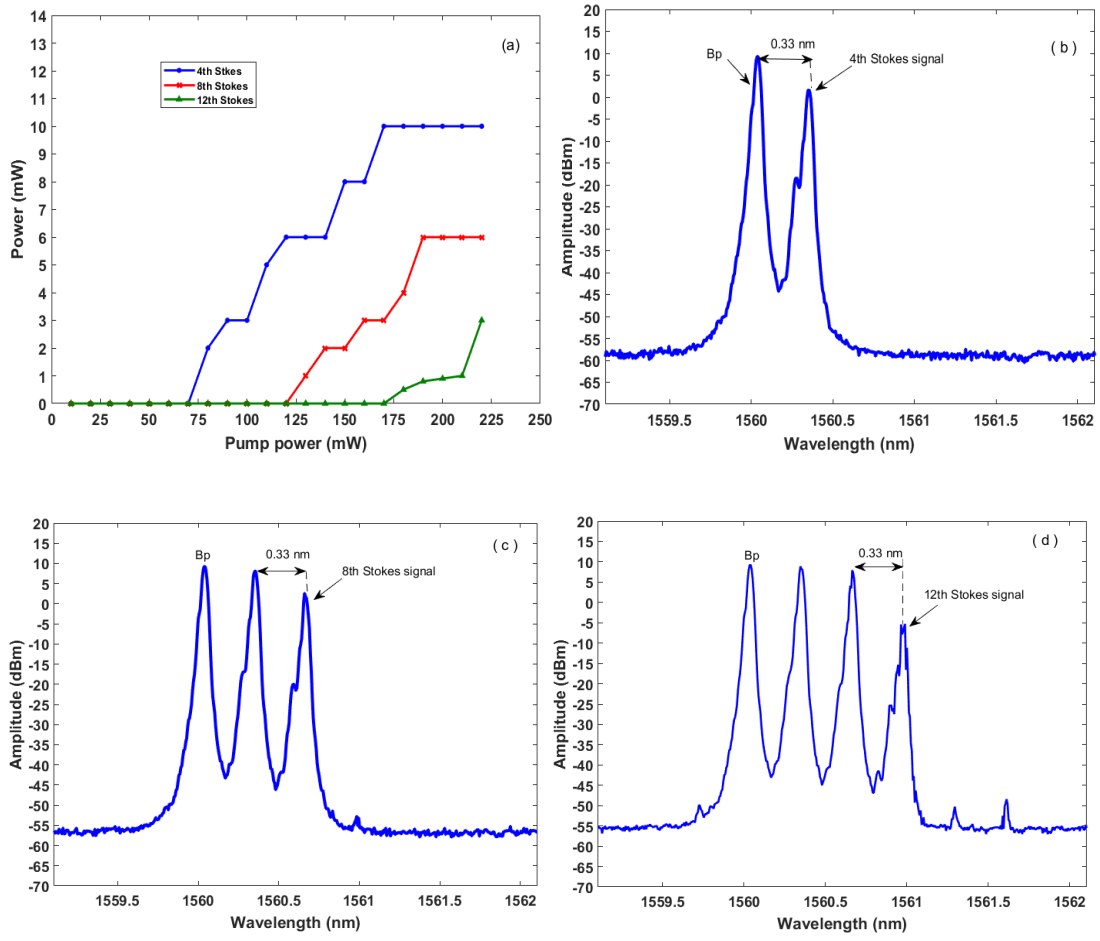


Figure 4.24 Threshold power for S4, S8, and S12. (a) Stokes power variation as a function of 1480 pump power, (b, c, and d) output spectrum for S4, S8, and S12 at the threshold power of 70, 120, and 170 mW respectively.

The 1480 nm pump power was varied and the value of the pump power at which all these Stokes signals were generated was recorded. By referring to Figure 4.24a, the required pump power for the 1st 0.33 nm Stokes signal was 70 mW. Further increment in pump power, the 1st 0.33 nm Stokes power was increased. With the increment of the 1st Stokes power, 2nd 0.33 nm Stokes signal is generated at 120 mW of 1480 pump power. As the 2nd order 0.33 nm Stokes signal appeared, the 1st quadruple Stokes tend to be saturated, and it was totally saturated once the 2nd quadruple Stokes power became effective. The 1480 was increased further, so far at the value of 170 mW, the 3rd 0.33 nm Stokes signal was oscillated and once its power was effective, the 2nd quadruple Stokes signal was saturated. More results were recorded for the output spectrum power of the 1st and the 2nd quadruple Stokes signal at the required pump power for each one of them to be oscillated as depicted in Figure 4.24 (b, c, and d) respectively.

4.5.4 Stokes Power Variation as a Function of BP Power

Further results were conducted to show the effect of the BP power variation on the generated quadruple Stokes powers. Figure 4.25 illustrates the Stokes power variation as a function of BP power. Same BP wave- length of 1560 nm (at the center wavelength of the erbium gain) was used. BP power was varied from 5 dBm to the maximum value of 14 dBm in the step of 1 dBm. Within the BP power variation, the generated quadruple Stokes powers were recorded. In general, the generated Stokes power is mainly depending on the induced gain inside EDFA1 and EDFA2 sections at certain BP power. Refereeing to Figure 4.25a, the 4th Stokes power slightly increased with the increment of BP power until it will reach the maximum power value. This is due to at high BP power, both of EDFA1 and EDFA2 achieve the maximum output power. On the other side, 8th Stokes power shows saturation in its value within the BP power variation. The reason can be attributed to the fact that the generated 4th Stokes power values (subsequent BP power for 8th Stokes signal) were almost at high power that saturate both of EDFA1 and EDFA2. Different behavior was observed for the 12th Stokes power which was highly affected by the BP power variation. It was rapidly increased with the increment of the BP power. At such low BP powers (smaller than 8 dBm), EDFA1 and EDFA2 were not saturated so higher induced gain can achieved.

Further increment in BP power, EDFA1 starts to saturate and led to saturate EDFA2 as well. Therefore, the saturation in the 12th Stokes power was takes place. Finally, when the EDFA1 reached its maximum output power, EDFA2 will be saturated more that decrease the generated Stokes power. More results were recorded for the output spectrum power of the 4th, 8th, and 12th quadruple Stokes signal at different BP powers of 12, 13 and 14 dBm as depicted in Figure 4.25(b, c, and d) respectively. It is further proving the saturation and the reduction in the 8th and the 12th Stokes power.

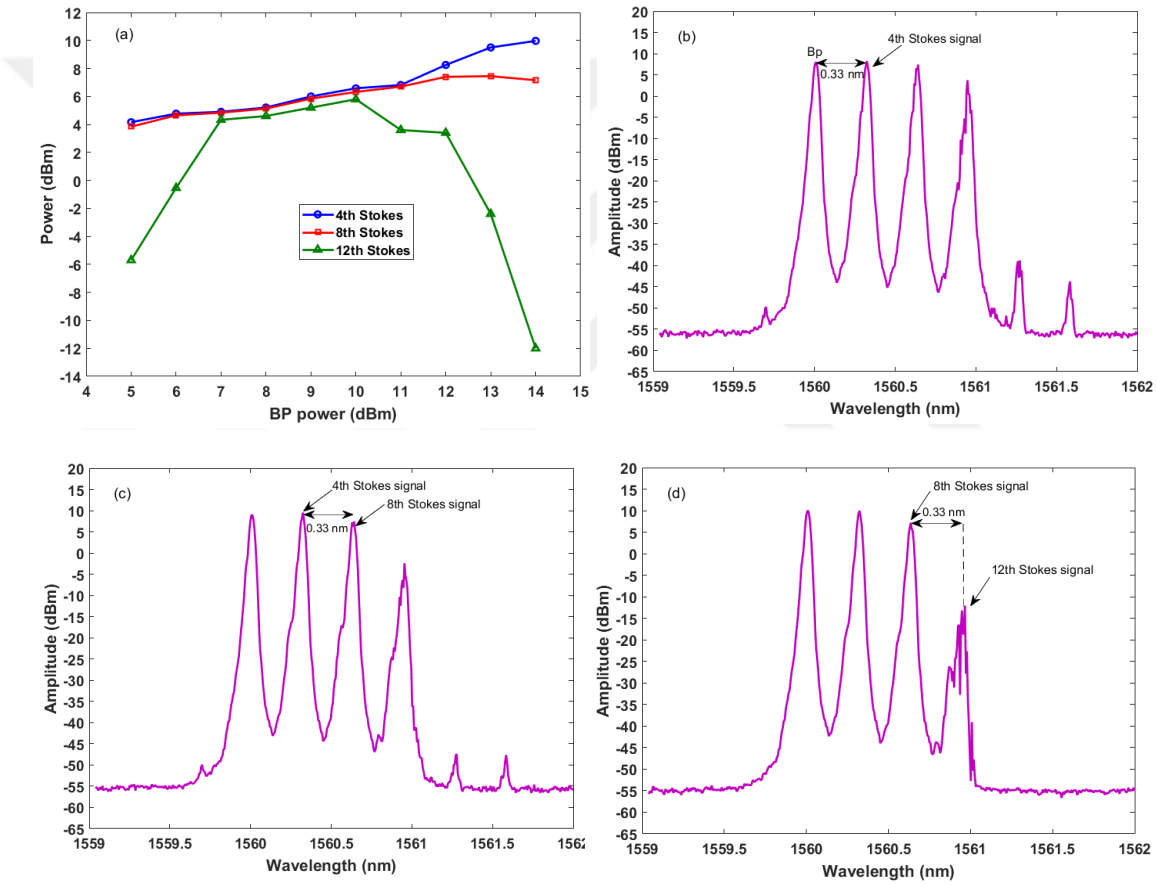


Figure 4.25 (a) Stokes power variation as a function of BP power, (b, c, and d) output spectrum for S4, S8, and S12 at the different BP power of 12, 13, and 14 dBm respectively.

4.5.5 Output Laser Comb Spectrum of the Multi-Output Ports

Figure 4.26 illustrates the output spectrum of the laser comb at a maximum pump power of 225 mW and Bp power of 20 mW. BP wavelength was set at 1560 nm (central

wavelength of free running cavity modes). Four quadruple Stokes signals (BP, S4, S8, S12) with equally wave- length spacing of 0.33 nm were achieved at out1 with an output ratio of 50% as depicted in Figure 4.26a. High Stokes peak powers of 9.2, 9, 7.5, and 4.5 dBm were observed for the generated Stokes signals respectively. Out2 also exhibited four 40 GHz channel spacing Brillouin Stokes signals (S1, S5, S9, S13) at output ratio of 10% as illustrated in Figure 4.26b.

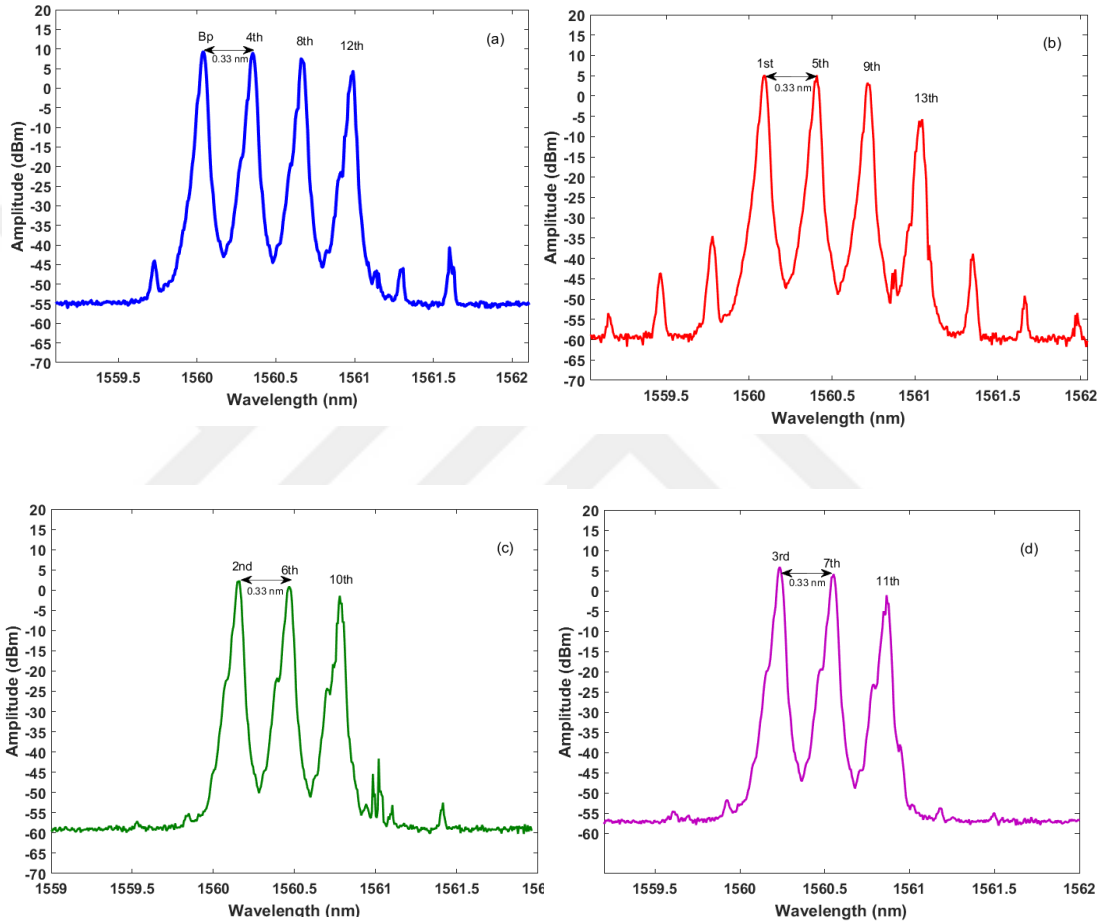


Figure 4.26 The output spectrum of the multi-output ports laser comb at a maximum pump power of 225 mW and BP power of 20 mW (a) out1 (b) out2 (c) out3 (d) out4.

Peak powers of 5, 5, 3, and −5 dBm were observed for the generated Stokes signals respectively. In addition, Figure 4.26c shows another 40 GHz Stokes signals (S2, S6, S10) with a maximum peak power of 2.5, 1, and −1.5 dBm at out3 with an output ratio of 10%. Furthermore, Figure 4.26d illustrates more 40 GHz Stokes signals (S3, S7, S11) which has peak powers of 6, 4.5, and −1 dBm respectively were recorded at out4

with 10% output ratio. The observed high stokes powers at out4 was higher than the output Stokes power at out2 that is because the generated Stokes signals (S3, S7, S11) with experience an additional gain within EDFA2 section. Also, it can be noticed from the results, that large optical signal to noise ratios (OSNRs) more than 50 dB was recorded for all generated stokes signals. According to these different output ports, up to 14 Stokes signals with a quadruple channel spacing of 0.33 nm were achieved.

4.5.6 Output Channels Tunability

The tunability of MBEFL cavity is illustrated in Figure 4.27 at maximum pump powers of 225 mW and 20 mW for 1480 nm and BP, respectively. The proposed structure shows widely tuning range up to 60 nm (1530–1590) nm in the absence of self lasing cavity modes. Many parameters were contributed for achieving such wide range; high BP power, pre-amplification technique, and capturing the residual pump power outside the cavity. High BP power cause an additional Brillouin gain required to reach the threshold power. This additional Brillouin gain allowed the Brillouin Stokes signal to be tuned for a wider range [131].

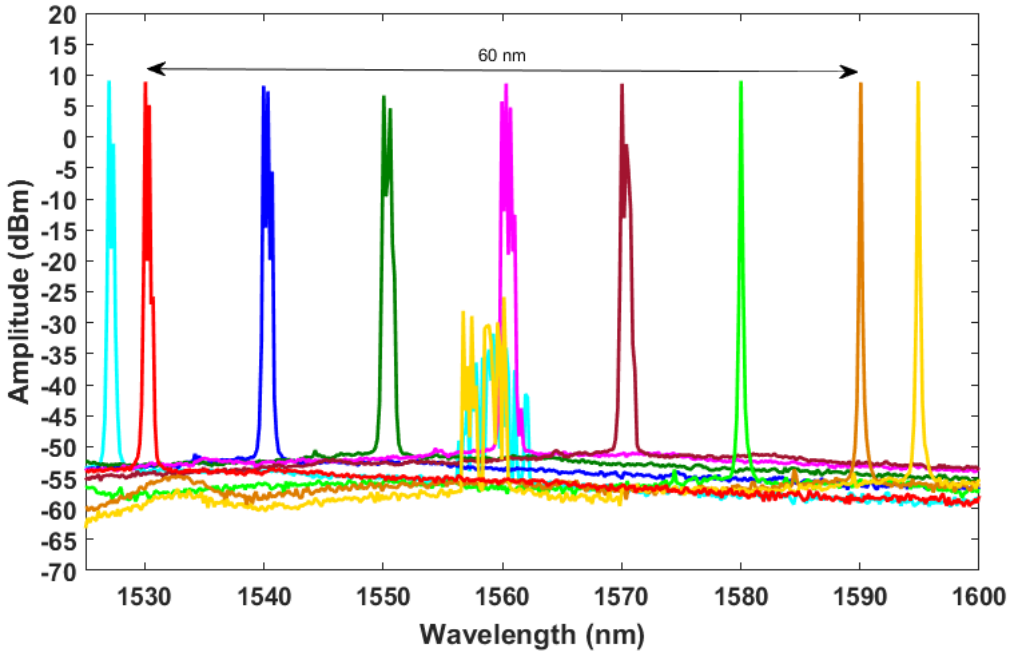


Figure 4.27 Output channels tunability of MBEFL cavity at different wavelengths with BP and pump powers of 20 mW and 225 mW, respectively.

In the pre- amplification technique, the injected BP to the Brillouin gain media collects more energies through EDFA1 section. due to the high BP power intensities, the generated Brillouin Stokes signal intensity is significantly increased. Regarding to the high Brillouin Stokes power, EDFA2 section forced to be worked deeply in the saturation regime. In the saturation, the effect of homogeneous saturation along the spectral gain led to achieve uniform gain. Subsequently, the free running modes gain is also saturated under the cavity losses, so it can be totally suppressed in the laser cavity [12]. Using high 1480 nm pump power of 225 mW, the residual pump power at the end of EDFA2 section was effective as illustrated in Figure 4.28. This residual power takes more energy in EDFA1 that can cause high competition with BP power and reduce the cavity tunability. Therefore, WSC was used to extract the residual pump power outside the cavity to achieve wider tuning range [132]. Comparing our results with other results presented by [31,132–134] that they used filtering technique for controlling free running mode oscillation, our results illustrates wider tuning range and no filtering technique is needed.

4.5.7 Impact of wave selective coupler on the performance

Figure 4.28 shows the effect of inclusion WSC after EDFA2 section. Figure 4.28a illustrates the output spectrum of the residual 1480 pump power at the pump port of the WSC at the maximum pump power value of 225 mW.

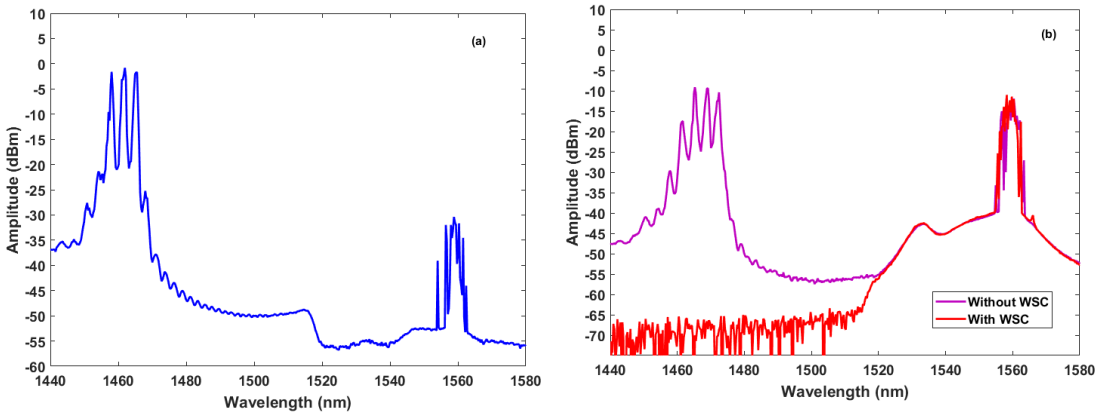


Figure 4.28 Output spectrum at the maximum 1480 pump power of 225 mW, (a) the residual 1480 nm pump power at WSC. (b) free running modes at out4 with and without WSC with 10% output ratio.

Extracting the residual pump power effect is indicated in Figure 4.28b. It is quite clear that by inclusion WSC the residual pump was captured outside the cavity. These unwanted modes can directly affect the laser cavity tunability through increasing the competition with the BP power.

4.5.8 Output Spectrum of the Generated Stokes Signals

Figure 4.29 shows the output spectrum of the laser comb at different BP wavelengths within the entire tuning range; 1530, 1540, 1550, 1560, 1570, 1580 and 1590 nm. Maximum power of 225 mW and 20 mW was used for 1480 nm and BP respectively. BP wavelengths of 1530 nm and 1590 nm exhibited two quadruple output Stokes signals as shown in Figure 4.29(a, g). The reduction in the number of channels was due to BP wavelengths which was a bit far from the central wavelength of the Erbium gain (1560 nm). Therefore, BP and the induced 1st quadruple Stokes signal experience low gain in EDFA1 so it was not able to generate higher order quadruple Stokes signal. 1st quadruple Stokes signal peak power of 4 dBm was achieved for these two different signals wavelengths. In addition, the gain difference between BP and 1st quadruple Stokes signal for these two different BP wavelengths was 5.3 dB. As the BP wavelength was tuned to be closer to the self lasing cavity modes oscillation (Erbium gain), three output quadruple Stokes channels with highest output peak power were produced at 1540 nm as depicted in Figure 4.29b. Up to 8.2 dBm and 5 dBm were measured for the 1st and the 2nd quadruple Stokes signals and the gain difference between the BP and the 1st stokes was 1.8 dB. At BP wavelengths ranges of 1550 nm to 1580 nm, the proposed structure shows four output channels with no gain difference between BP and the 1st quadruple signal as illustrated in Figure 4.29(c, d, e and f). Within the entire tuning range starting from 1530 nm to 1580 nm in the increment of 10 nm, the difference in peak power between the 40 GHz and 22 GHz were 44.6, 47, 49, 49, 48.5, 47.5 and 41.3 dB, respectively. In addition, high OSNRs almost more than 50 dB were recorded for the generated Stokes signals in the tuning range bandwidth.

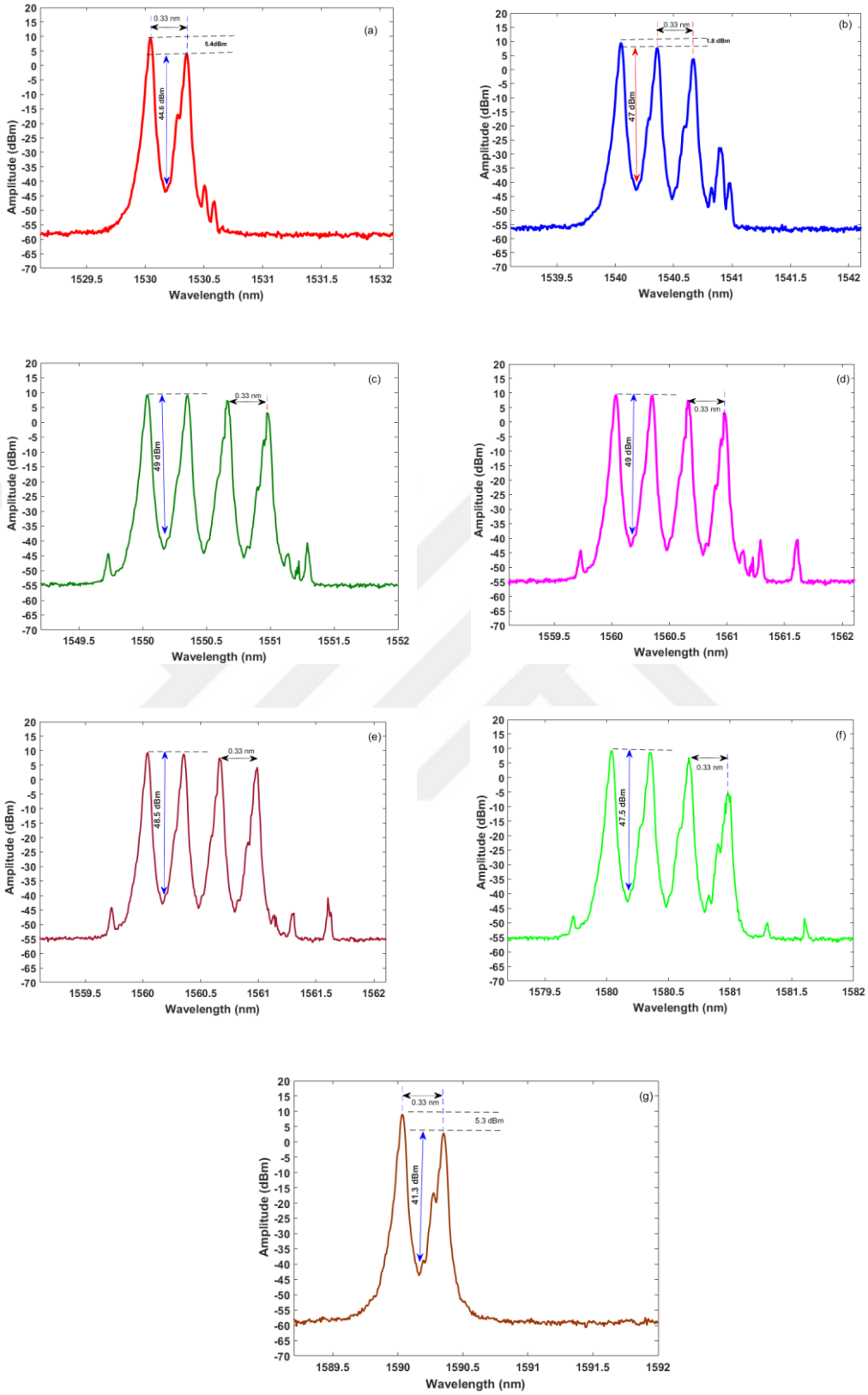


Figure 4.29 Output spectrum of the generated Stokes signals at different BP wavelength at the maximum 1480 nm pump powers of 225 mW and 20 mW of Bp power

4.5.9 Peak Brillouin Stokes power stability

Figure 4.30 depicts the fluctuation in the peak power (maximum Stokes power) for the generated 40 GHz channels within one hour. The stability of the output Stokes signals powers were investigated over 60 min for every 5 min at the BP power of 20 mW at 1560 nm wavelength and 1480 nm pump power of 225 mW. The four generated 40 GHz Brillouin Stokes channels (BP, S4, S8, and S12) illustrate high stable operation within the entire investigation period. Maximum power fluctuations of 0.07 dB, 0.7 dB, 0.91 dB and 1.72 dB were recorded for the BP, S4, S8, and S12 Stokes signals, respectively. High fluctuation was observed for S12 signal due to this signal does not reach its saturation level thus it became highly affected by the gain fluctuation inside the cavity.

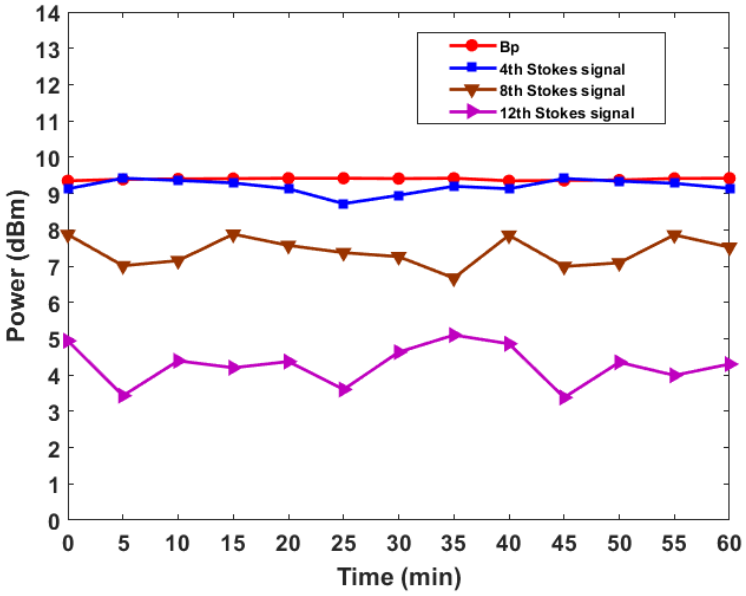


Figure 4.30 Peak power stability within a period of one hour for the Bp, S4, S8, and S12 Brillouin Stokes signals at a pump power of 225 mW and a BP wavelength of 1560 nm with a power of 20 mW.

4.6 Quintuple Brillouin frequency shift (50 GHz)

4.6.1 Experimental Setup

Figure 4.31 illustrates the experimental setup of the proposed 50 GHz MBEFL cavity. The cavity structure consisted of 3-port circulator (Cir1) and two 4-ports Circulators (Cir2 and Cir3), 50:50 coupler (this ratio was used so that the inserted BP power can

be effectively large and able to compensate the free running modes achieved by EDFA1), four 10:90 optical couplers (C1, C2, C3, and C4) these low output ratios were used to make sure that high Brillouin gain power for all generated Stokes signal can be lunched through the cavity to generate the higher order Stokes signals, three dispersion-compensating fibers (DCF1: 6km, DCF2: 6km, and DCF3: 3km) as a Brillouin gain medium, two EDFA sections consisted of an erbium-doped fiber (EDF) with a length of 10 m type M12, 5m M5 type, 1480 nm pump power unit, wave division multiplexer (WDM) coupler, and two wave selective couplers (WSC1, and WSC2). WSC1 was used to pump the EDFA2 section and WSC2 was implemented to extract the residual pump power outside the cavity. A Brillouin signal was provided by an external tunable laser source (TLS) with a maximum power of 14 dBm and wavelength range of 150 nm (1480–1630) nm. An optical isolator was connected directly to the TLS and to DCF3 to prevent any reflection signal back. Optical spectrum analyzer (OSA) with a resolution of 0.03 nm was connected to the multi-output ports (port 1, port2, port3, port4 and port5) to monitor the induced quintuple Brillouin Stokes signals.

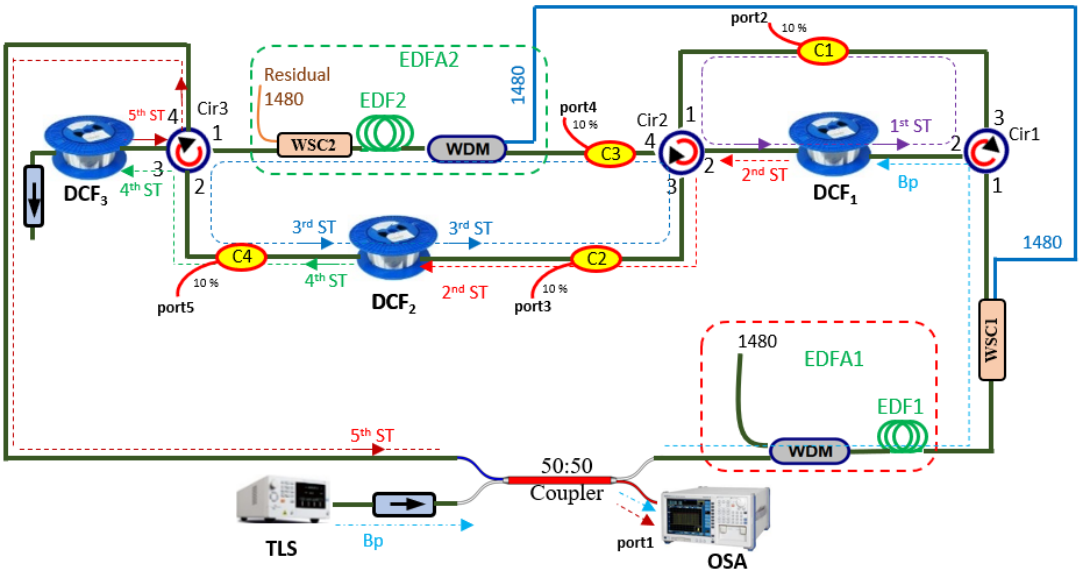


Figure 4.31 Experimental setup of the proposed MBEFL cavity.

Firstly, BP signal was injected to DCF1 though 3-dB coupler and port 2 of Cir1. Once the BP signal reached the threshold power, 1st Stokes signal (S1) with down shift

frequency of 0.08 nm was generated and propagated in opposite direction to the lunched BP signal then to be inserted to another end of the DCF1 via port 2 of Cir2. The generated S1 signals started to be circulated between Cir1 and Cir2 due to the unidirectional propagation of these two circulators. At this time, when S1 exceed the threshold, 2nd order Stokes signal (S2) with a down shift frequency of 0.17 nm was generated. The generated S2 signal was directed through Cir2 port 3 to be inserted to DCF2. Now the 3rd order Stokes signal (S3) with a wavelength spacing of 0.25 nm can be generated if the inserted S2 signal exceeded the threshold power. The produced S3 signal travel through Cir2 (port3 to port4) then to be injected to EDFA2 section for accumulating more gain and reinserted to other end of DCF2 via port 2 of Cir3. If the amplified S3 signal became higher than the threshold, 4th Stokes signal can be generated which will travel to DCF3 via port3 of Cir3. Same procedure can take place and the 5th Stokes signal can be achieved once the inserted 4th Stokes signal reached the threshold value. The generated 5th Stokes signal travel through cir3 (port 4) and 3-dB coupler before the first-round trip. Higher order Stokes signal with 0.4 nm wavelength spacing can be generated at the same way until the total gain become below the threshold value.

4.6.2 Self Lasing Cavity Modes

Figure 4.32 illustrates the self lasing cavity modes in the absence of BP power at 220 mW of 1480 nm pump power within 60 nm span (1530–1590) nm. The self lasing cavity mode has 10 nm band (1555– 1565 nm) at the center wavelength of 1562 nm. These oscillation modes were observed to select the proper Bp wavelength at which the maximum gain can be obtained. The self lasing cavity modes are mainly depending on two parameters; the emission spectrum of the Erbium ions and the total gain provided by the cavity structure. In another word, Erbium ions emission is related to the physical properties of the Erbium types that already used in EDFA1 and EDFA2 and these emission bands are lies usually between 1535 to 1565 nm (C-band region). These modes can be shifted towards L-band region (1570– 1590 nm) if there is strong feedback inside the cavity [105]. On the other side, it can be also shifted to the shorter wavelength if the losses inside the cavity was increased [106]. Therefore, the free running modes (Erbium gain) is strongly dependent on the total gain.

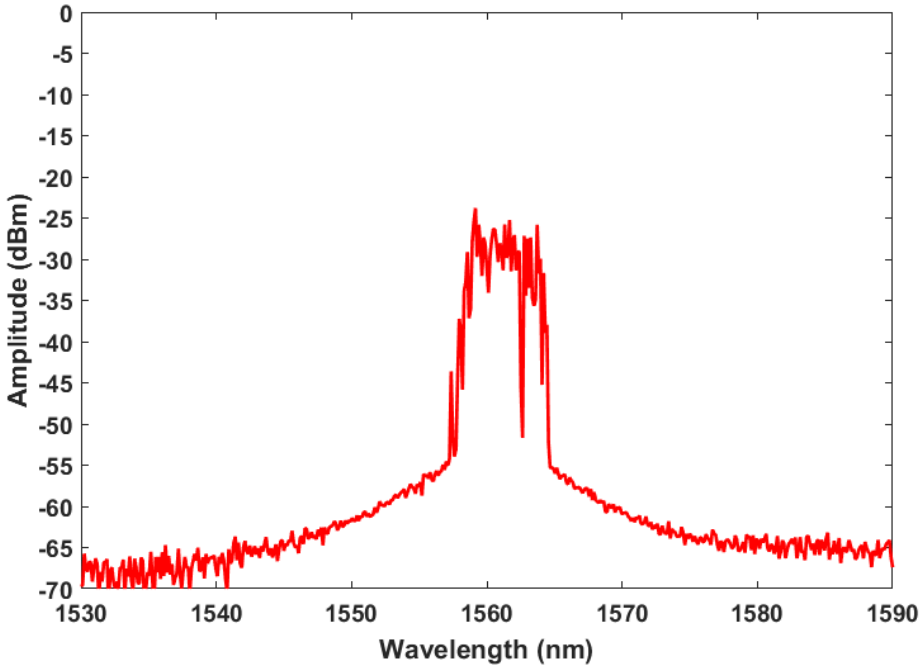


Figure 4.32 Free running modes (Erbium gain) at the maximum pump power of 220mW.

4.6.3 Output Spectrum for The Generated Stokes Signals at the Threshold Power

The pump power values at which the quintuple (0.4 nm channel spacing) Stokes signals S5, S10 and S15 at fixed BP power of 20 mW appeared was recorded as depicted in Figure 4.33. The optimal BP wavelength of 1562 nm, which lies in the center of free running modes, was utilized. From Figure 4.33a, 1st order quintuple Stokes signal (S5) appeared at 60 mW pump power. With the increment of the pump power, S5 Stokes power effectively increased. Further increasing in the pump power, beyond 130 mW, 2nd order quintuple Stokes signal (S10) was generated. As the generated S10 signal became effective at 160 mW, S5 signal power tends to be saturated. Since the pump power was increased further, so far at the value of 200 mW, the 3rd order quintuple Stokes signal (S15) was oscillated. Once the generated S15 Stokes power becomes active, S10 signal power was saturated. In addition, the output spectrum of the generated quintuple Stokes signals was recorded as the required pump power for these Stokes signals as depicted in Figure 4.33b.

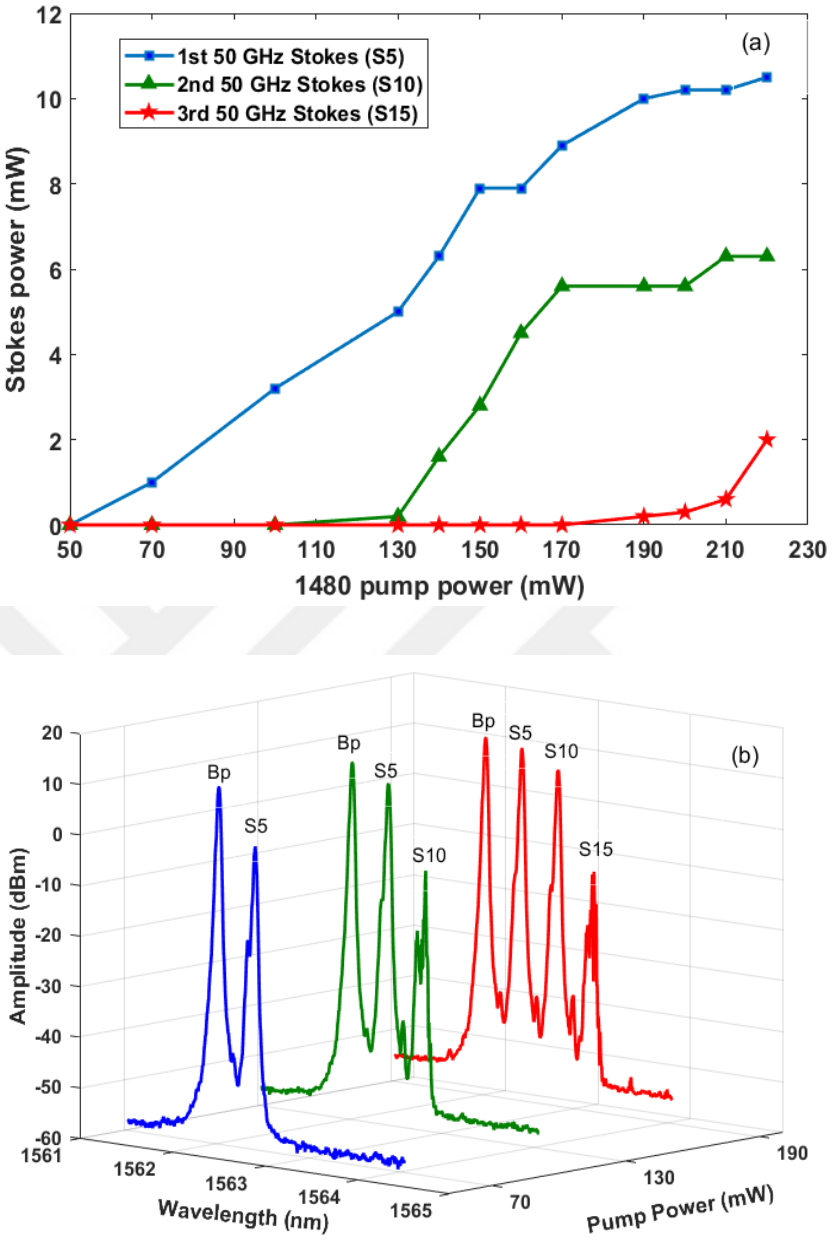


Figure 4.33 (a): Quintuple Stokes signals power vs 1480 pump power. (b): Output Spectrum for the generated Stokes signals at the threshold power (required 1480 pump power for each Stokes signal.

4.6.4 The Output Laser Comb Spectrum of the Multi-Output Ports

Figure 4.34 shows the output spectrum at different output ports of the generated quintuple Stokes signals at the maximum pump and BP powers of 220 mW and 20 mW respectively. Again, BP wavelength was chosen to be at the center of the self

lasing cavity modes oscillations at 1560 nm. Up to 4 quintuple Stokes signals (BP, S5, S10, and S15) with same channel spacing of 0.4 nm were observed at port1 with output ratio 50% as presented in Figure 4.34a.

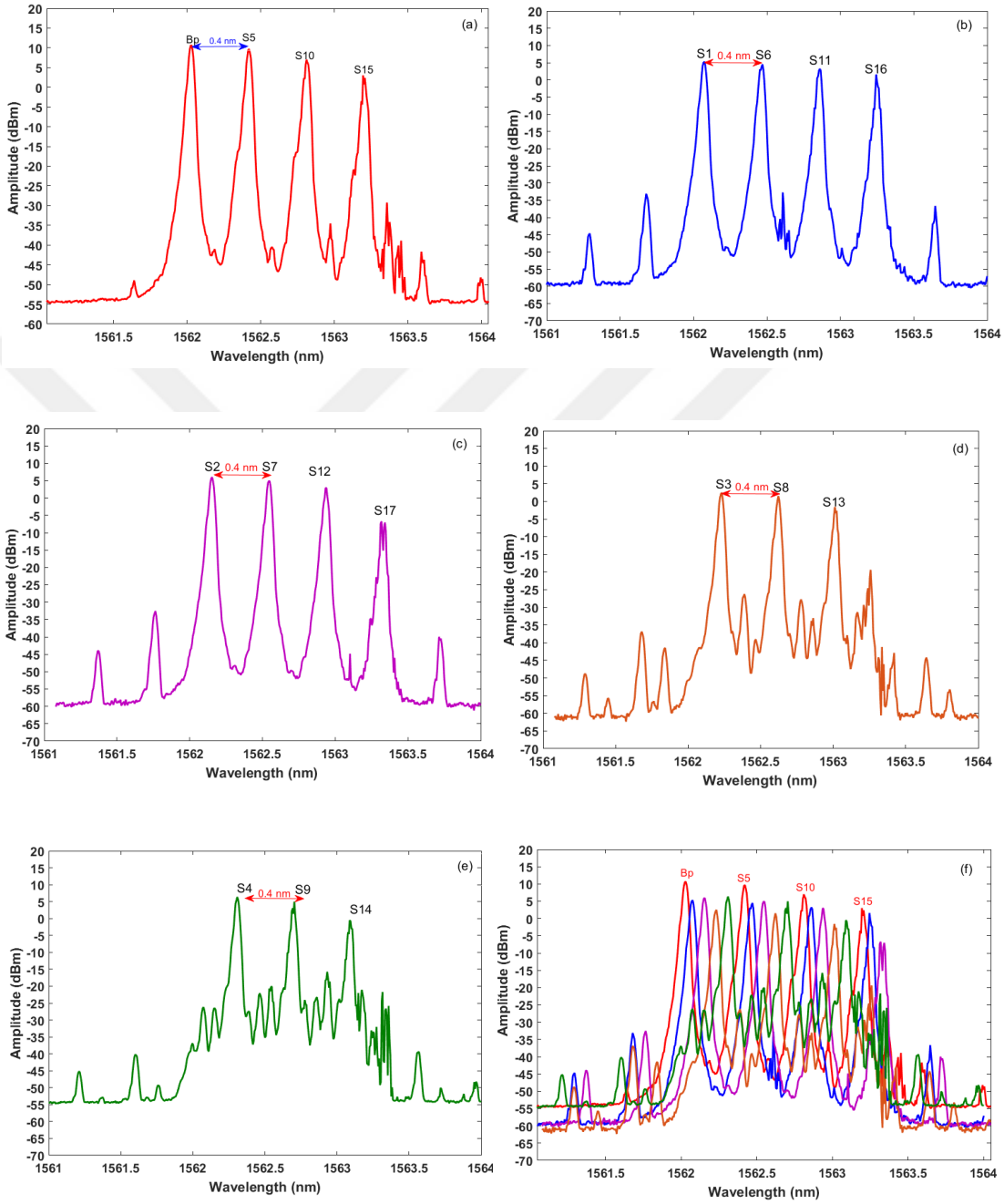


Figure 4.34 The output spectrum of the multi-output ports laser comb at a maximum pump power of 220 mW and BP power of 20 mW (a) port1 (b) port2 (c) port3 (d) port4 (e) port5 (f) All ports.

The recorded Stokes signals show high peak powers of 10.6, 9.6, 7, and 2.4 dBm for BP, S5, S10, and S15 respectively. Port2 likewise displayed four 5th channel spacing signals (S1, S6, S11, S16) with an output ratio of 10% as recorded in Figure 4.34b. Relatively high signals powers of 5.3, 4.4, 3.2, and 1.5 dBm were noticed correspondingly. Furthermore, Figure 4.34c also illustrates 4 quintuple Brillouin Stokes signals (S2, S7, S12, and S17) with highest peak powers of 5.1, 4.2, 2.4 and −6.7 dBm at port3 with an output ratio of 10%. In addition, Figure 4.34d shows 3 quintuple Stokes signals (S3, S8, S13) that has peak signal powers of 2.5, 1.5, and −1.5 dBm respectively and observed at port4 with 10% output ratio. At port5, also 3 quintuple Stokes signals (S4, S9, and S14) were generated with a peak power of 6.4, 4.9, and −0.5 dBm respectively. Port5 shows higher Stokes power than port4 that is due to Stokes signals (S3, S8, S13) that generates (S4, S9 and S14) experience an additional gain inside EDFA2 section. Referring to Figure 4.34(a, b, and c), high optical signal to noise ratios (OSNRs) greater than 50 dB was observed for all generated stokes signals. On the other side port4 and port 5 still exhibit good OSNRs of 29 dB. Up to 18 different quintuple Stokes channels were generated at output ports (port1 to port5).

4.6.5 Output Channels Tunability

Figure 4.35 shows the laser cavity tunability at the maximum powers of both of BP and 1480 nm powers of 20mW and 220 mW respectively. Wide tuning range of 40 nm (1540–1580 nm) was achieved without free running modes oscillations. Achieving such wide tuning range can be attributed to three different techniques: high BP power, BP preamplification, and extraction the residual pump power out of the cavity. Using high BP power permits an additional Brillouin gain (above the threshold) that can be tuned over a wide tuning range [131]. In addition, EDFA1 was used to achieve pre-amplification for BP and for all generated quintuple Stokes signals (S5, S10, and S15). Due to the high gain provided by EDFA1, higher order quintuple Stokes signals can be generated with high intensities. As a result, EDFA2 section forced to be worked in saturation region and the homogeneous saturation along the spectral gain led to achieve uniform gain. Therefore, the lasing cavity modes is also saturated, and it can be easily suppressed [12].

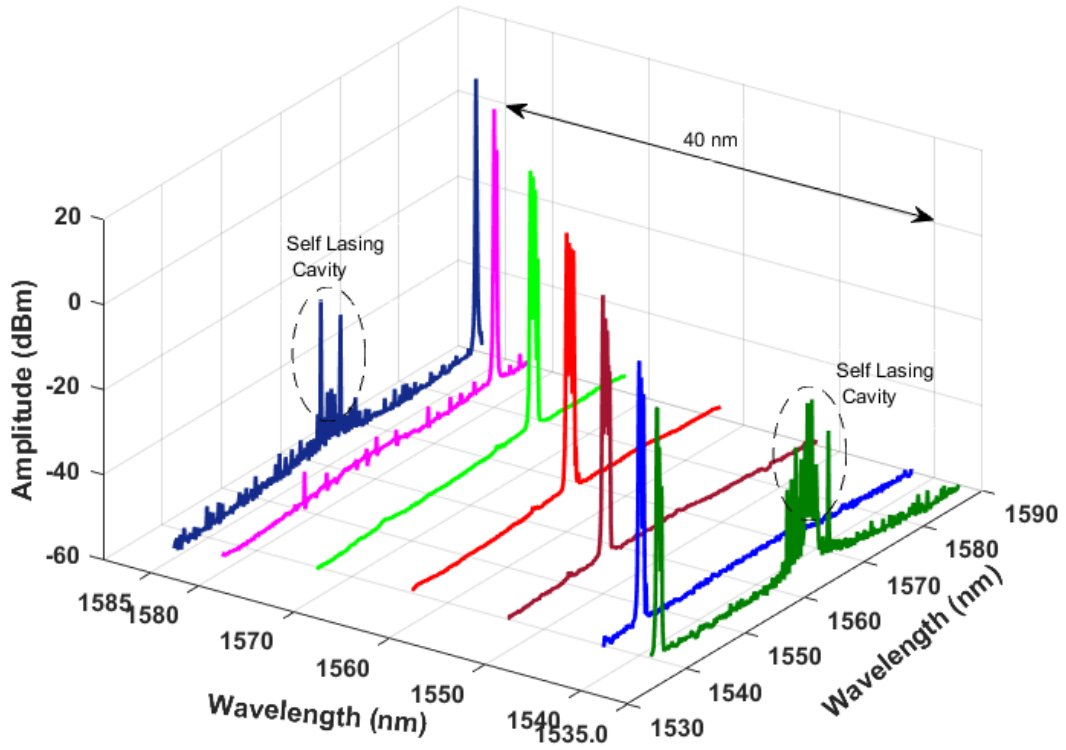


Figure 4.35 Output channels tunability of MBEFL cavity at different wavelengths at maximum of BP and 1480 nm powers of 20 mW and 220 mW respectively.

In our proposed structure, WSC2 was used in order to capture the residual pump power outside the cavity. Referring to Figure 4.31, if WSC2 is not included the residual pump after EDFA2 section will propagates inside the cavity that make more competition with Brillouin gain and reduce the cavity tunability. Hence, WSC2 was implemented to reduce the residual pump power competition with the BP power [132]. To show the effect of residual pump power, Figure 4.36 illustrates the inclusion WSC2 after EDFA2 section with a percentage output ratio of 10%. It is quite clear that the residual pump power was totally captured via WSC2. Using these three techniques, wider tuning range was achieved without filtering.

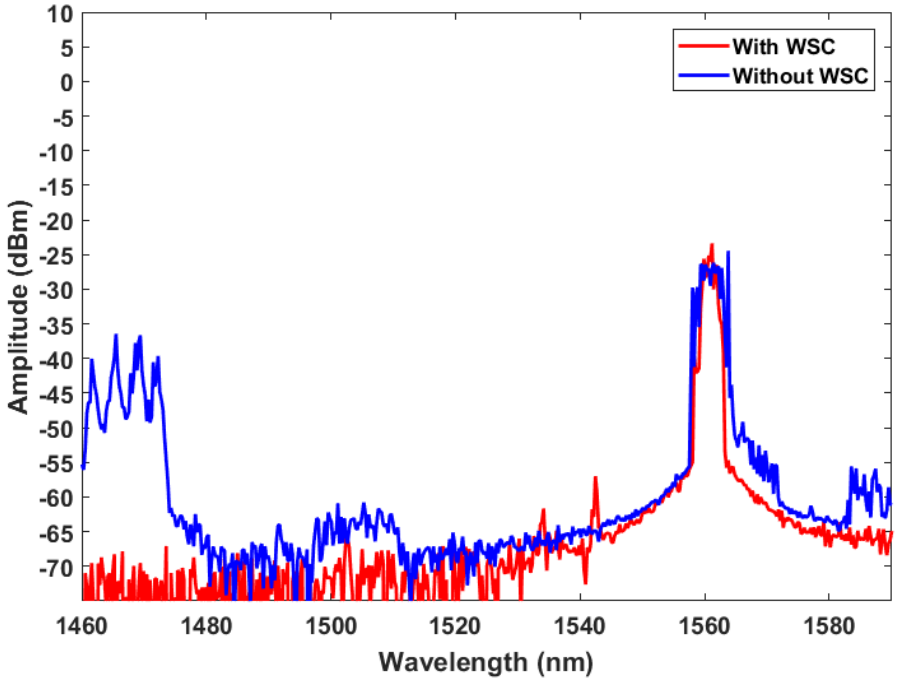


Figure 4.36 Free running modes with and without WSC2 with output ratio 10% after EDFA2 section

4.6.6 Output Spectrum of Stokes Signals Generated at Different BP Wavelength

The output laser spectrum at different BP wavelengths within the tuning bandwidth range; 1540, 1550, 1560, 1570, and 1580 is depicted in Figure 4.37. Same power of 20 mW and 220 mW were used for BP and 1480 nm respectively. BP wavelengths of 1540 nm exhibited three quintuple output Stokes signals as shown in Figure 4.37a. up to 10.5, 8.4 and 0.9 dBm were recorded for BP, S5 and S10 respectively which means that the gain difference between Bp and S5 was only 2.1 dB. Tuning the BP wavelength to 1550 nm to be closer to the free running modes center as depicted in Figure 4.37b, four quintuple Stokes signals were observed with 10.7, 9, 4.3, and −6.7 dBm for BP, S5, S10, and S15 respectively. At this time, the gain difference between BP and S5 was reduced to 1.7 dB. Figure 4.37(c, d) shows the laser spectrum at Bp wavelengths of 1562 nm and 1570 nm respectively, both BP wavelengths illustrates almost no gain difference between BP and the S5 signal. This is because these two BP values, which are very close to Erbium gain, can experience highest gain within the laser cavity. As the BP wavelength was tuned further to 1580 nm, three Stokes signals were generated as shown in Figure 4.37e. At such wavelength, that tuned out of Erbium gain center,

the generated Stokes number was reduced to three and the gain difference between BP and the first quintuple Stokes signals was increased to 1.5 dB. Within the whole tuning range bandwidth (1540–1580 nm), high optical signal to noise ratio more than 50 dB were achieved. For further improvement, Figure 4.37f was conducted to show the effect of the wavelength of the BP on the generated Stokes signals power.

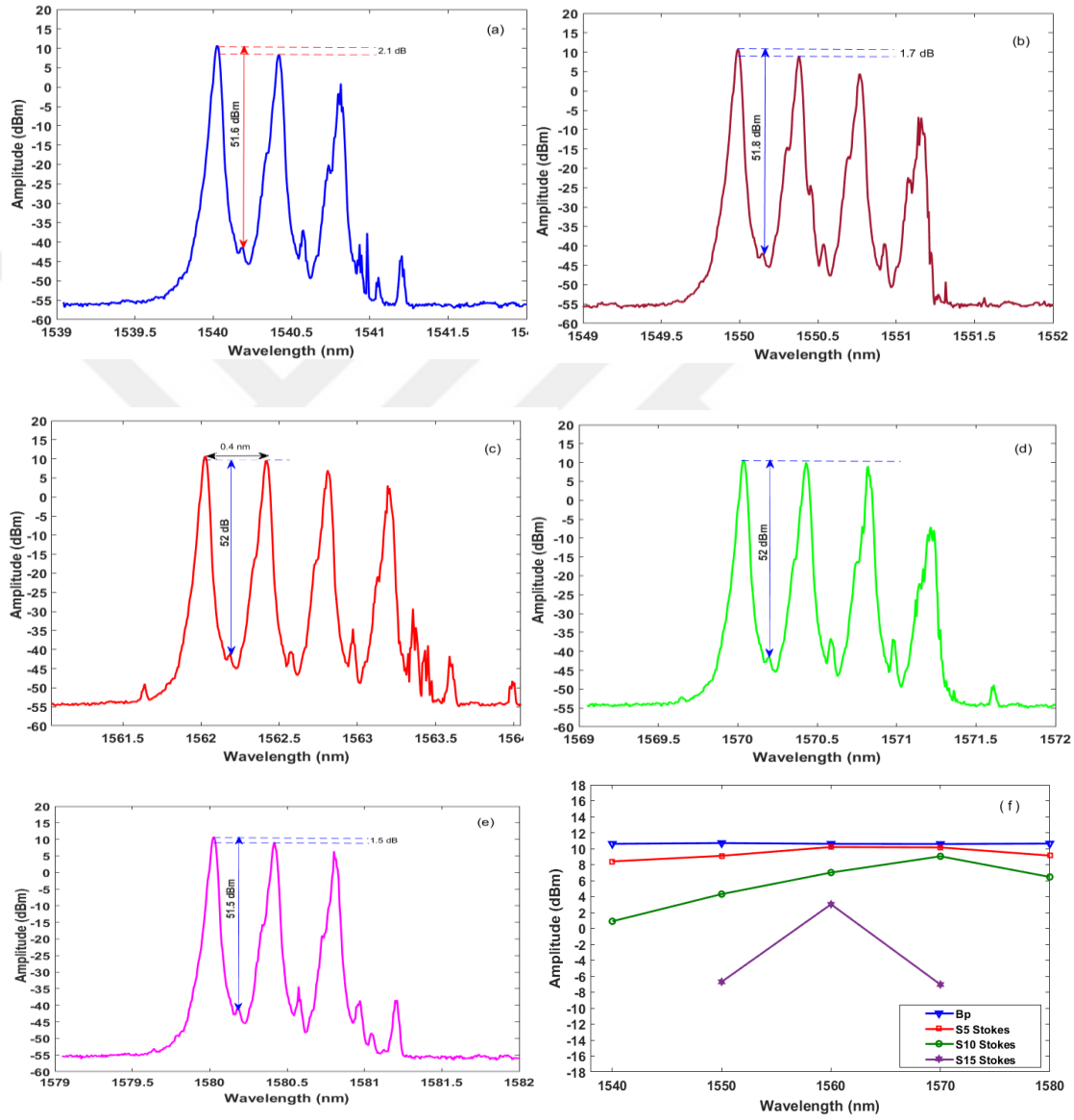


Figure 4.37 Output spectrum of Stokes signals generated at different Bp wavelength (a) 1540 (b) 1550 (c) 1562 (d) 1570 (e) 1580 (f) quintuple Stokes peak powers at different Bp wavelength.

4.6.7 Stokes Peak Power Fluctuation

Figure 4.38 illustrates the Stokes peak power fluctuation for the observed 50 GHz signals with one-hour duration. Stokes signals powers stability was examined over 60 min for every 5 min with BP and 1480 nm pump powers of 20 mW and 220 mW respectively. The quintuple Brillouin Stokes signals (BP, S5, S10, and S15) show an excellent stable operation during the whole investigation period. The recorded power fluctuations of 0.1 dB, 0.5 dB, 0.9 dB, and 1.9 dB were observed for the BP, S5, S10, and S15 Stokes signals, respectively. Relatively higher power fluctuation was noticed for S15 Stokes signal (below 3 dB) compared to other Stokes signals which is because this Stokes signal power did not reach the saturation level, hence it shows more gain oscillation inside the cavity.

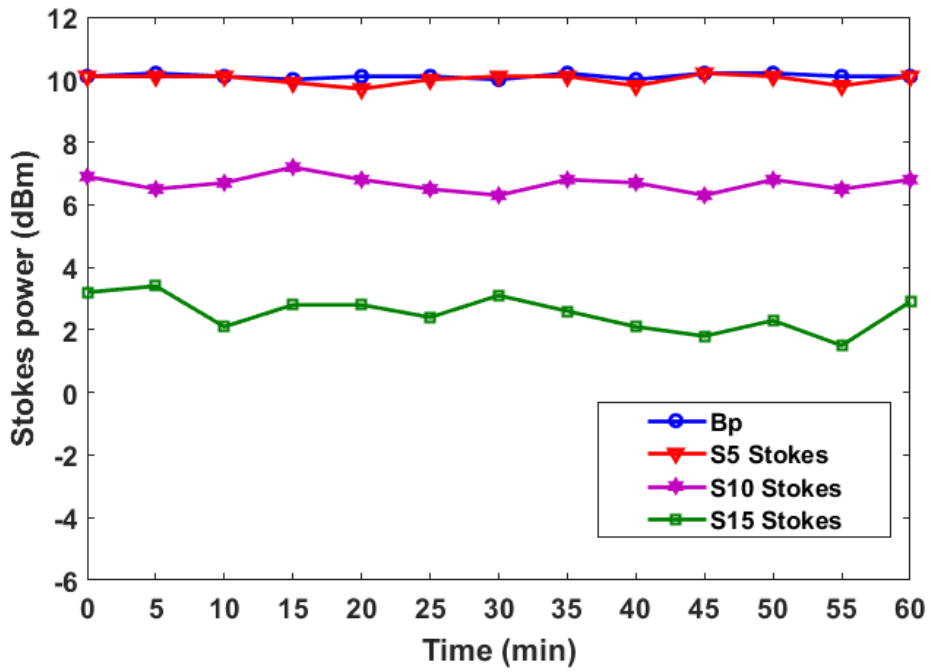


Figure 4.38 Peak power stability within a period of one hour for the BP, S5, S10, and S15 Brillouin Stokes signals at a pump power of 220mW and a Bp wavelength of 1562 nm with power of 20 mW.

CHAPTER 5

CONCLUSIONS AND FURTHER WORKS

5.1 Conclusions

Started with single Brillouin frequency shift design, the tunability of MBEFL utilizing a PEDF as an absorber section was effectively enhanced experimentally. An average of 10 signals can be tuned over a wide tuning range of 65 nm, that cover both of C and L-bands, from 1540 nm to 1605 nm at 1480 nm pump and Brillouin pump powers of 230 and 10 mW, respectively. The enhancement is attributed to both of PEDF absorption and emission bands in addition to its location inside the laser cavity. The main goal of using such PEDF was to reduce the free running modes competition towards BP power.

Then according to investigation study in double Brillouin frequency cavity, the influence of the bidirectional signal propagation on the Stokes power as well as on the SBS threshold has been experimentally demonstrated. 1st stokes signal power was examined in two different configurations of conventional technique and ring BFL cavity. High Stokes power was observed in ring BFL cavity in relatively short SMF length. This provided gain within the laser cavity was highly attenuated in long SMF length. In addition, SBS threshold was also studied using different SMF lengths. the threshold was reduced up to 90% in ring BFL cavity compared to conventional technique. Finally, the provided Brillouin gain and the Stokes threshold power in ring BFL cavity and linear BFL cavity were tested to show the effect of the loss path on the generated Stokes power. In addition, the effect of the 1st Stokes signal power saturation due to the generated of 2nd Stokes signal has been presented for these two different configurations

Thirdly, related to the triple Brillouin frequency shift cavity, a MBEFL with a triple Brillouin wavelength spacing (0.25 nm) Stokes signals is success- fully experimentally demonstrated. Up to 6 triple Stokes signals were presented at the center of the Erbium gain. Wide laser cavity tunability of 50 nm (1530–1580 nm) was recorded without self

lasing cavity modes due to using high Bp power and extracting the residual pump power outside the cavity. high OSNRs more than 45 dB, High Stokes powers of about 8 dBm, and good stability less than 2 dB were observed for the generated triple Stokes signals.

Moreover, within the quadruple Brillouin frequency shift design, a multi output port with a quadruple wavelength spacing (0.33 nm) Stokes signals utilizing MBEFL cavity is experimentally demonstrated successfully. Up to 14 Stokes signals with a channel spacing of 0.33 nm were recorded at these four output ports. Wide laser cavity tunability of 60 nm (1530–1580 nm) was presented in the absence of free running modes oscillation as a result to using high Bp power, pre-amplification technique, and capturing the residual pump power outside the cavity. For all generated Stokes signals, high peak powers and large OSNRs were presented

Finally, for large Brillouin frequency shift of 50 GHz, a multi output port with a quintuple wavelength spacing (0.4 nm) Stokes signals utilizing dual ring MBEFL cavity is experimentally demonstrated successfully. Up to 18 Stokes signals with equally wave- length spacing of 0.4 nm were recorded at different five output ports. Broad cavity tunability of 40 nm (1540–1580 nm) was introduced in the absence of self lasing cavity mode oscillations without filter- ing methods using three different techniques high BP power, pre- amplification technique, and capturing the residual pump power out- side the cavity. High Stokes powers of about 10 dBm, high OSNRs more than 50 dB, and good stability less than 2 dB were observed for the generated quintuple Stokes signals.

5.2 Novelty Contribution

The design and the analysis of different Brillouin frequency shift lines is addressed in this thesis. An investigation, enhancement, and new generation structures are presented in this study. The main contributions of this experimental research can be summarized as follows:

- Enhancing the laser cavity tunability in the single channel spacing fiber laser cavity using simple and cheap PEDF.

- Estimating and deriving the SBS threshold equation in the presence of Brillouin gain within double pass channel spacing cavity.
- Improving both of tuning range and number of the generated Stokes lines in triple Brillouin frequency shift cavity. Simple techniques are used for the improvement issue.
- Generating a new and an efficient multiwavelength quadruple channel spacing line that can be used for DWDM communication system.
- Generating a new and widest multiwavelength Brillouin frequency shift signals of 50 GHz that is more suitable for DWDM systems.
- The experimental conducted results in thesis (section 4.3 to section 4.6) are published in SCI index journals [136–139]

5.3 Recommendations for Further Work

Further experimental study could be conducted by inclusion the four-wave mixing effect in the 40 and 50 GHz cavities in order to improve the generated Stokes lines with a high flatness channel bandwidth. In addition, the new system can get a benefit from the generated anti-Stokes channels which has the same Brillouin frequency shift of the inserted Stokes channels. Finally, an external four-wave mixing cavity could be incorporated with the internal fiber laser cavity to reduce the complexity of the phase matching inside the Brillouin cavity.

REFERENCES

[1] Schneider, T., “Four-Wave-Mixing (FWM)”, Berlin , Springer , 2004.

[2] Agrawal, G. P., “Optical Signal Generation”, New York ,John Wiley & Sons, Ltd, 2005.

[3] Agrawal, G. P., “Nonlinear Fiber Optics” , Berlin, Springer , 2007.

[4] Agrawal, G. P., “WDM Systems” , New York , John Wiley & Sons, Ltd, 2005.

[5] Chiao, R. Y., Townes, C. H., and Stoicheff, B. P. Stimulated Brillouin Scattering and Coherent Generation of Intense Hypersonic Waves. Phys. Rev. Lett., *(12)*, (21) 592–595. 1964.

[6] ITU-T, “G.694.1, "Spectral grids for WDM applications: DWDM frequency grid,”, 02/2012, from https://www.itu.int/rec/T-REC-G.694.1/en, 2012,

[7] Shen, Y., Zhang, X., and Chen, K. All-optical generation of microwave and millimeter wave using a two-frequency Bragg grating-based Brillouin fiber laser. Journal Light. Technol, *(23)*, (5) 1860–1865. 2005.

[8] Turitsyna, E. G. and Webb, S. Simple design of FBG-based VSB filters for ultra-dense WDM transmission. ELECTRONICS LETTERS, *(41)*, (2) 40–41. 2005.

[9] Al-Mansoori, M. H., Abd-Rahman, M. K., Mahamd Adikan, F. R., and Mahdi, M. A. Widely tunable linear cavity multiwavelength Brillouin-Erbium fiber lasers. Opt. Express, *(13)*, (9) 3471. 2005.

[10] Salman, A. and Al-Janabi, A. Multiwavelength Q-switched erbium-doped fibre laser-based aluminum nanoparticles saturable absorber and sagnac loop filter. Laser Phys, *(29)*, (7) 65103, 2019.

[11] Saharudin, S., Abdullah, M. K., and Mahdi, M. A. Enhancement of Brillouin stokes powers in multiwavelength fiber laser utilizing band-pass filter. Microw.

Opt Technol Lett, *(40)*, (5) 408–410. 2004.

[12] Al-Mansoori, M. H. and Mahdi, M. A. Tunable range enhancement of Brillouin-erbium fiber laser utilizing Brillouin pump preamplification technique. Opt. Express, *(16)*, (11) 7649. 2008.

[13] Al-Mansoori, M. H., Mahdi, M. A., and Premaratne, M. Novel multiwavelength L-band Brillouin-Erbium fiber laser utilizing double-pass Brillouin pump preamplified technique. IEEE J. Sel. Top. Quantum Electron., *(15)*, (2) 415–421. 2009.

[14] Dong, B., Zhou, D. P., and Wei, L. Tunable multiwavelength Brillouin-Erbium fiber laser by controlling self-lasing cavity modes' oscillation. Opt. Fiber Technol, *(16)*, (1) 17–19. 2010.

[15] Al-Mashhadani, T. F., Al-Mansoori, M. H., Jamaludin, M. Z., Abdullah, F., Abass, A. K., and Rawi, N. I. M. Tunable multiwavelength L-band Brillouin-Erbium fiber laser utilizing passive EDF absorber section. Opt. Fiber Technol., *(19)*, (6) 593–597. 2013.

[16] Hänisch, C., Heuer, A., and Menzel, R. Threshold reduction of stimulated Brillouin scattering (SBS) using fiber loop schemes. Appl. Phys. B, *(73)*, (8) 851–854. 2001.

[17] Radmore, P. M. Solutions of the SBS equations in single mode optical fibres and implications for fibre transmission systems. Electron. Lett., *(26)*, (7) 434-436.1990.

[18] Kobyakov, A., Darmanyan, S. A., and Chowdhury, D. Q. Exact analytical treatment of noise initiation of SBS in the presence of loss. Opt. Commun., *(260)*, (1) 46–49. 2006.

[19] Lee, C. C. and Chi, S. Measurement of stimulated-Brillouin-scattering threshold for various types of fibers using Brillouin optical-time-domain reflectometer. IEEE Photonics Technol. Lett., *(12)*, (6) 672–674. 2000.

[20] Kovalev, V. I. and Harrison, R. G. Threshold for stimulated Brillouin scattering in optical fiber. Opt. Express, (15), (26) 17625–17630. 2007.

[21] Inoue, K. Brillouin threshold in an optical fiber with bidirectional pump lights. Opt. Commun., *(120)*, (2) 34–38. 1995.

[22] Ajiya, M., Mahdi, M. A. A., Al-Mansoori, M. H. H., Shee, Y. G. G., Hitam, S., and Mokhtar, M. Reduction of stimulated Brillouin scattering threshold through pump recycling technique. Laser Phys. Lett., *(6)*, (7) 535–538. 2009.

[23] Al-Mashhadani, T. F., Al-Mansoori, M. H., Jamaludin, M. Z., Abdullah, F., and Abass, A. K. Influence of a bidirectional recycling residual pump on the Stokes signal characteristics of a linear cavity Brillouin fiber laser. Laser Phys., *(23)*, (8) 121-125. 2013.

[24] Agrawal, G., "*Nonlinear fiber optics"*. New York. Elsevier Inc., 2000.

[25] Cowle, G. J. and Stepanov, D. Y. Hybrid Brillouin/erbium fiber laser. Opt. Lett., *(21)*, (16) 1250–1252. 1996.

[26] Ahmad, H. Stokes signal saturation in tunable BEFL system. Electron. Lett., *(34)*, (18) 1751-1752(1).1998.

[27] Lim, D. S., Lee, H. K., Kim, K. H., Kang, S. B., Ahn, J. T., and Jeon, M.-Y. Generation of multiorder Stokes and anti-Stokes lines in a Brillouin erbium-fiber laser with a Sagnac loop mirror. Opt. Lett.,*(23)*, (21) 1671, 1998.

[28] Almusafer, W. K. H., Jamaludin, M. Z., Abdullah, F., Al-Mansoori, M. H., Ajiya, M., and Mahdi, M. A. Widely Tunable C +L Bands Multiwavelength BEFL with Double-Brillouin Frequency Shifts. IEEE Photonics J., *(4)*, (5) 1720–1727. 2012.

[29] Mohd Nasir, M. N., Yusoff, Z., Al-Mansoori, M. H., Abdul Rashid, H. A., and Choudhury, P. K. Widely tunable multi-wavelength Brillouinerbium fiber laser utilizing low SBS threshold photonic crystal fiber. Opt. Express, *(17)*, (15) 12829. 2009.

[30] Huang, Y., Zhan, L., Ji, J. H., Luo, S. Y., and Xia, Y. X. Multiwavelength self-seeded Brillouin-erbium fiber laser with 45-nm tunable range. Opt. Commun., (281), (3) 452–456. 2008.

[31] Song, Y. J., Zhan, L., Hu, S., Ye, Q. H., and Xia, Y. X. Tunable multiwavelength Brillouin-Erbium fiber laser with a polarization-maintaining fiber Sagnac loop filter. IEEE Photonics Technol. Lett., *(16)*, (9) 2015–2017, 2004.

[32] Ahmad, H., Razak, N. F., Zulkifli, M. Z., Ismail, M. F., Munajat, Y., and Harun, S. W. Tunable single Stokes extraction from 20 GHz Brillouin fiber laser using ultranarrow bandwidth optical filter. Appl. Opt., (53), (29) 6944. 2014.

[33] Mamdoohi, G., Sarmani, A. R., Abas, A. F., Yaacob, M. H., Mokhtar, M., and Mahdi, M. A. 20 GHz spacing multi-wavelength generation of Brillouin-Raman fiber laser in a hybrid linear cavity. Opt. Express, *(21)*, (16) 18724. 2013.

[34] Tang, J., Sun, J., Chen, T., and Zhou, Y. A stable optical comb with double-Brillouin-frequency spacing assisted by multiple four-wave mixing processes. Opt. Fiber Technol., *(17)*, (6) 608–611. 2011.

[35] Shirazi, M. R., Biglary, M., Harun, S. W., Thambiratnam, K., and Ahmad, H. Bidirectional multiwavelength Brillouin fiber laser generation in a ring cavity. J. Opt. A Pure Appl. Opt., *(10)*, (5) 8–11. 2008.

[36] Zhou, X., Hu, K., Wei, Y., Bi, M., and Yang, G. An L-band multi-wavelength Brillouin-erbium fiber laser with switchable frequency spacing. Laser Phys., *(27)*, (1) 15103. 2017.

[37] Qian, L., Fen, D., Xie, H., and Sun, J. A novel tunable multi-wavelength Brillouin fiber laser with switchable frequency spacing. Opt. Commun., *(340)*, (5) 74–79.2015.

[38] Zhou, X. Multi-Wavelength Brillouin Fiber Laser with Triple Brillouin Frequency Spacing. IEEE Photonics Technol. Lett., *(28)*, (21) 2379–2382. 2016.

[39] Wang, X. Frequency spacing switchable multiwavelength Brillouin erbium fiber laser utilizing cascaded Brillouin gain fibers. Appl. Opt., *(55)*, (23) 6475. 2016.

[40] Al-Mansoori, M. H., Al-Sheriyani, A., Al-Nassri, S., and Hasoon, F. N. Generation of efficient 33 GHz optical combs using cascaded stimulated Brillouin scattering effects in optical fiber. Laser Phys., *(27)*, (6)121-124. 2017.

[41] Wang, Z., Wang, T., Jia, Q., Ma, W., Su, Q., and Zhang, P. Triple Brillouin frequency spacing multiwavelength fiber laser with double Brillouin cavities and its application in microwave signal generation. Appl. Opt., *(56)*, (26) 7419, 2017.

[42] Al-Mansoori, M. H., Al-Sheriyani, A., Younis, M. A. A., and Mahdi, M. A. Widely tunable multiwavelength Brillouin-erbium fiber laser with triple Brillouin-shift wavelength spacing. Opt. Fiber Technol., (41), (5) 21–26. 2018.

[43] Jia, Q., Zhang, P., Wang, T., Li, X., and Bo, B. 40 GHz narrow linewidth frequency-switched microwave signal generation based on a single-longitudinal-mode double-Brillouin-frequency spaced Brillouin fiber laser. Appl. Opt., *(56)*, (19) 5323. 2017.

[44] Schneider, T., "*Nonlinear Impairments*", Berlin , John Wiley & Sons, Ltd, 2005.

[45] Zalehan, E. A. M., Ahmad Hambali, N. A. M., Wahid, M. H. A., Shahimin, M. M., and Roshidah, N. S-band multiwavelength Brillouin-Raman fiber laser utilizing an optical reflector. Optik (Stuttg)., *(130)*, (7) 818–824. 2017.

[46] Schneider, T., "Self- and Cross-Phase Modulation", Berlin, ,Springer Berlin Heidelberg. 2004.

[47] Islam, M. N., Mollenauer, L. F., Stolen, R. H., Simpson, J. R., and Shang, H. T. Cross-phase modulation in optical fibers. Opt. Lett., *(12)*, (8) 625–627. 1987.

[48] Abu Bakar, M. H., Mahamd Adikan, F. R., Ibrahim, N. H., and Mahdi, M. A.

L-band R-EDFA/Raman hybrid amplifier with enhanced higher-order pumping scheme utilizing stimulated Raman scattering. Opt. Commun., *(291)*, (6) 155–161. 2013.

[49] Ippen, E. P. and Stolen, R. H. Stimulated Brillouin scattering in optical fibers. Appl. Phys. Lett., *(21)*, (11) 539–541. 1972.

[50] Chraplyvy, A. R. Limitations on lightwave communications imposed by optical-fiber nonlinearities. J. Light. Technol., *(8)*, (10) 1548–1557. 1990.

[51] Uesugi, N., Ikeda, M., and Sasaki, Y. Maximum single frequency input power in a long optical fibre determined by stimulated Brillouin scattering. Electron. Lett., *(17)*, (11) 379–380. 1981.

[52] Gaeta, A. L. And Boyd, R. W. Stımulated Brıllouın Scatterıng In The Presence Of External Feedback. J. Nonlinear Opt. Phys. Mater., *(1)*, (3) 581–594. 1992.

[53] Melloni, A., Frasca, M., Garavaglia, A., Tonini, A., and Martinelli, M. Direct measurement of electrostriction in optical fibers. Opt. Lett., *(23)*, (9) 691–693. 1998.

[54] Tang, C. L. Saturation and Spectral Characteristics of the Stokes Emission in the Stimulated Brillouin Process. J. Appl. Phys., *(37)*, (8) 2945–2955. 1966.

[55] Enns, R. H. and Batra, I. P. Saturation and depletion in stimulated light scattering. Phys. Lett. A, *(28)*, (8) 591–592. 1969.

[56] Chen, L. and Bao, X. Analytical and numerical solutions for steady state stimulated Brillouin scattering in a single-mode fiber. Opt. Commun., *(152)*, (3) 65–70. 1998.

[57] Ou, Z., Li, J., Zhang, L., Dai, Z., and Liu, Y. An approximate analytic solution of the steady state Brillouin scattering in single mode optical fiber without neglecting the attenuation coefficient. Opt. Commun., *(282)*, (18) 3812–3816. 2009.

[58] Al-Mashhadani, T. F., Jamaludin, M. Z., Al-Mansoori, M. H., Abdullah, F., and Abass, A. K. Modeling of multi-wavelength brillouin fiber laser based on analytical solutions in a linear cavity. Fiber Integr. Opt., *(31*),(6) 383–396.2012.

[59] Smith, R. G. Optical Power Handling Capacity of Low Loss Optical Fibers as Determined by Stimulated Raman and Brillouin Scattering. Appl. Opt., *(11)*, (11) 2489–2494,. 1972.

[60] Haus, H. A. Applications of Nonlinear Fiber Optics. Phys. Today, *(55)*, (6) 58–59. 2002.

[61] van Deventer, M. O. and Boot, A. J. Polarization properties of stimulated Brillouin scattering in single-mode fibers. J. Light. Technol., *(12)*, (4) 585–590. 1994.

[62] Botineau, J., Picholle, E., and Bahloul, D. Effective stimulated Brillouin gain in singlemode optical fibres. Electron. Lett., *(31)*, (23) 2032–2034. 1995.

[63] Shiraki, K., Ohashi, M., and Tateda, M. Suppression of stimulated Brillouin scattering in a fibre by changing the core radius. Electron. Lett., *(31)*, (8) 668–669. 1995.

[64] Shiraki, K., Ohashi, M., and Tateda, M. Performance of strain-free stimulated Brillouin scattering suppression fiber. J. Light. Technol., *(14)*, (4) 549–554. 1996.

[65] Aoki, Y., Tajima, K., and Mito, I. Input power limits of single-mode optical fibers due to stimulated Brillouin scattering in optical communication systems. J. Light. Technol., *(6)*, (5) 710–719. 1988.

[66] Willems, F. W., van der Plaats, J. C., and Muys, W. Harmonic distortion caused by stimulated Brillouin scattering suppression in externally modulated lightwave AM-CATV systems. Electron. Lett., *(30)*, (4) 343–345. 1994.

[67] Willems, F. W., Muys, W., and Leong, J. S. Simultaneous suppression of stimulated Brillouin scattering and interferometric noise in externally

modulated lightwave AM-SCM systems. IEEE Photonics Technol. Lett., *(6)*, (12) 1476–1478. 1994.

[68] Nikles, M., Thevenaz, L., and Robert, P. A. Brillouin gain spectrum characterization in single-mode optical fibers. J. Light. Technol., *(15)*, (10) 1842–1851. 1997.

[69] Ruffin, A. B., Li, M.-J., Chen, X., Kobyakov, A., and Annunziata, F. Brillouin gain analysis for fibers with different refractive indices. Opt. Lett., *(30)*, (23) 3123–3125. 2005.

[70] Shimizu, T., Nakajima, K., Shiraki, K., Ieda, K., and Sankawa, I. Evaluation methods and requirements for the stimulated Brillouin scattering threshold in a single-mode fiber. Opt. Fiber Technol., *(14)*, (1). 2008.

[71] Al-Asadi, H. A., Al-Mansoori, M. H., Ajiya, M., Hitam, S., Saripan, M. I., and Mahdi, M. A. Effects of pump recycling technique on stimulated Brillouin scattering threshold: a theoretical model. Opt. Express, *(18)*, (21) 22339. 2010.

[72] Dämmig, M., Zinner, G., Mitschke, F., and Welling, H. Stimulated Brillouin scattering in fibers with and without external feedback. Phys. Rev. A, *(48)*, (4) 3301–3309. 1993.

[73] Kovalev, V. I. and Harrison, R. G. Abnormally low threshold gain of stimulated Brillouin scattering in long optical fiber with feedback. Opt. Express, *(16)*, (16) 12272–12277. 2008.

[74] Cowle, G. J. and Stepanov, D. Y. Multiple wavelength generation with brillouin/erbium fiber lasers. IEEE Photonics Technol. Lett., *(8)*, (11) 1465–1467. 1996.

[75] Abd-rahman, M. K., Abdullah, M. K., and Ahmad, H. Multiwavelength , bidirectional operation of twin-cavity Brillouin r erbium fiber laser. Opt. Commun., *(181)*, (7) 135–139. 2000.

[76] Al-Mansoori, M. H., Bouzid, B., Ali, B. M., Abdullah, M. K., and Mahdi, M.

A. Multi-wavelength Brillouin-Erbium fibre laser in a linear cavity. Opt. Commun., *(242)*, (1–3) 209–214. 2004.

[77] Song, Y. J., Zhan, L., Hu, S., Ye, Q. H., and Xia, Y. X. Tunable multiwavelength Brillouin-Erbium fiber laser with a polarization-maintaining fiber Sagnac loop filter. IEEE Photonics Technol. Lett., *(16)*, (9) 2015–2017. 2004.

[78] Abdullah, M. K., Shaharudin, S., Mahdi, M. A., and Endut, R. A widely tunable hybrid brillouin-erbium fiber laser (BEFL) system. Opt. Laser Technol., *(36)*, (7) 567–570. 2004.

[79] Al-Mansoori, M. H., Abdullah, M. K., Ali, B. M., and Mahdi, M. A. Hybrid Brillouin/Erbium fibre laser in a linear cavity for multi-wavelength communication systems. Opt. Laser Technol., *(37)*, (5) 387–390. 2005.

[80] Harun, S. W., Cheng, X. S., and Ahmad, H. An efficient S-band brillouin erbium fiber laser with additional EDFA. Opt. Laser Technol., *(39)*, (3) 616–618. 2007.

[81] Al-Mansoori, M. H., Adikan, F. R. M. M., Naji, A. W., Abdullah, M. K., and Mahdi, M. A. Multi-wavelength Fabry-Pérot Brillouin-Erbium fibre laser. Optik (Stuttg)., *(117)*, (3) 128–130. 2006.

[82] Cheng, X. S., Harun, S. W., and Ahmad, H. Effects of output coupler reflectivity on the performance of a linear cavity Brillouin/erbium fiber laser. Pramana - J. Phys., *(68)*, (3) 451–456. 2007.

[83] Huang, Y., Zhan, L., Ji, J. H., Luo, S. Y., and Xia, Y. X. Multiwavelength self-seeded Brillouin-erbium fiber laser with 45-nm tunable range. Opt. Commun., *(281)*, (3) 452–456. 2008.

[84] Hambali, N. A. M., Mahdi, M. A., Al-Mansoori, M. H., Abas, A. F., and Saripan, M. I. Investigation on the effect of EDFA location in ring cavity Brillouin-Erbium fiber laser. Opt. Express, *(17)*, (14) 11768. 2009.

[85] Tang, J., Sun, J., Zhao, L., Chen, T., Huang, T., and Zhou, Y. Tunable multiwavelength generation based on Brillouin-erbium comb fiber laser assisted by multiple four-wave mixing processes. Opt. Express, *(19)*, (15) 14682. 2011.

[86] Al-Mansoori, M. H. and Mahdi, M. A. Characteristics of multiple wavelengths l-band brillouin-erbium comb fiber laser at low pumping powers. 2008 Int. Electron. Des. ICED 2008, pp. 3–6, 2008.

[87] Samsuri, N. M., Zamzuri, A. K., Al-Mansoori, M. H., Ahmad, A., and Mahdi, M. A. Brillouin-Erbium fiber laser with enhanced feedback coupling using common Erbium gain section. Opt. Express, *(16)*, (21) 16475. 2008.

[88] Al-Mansoori, M. H. and Mahdi, M. A. Multiwavelength L-band brillouin-erbium comb fiber laser utilizing nonlinear amplifying loop mirror. J. Light. Technol., *(27)*, (22) 5038–5044. 2009.

[89] Al-Mansoori, M. H., Mahdi, M. A., and Premaratne, M. Novel multiwavelength L-band Brillouin-Erbium fiber laser utilizing double-pass Brillouin pump preamplified technique. IEEE J. Sel. Top. Quantum Electron., *(15)*, (2) 415–421. 2009.

[90] Tian, J., Yao, Y., Xiao, J. J., Xu, X., and Chen, D. Multiwavelength erbium-doped fiber laser based on intensity-dependent transmission in a linear cavity. J. Appl. Phys., *(109)*, (11) 1–5. 2011.

[91] Rahman, Z. A., Hitam, S., Abas, A. F., and Mahdi, M. A. Multiwavelength Brillouin fiber laser with enhanced reverse-S-shaped feedback coupling assisted by out-of-cavity optical amplifier. *(19)*, (22) 21238–21245. 2011.

[92] Ajiya, M., Mahdi, M. A., and Member, S. L-Band Multiwavelength BEFL With Amplifi ed Fiber Loop Mirror L-Band Multiwavelength BEFL With. IEEE Photonics J., *(4)*, (2) 0–8. 2012.

[93] Yaacob, M. H., Abas, A. F., Mahdi, M. A., and Mokhtar, M. Simple multiwavelength Brillouin – Erbium-doped fi ber laser structure based on short

SSMF. Opt. Commun., *(300)*, (6) 8–11. 2013.

[94] Al-Alimi, A. W., Yaacob, M. H., Abas, A. F., Mahdi, M. A., Mokhtar, M., and Al-Mansoori, M. H. 150-Channel Four Wave Mixing Based Multiwavelength Brillouin-Erbium Doped Fiber Laser. IEEE Photonics J., *(5)*, (4) 1501010, 2013.

[95] Rahman, Z. A., Hitam, S., Al-Mansoor, M. H., Bakar, M. H. A., and Mahdi, M. A. Capacity enhancement of virtual-mirror-based multiwavelength Brillouin-erbium fiber laser. Microw. Opt Technol Lett, *(55)*, (11) 2549–2553, 2013.

[96] Abd-rahman, M. K., Nurdik, M. R., Rahim, N. S. A., and Brillouin-erbium, A. A. Self-Seeded Multiwavelength Dual-Cavity Brillouin-Erbium Fiber Laser. IEEE J. Sel. Top. Quantum Electron., *(20)*, (5) 125-129. 2014.

[97] Al-Alimi, A. W., Cholan, N. A., Yaacob, M. H., Abas, A. F., Alresheedi, M. T., and Mahdi, M. A. Wide bandwidth and flat multiwavelength Brillouin-erbium fiber laser. Opt. Express, *(25)*, (16) 19382. 2017.

[98] Al-Alimi, A. W., Sarmani, A. R., Al-Mansoori, M. H., Lakshminarayana, G., and Mahdi, M. A. Flat amplitude and wide multiwavelength Brillouin/erbium fiber laser based on Fresnel reflection in a micro-air cavity design. Opt. Express, *(26)*, (3) 3124, 2018.

[99] Ma, L., Zou, H., Xiong, H., Wu, H., and Zhang, Y. Multiwavelength generation by using a novel Brillouin-erbium fiber laser with double linear-cavity based on a double-pass Brillouin Pump (BP) amplification technique. Opt. Laser Technol., *(117)*, (6) 169–174. 2019.

[100] Ajiya, M., Mahdi, M. A., Al-Mansoori, M. H., Hitam, S., and Mokhtar, M. Seamless tuning range based-on available gain bandwidth in multiwavelength Brillouin fiber laser. Opt. Express, *(17)*, (8) 5944. 2009.

[101] Ajiya, M., Mahdi, M. A., Al-Mansoori, M. H., Mokhtar, M., and Hitam, S. Directivity influence of signals propagation through EDFA gain medium of Brillouin-erbium fiber laser. Opt. Commun., *(282)*, (21) 4266–4270. 2009.

[102] Ajiya, M., Mahdi, M. A., Al-Mansoori, M. H., Mokhtar, M., and Hitam, S. Broadly tunable multiple wavelength Brillouin fiber laser exploiting erbium amplification. J. Opt. Soc. Am. B, *(26)*, (9) 1789. 2009.

[103] Zhao, J., Yang, X., Tong, Z., Liu, Y., and Zhao, Q. Simple tunable multiwavelength Brillouin/Erbium fiber laser utilizing short-length photonic crystal fiber. Optik (Stuttg)., *(122)*, (12) 1046–1049. 2011.

[104] Mahdi, M. A., Al-Mansoori, M. H., and Premaratne, M. Enhancement of multiwavelength generation in the L-band by using a novel Brillouin-Erbium fiber laser with a passive EDF booster section. Opt. Express, *(15)*, (18) 11570, 2007.

[105] Al-Mashhadani, T. F., Jamaludin, M. Z., Al-Mansoori, M. H., Abdullah, F., and Abbas, A. K. Impact of booster section length on the performance of linear cavity brillouin-erbium fiber laser. J. Opt. Soc. Korea, *(18)*, (2) 162–166. 2014.

[106] Al-Mashhadani, T. F., Al-Mansoori, M. H., Jamaludin, M. Z., Abdullah, F., Abass, A. K., and Rawi, N. I. M. Tunable multiwavelength L-band Brillouin-Erbium fiber laser utilizing passive EDF absorber section. Opt. Fiber Technol., *(19)*, (6) 593–597. 2013.

[107] Oh, W. Y., Ko, J. S., Lim, D. S., and Seo, W. 10 and 20 GHz optical combs generation in Brillouin/erbium fiber laser with shared cavity of Sagnac reflector. Opt. Commun., *(201)*, (4–6) 399–403. 2002.

[108] Harun, S. W., Shirazi, M. R., Abdul-Rashid, H. A., and Ahmad, H. Multiwavelength source using a brillouin fiber laser. J. Nonlinear Opt. Phys. Mater., *(17)*, (2) 199–203. 2008.

[109] Harun, S. W., Shirazi, M. R., and Ahmad, H. A new configuration of multi-wavelength Brillouin fiber laser. Laser Phys. Lett., *(5)*, (1) 48–50. 2008.

[110] Shee, Y. G., Al-Mansoori, M. H., Ismail, A., Hitam, S., and Mahdi, M. A. Double Brillouin frequency shift through circulation of odd-order Stokes signal. Appl. Opt., *(49)*, (20) 3956–3959. 2010.

[111] Shee, Y. G., Ismail, A., Hitam, S., and Mahdi, M. A. Multiwavelength Brillouin-erbium fiber laser with double-Brillouin-frequency spacing. Opt. Express, *(19)*, (3) 1699–1706. 2011.

[112] Parvizi, R., Ali, N. M., Harun, S. W., Moghavvemi, M., Arof, H., and Ahmad, H. Multi-wavelength Brillouin fiber laser using dual-cavity configuration. Laser Phys., *(21)*, (1) 205–209. 2011.

[113] Parvizi, R., Arof, H., Ali, N. M., Ahmad, H., and Harun, S. W. 0.16 nm spaced multi-wavelength Brillouin fiber laser in a figure-of-eight configuration. Opt. Laser Technol., *(43)*, (4) 866–869. 2011.

[114] Shee, Y. G. et al. Millimeter wave carrier generation based on a double-Brillouin-frequency spaced fiber laser. Opt. Express, *(20)*, (12) 13402–13408. 2012.

[115] Zhao, J. F., Liao, T. Q., Zhang, C., Zhang, R. X., Miao, C. Y., and Tong, Z. R. Double Brillouin frequency spaced multiwavelength Brillouin-erbium fiber laser with 50 nm tuning range. Laser Phys., *(22)*, (9) 1415–1418. 2012.

[116] Ahmad, B. A., Al-Alimi, A. W., Abas, A. F., Mokhtar, M., Harun, S. W., and Mahdi, M. A. Double spacing multi-wavelength L-band Brillouin erbium fiber laser with Raman pump. J. Mod. Opt., *(59)*, (19) 1690–1694. 2012.

[117] Ahmad, B. A., Al-Alimi, A. W., Abas, A. F., Mokhtar, M., Harun, S. W., and Mahdi, M. A. Compact Brillouin fiber laser based on highly nonlinear fiber with 51 double spacing channels. IEEE Photonics J., *(4)*, (4) 1087–1094. 2012.

[118] Tan, S. J., Harun, S. W., Ali, N. M., Ismail, M. A., and Ahmad, H. A multi-wavelength Brillouin Erbium fiber laser with double brillouin frequency spacing and Q-switching characteristics. IEEE J. Quantum Electron., *(49)*, (7) 595–598. 2013.

[119] Li, J., Chen, T., Sun, J. Q., and Shen, X. Double-brillouin-frequency spaced multiwavelength generation in a ring brillouin-erbium fiber laser. Chinese Phys. Lett., *(30)*, (2) 1122. 2013.

[120] Zhao, J. F., Zhang, C., Miao, C. Y., Ji, Z. H., Cao, Y., and Tong, Z. R. A widely tunable double-Brillouin-frequency spaced multiwavelength fiber laser with a 110 nm tuning range. Laser Phys., *(23)*, (6). 2013.

[121] Abass, A. K., Al-Mansoori, M. H., Jamaludin, M. Z., Abdullah, F., Al-Mashhadani, T. F., and Ali, M. H. L-band multi-wavelength brillouin-raman fiber laser with 20-GHz channel spacing. Fiber Integr. Opt., *(33)*, (2) 56–67, 2014.

[122] Zhou, X., Liu, Y., and Yuan, S. A novel double-Brillouin-frequency spaced multi-wavelength Brillouin erbium-doped fiber laser based on non-linear amplified fiber loop mirror. Optik (Stuttg)., *(125)*, (18) 5218–5220. 2014.

[123] Kuo, H. L. and Lin, W. P. Double-Brillouin-frequency spaced multiwavelength generation in one loop structure. Opt. Lett., *(39)*, (15) 4565. 2014.

[124] Tiu, Z. C., Aidit, S. N., Hassan, N. A., Ismail, M. F. Bin, and Ahmad, H. Single and Double Brillouin Frequency Spacing Multi-Wavelength Brillouin Erbium Fiber Laser with Micro-Air Gap Cavity. IEEE J. Quantum Electron., *(52)*, (9). 2016.

[125] Wang, X. Frequency spacing switchable multiwavelength Brillouin erbium fiber laser utilizing cascaded Brillouin gain fibers. Appl. Opt., *(55)*, (23) 6475. 2016.

[126] Pan, S. and Yao, J. Frequency-switchable microwave generation based on a dual-wavelength single-longitudinal-mode fiber laser incorporating a high-finesse ring filter. Opt. Express, *(17)*, (14) 12167. 2009.

[127] Zhou, X., Ge, C., and Wei, Y. A tunable multi-wavelength Brillouin–erbium fiber laser with fourfold Brillouin frequency spacing. Opt. Quantum Electron., *(49)*, (4) 166. 2017.

[128] Al-Mashhadani, T. F. Erbium gain effects on Stokes signal performance in a Fabry–Perot Brillouin Erbium fiber laser. Opt. Quantum Electron., *(51)*, (6) 1–9. 2019.

[129] Al-Mashhadani, T. F., Al-Mashhadani, M. K. S., Yucel, M., and Goktas, H. H. Influence of bidirectional cavity structure on the Brillouin Stokes signal characteristics in ring BFL. Optik (Stuttg)., *(185)*, (4) 359–363. 2019.

[130] Al-Mashhadani, T. F., Al-Mansoori, M. H., Jamaludin, M. Z., Abdullah, F., and Abass, A. K. Influence of a bidirectional recycling residual pump on the Stokes signal characteristics of a linear cavity Brillouin fiber laser. Laser Phys., *(23)*, (8) 85111. 2013.

[131] Al-Mansoori, M. H., Abd-Rahman, M. K., Mahamd Adikan, F. R., and Mahdi, M. A. Widely tunable linear cavity multiwavelength Brillouin-Erbium fiber lasers. Opt. Express, *(13)*, (9) 3471. 2005.

[132] Abass, A. K., Al-Mansoori, M. H., Jamaludin, M. Z., Abdullah, F., Al-Mashhadani, T. F., and Ali, M. H. Enhancing performance of multiwavelength Brillouin–Raman fiber laser by capturing residual pump power. Appl. Opt., *(53)*, (23) 5187. 2014.

[133] Ahmad, H., Razak, N. F., Zulkifli, M. Z., Ismail, M. F., Munajat, Y., and Harun, S. W. Tunable single Stokes extraction from 20 GHz Brillouin fiber laser using ultranarrow bandwidth optical filter. Appl. Opt., *(53)*, (29) 6944. 2014.

[134] Gan, G. K. W., Yeo, K. S., Adikan, F. R. M., and Shee, Y. G. Four-wave-mixing-assisted Brillouin fiber laser with double-Brillouin-frequency spacing. Opt. Fiber Technol., *(21)*, (6) 198–201. 2015.

[135] Al-Mansoori, M. H., Al-Sheriyani, A., Younis, M. A. A., and Mahdi, M. A. Widely tunable multiwavelength Brillouin-erbium fiber laser with triple Brillouin-shift wavelength spacing. Opt. Fiber Technol., *(41)*, (5) 21–26. 2018.

[136] Al-Mashhadani, T. F., Al-Mashhadani, M. K. S., Goktas, H. H., Yucel, M., and Celebi, F. V. Widely triple Brillouin frequency shift multiwavelength Brillouin erbium fiber laser. Opt. Quantum Electron., *(52)*, (4)228. 2020.

[137] Al-Mashhadani, M. K. S., Al-Mashhadani, T. F., and Goktas, H. H. Broadly tunable 40 GHz Brillouin frequency spacing multiwavelength Brillouin–

Erbium fiber laser for DWDM. Opt. Commun., *(451)*, (3) 116–123. 2019.

[138] Al-Mashhadani, T. F., Al-Mashhadani, M. K. S., Yucel, M., and Goktas, H. H. Influence of bidirectional cavity structure on the Brillouin Stokes signal characteristics in ring BFL. Optik (Stuttg)., *(185)*, 359–363. 2019.

[139] Al-Mashhadani, M. K. S., Al-Mashhadani, T. F., and Goktas, H. H. Tunable 50 GHz laser comb generation of multiwavelength Brillouin erbium fiber laser. Opt. Commun., *(464)*, 125542. 2020.